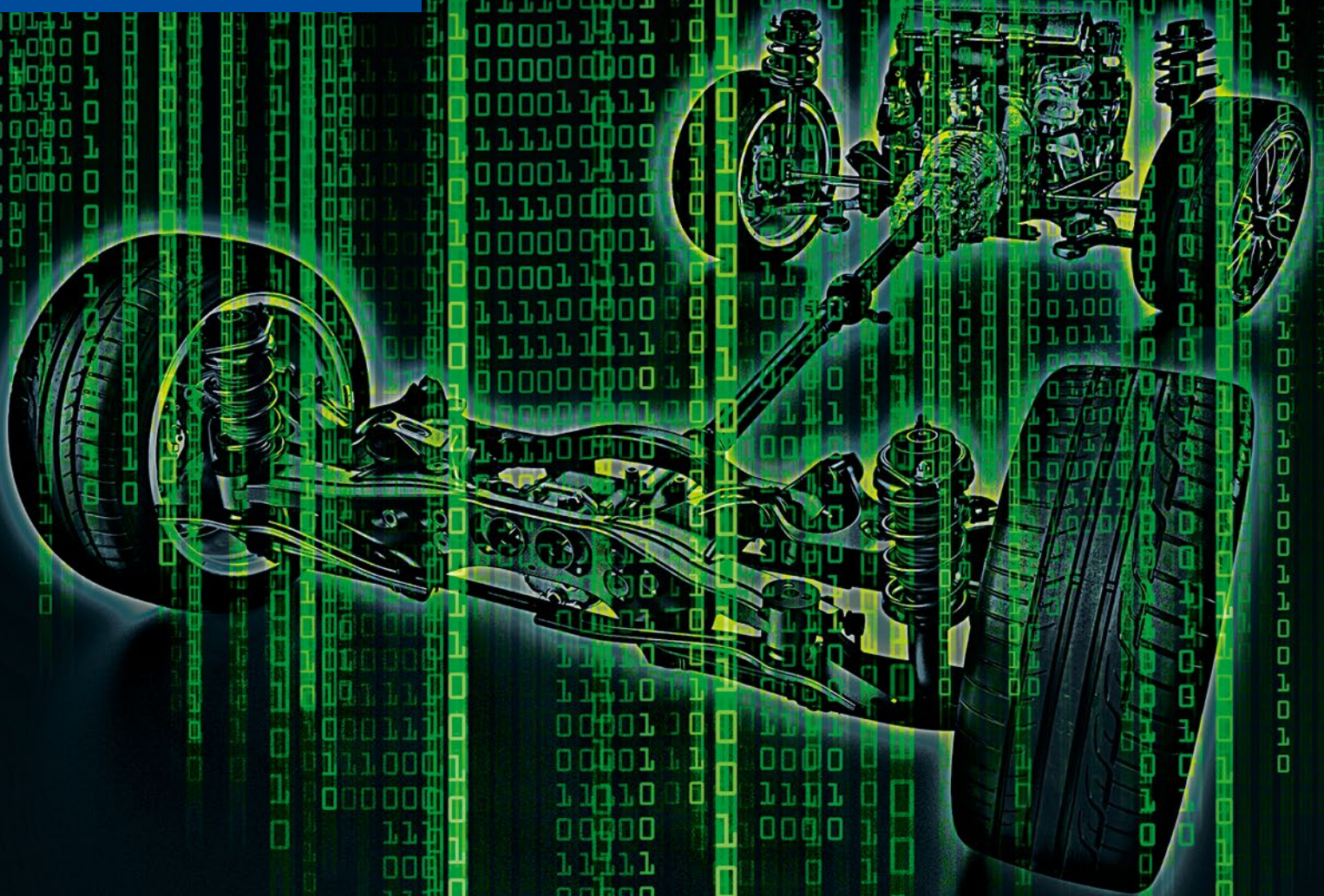


MTZ

12 December 2015 | Volume 76



COVER STORY

Cross-linking of the Drivetrain

MODERN METHODS

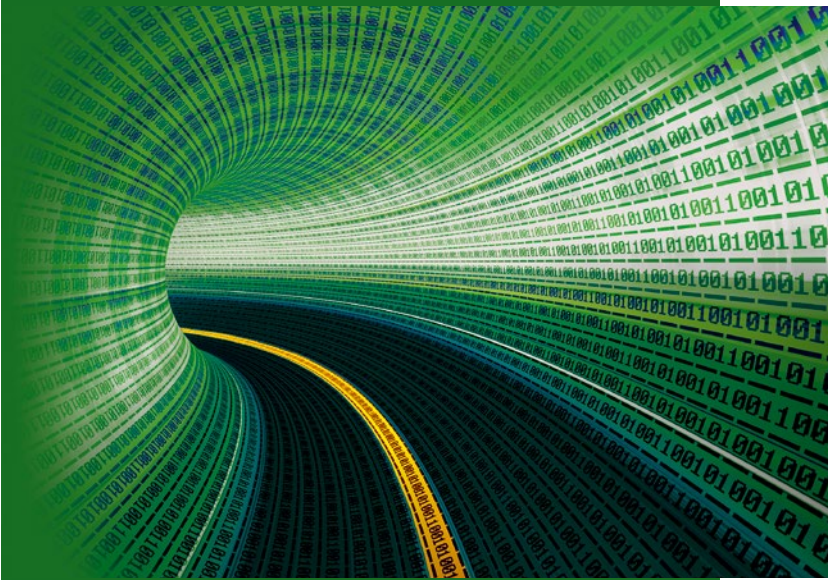
for Optimising Cylinder Distortions

IN-CYCLE CONTROL

Offers High Potential for New Combustion Concepts

QUICK ASHING

of Particulate Filters



COVER STORY

Cross-linking of the Drivetrain

In order to make vehicles even more efficient in the future, there will be greater focus on the entire powertrain and its management. We first take a look at the optimised interaction between individual components. We also consider how environmental data can be used for a predictive operating strategy.

4 Managing Diversity in the Drivetrain of the Future
Uwe Wagner, Martin Scheidt, Manfred Kraus [Schaeffler],
Hartmut Faust [LuK]

10 Connected Energy Management with a Backend-based
Driving Strategy as an Example
Friedrich Graf, Siegmund Deinhard, Christian Bottke,
Stefan Grubwinkler [Continental]

DEVELOPMENT**MEASURING TECHNIQUES**

16 Influencing Parameters in Emissions Measurement of Plug-in Hybrid Vehicles
Matthias Schröder [Horiba]

DEVELOPMENT METHODS

22 Modern Methods for Optimising Cylinder Distortions
Michael Berg, Hubert Schultheiß,
David Musch, Thomas Hilbert [IAV]

COOLING

30 Electrical 48-V Main Coolant Pump to Reduce CO₂ Emissions
Karl-Martin Fritsch, Stephan Weber,
Michael Krappel, Alfred Elsäßer [Mahle]

ENGINE MANAGEMENT

36 In-cycle Control Offers High Potential for New Combustion Concepts
Bastian Lehrheuer, Maximilian Wick,
Jakob Andert [RWTH Aachen University],
Jesse Lakemeier [dSpace]

CALCULATION AND SIMULATION

42 A New Global Algebraic NO_x Emissions Formation Model for Natural Gas Engines
Georgios Bikas [Delphi],
Konstantinos Michos, Ioannis Vlaskos [Ricardo]

RESEARCH

49 Peer Review

EXHAUST AFTERTREATMENT

50 Quick Ashing of Particulate Filters
Fabian Sonntag, Peter Eilts
[TU Braunschweig]

RUBRICS | SERVICE

3 Editorial
48 Imprint, Scientific Advisory Board

Time Window

Dear Reader,

actually, the IAA offered enough forward-looking topics to underline the innovative power of the automotive industry. But after „Dieselgate“ at Volkswagen, nothing remains – unfortunately! Instead, public perception is dominated by a scandal which consequences will cast a shadow not only over Volkswagen, but rather over an entire industry.

Because it has been known for years that the official fuel consumption and emissions indications deviate from the real-world values and that actual NO_x emissions from vehicles are many times higher in real operation than on test benches. The continuing high levels of NO₂ in German cities resulting from these emissions are nothing new either. Nevertheless, all parties have been haggling for years over new testing procedures, exceptions and the right time to introduce them – as if they were at a cattle market. Instead, it should be about the kind of world we want to leave to our children.

What is important now is, at long last, to introduce a worldwide harmonised test cycle (WLTC) with new test procedures (WLTP) quickly, sustainably and effectively to take account of Real Driving Emissions (RDE). However, what is even more important is that the automotive industry uses the narrow time window that is now available before the European and national political decision-makers set their own parameters, and that it goes on the offensive in addressing the subject of clean diesel technology. Only in this way will it be able to show how NO_x emissions can be reduced by using innovative technology and document that it is taking the issue of RDE seriously. ATZ and MTZ would be happy to deal extensively with this issue, applying the full range of knowledge available. Until now, this has all too often failed due to a lack of willingness in the industry to make informa-

tion available. But it is now time to do this, thus underlining the innovative power and responsibility of the companies involved.

Electric mobility is now unstoppable, and especially after this scandal it is likely to develop more rapidly than previously forecast. The 48-V theme will find its way, both top-down and bottom-up, into future vehicle models – in particular as a vehicle electrical system for hybrid vehicles. But these also require an internal combustion engine. If we want to prevent this engine, and especially the diesel, from being written off as „dirty“ in the coming decades of transition to the age of electrification, immediate and proactive measures are necessary.

The aim is therefore to use this time window effectively and powerfully. ATZ and MTZ will focus even more strongly on this area, and we are looking forward to the topics raised by the industry.

Best regards,



Dr. Alexander Heintzel
Editor in Chief





© Schaeffler

Managing Diversity in the Drivetrain of the Future

In order to fulfil future requirements, the range of technical solutions for combustion engines, electric motors, transmissions and chassis is becoming more diverse. In future, efficient measures towards reduced consumption will particularly emerge through developments that optimise the interaction between individual components. For automotive suppliers like Schaeffler, this represents a significant opportunity.



MORE COMPLEX DRIVETRAINS

Reduction of CO₂ and other harmful emissions will remain one of the dominant trends in automotive development over the coming years. The main drivers of this trend are the increasingly strict legal requirements — not only in Europe, but worldwide. To achieve the ambitious emissions targets, technical solutions are required that increase overall efficiency. The electrification of the drivetrain will play a pivotal role in this regard. At the same time, other trends like automated driving offer additional opportunities to reduce CO₂ emissions, such as through predictive control strategies that use route information.

Against this backdrop, the prognoses for drivetrain technology point clearly in one direction: The drivetrain is becoming more complex and increasingly electrified, **FIGURE 1**. However, car buyers are not fully prepared to share the resulting additional costs, meaning all technical solutions are under enormous cost pressure. The following article illustrates the opportunities and challenges facing suppliers of drivetrain components.

APPROACHES TO INCREASE EFFICIENCY IN THE DRIVETRAIN

The main approaches that can be taken to optimise the energy balance, **FIGURE 2**, can be roughly divided into three categories:

- consistent reduction of losses caused by undesirable friction and mass in the entire drivetrain
- right-sizing with turbocharging of the combustion engine and increasing variability in order to achieve a very

efficient, specific fuel consumption in a wide area of the engine map; this also includes optimisation of the downstream transmission, so that the combustion engine can be run in its optimal range

- increasing electrification of the drivetrain to use the energy that is generated by load point shifting and recuperation, for boosting and electric driving.

POTENTIAL AND MEASURES TOWARDS INCREASED EFFICIENCY

There are several fields showing potentials to improve the overall efficiency of the drivetrain. These are being discussed below.

ENGINE

The combustion engine used in **FIGURE 2** exhibits a medium effective efficiency of 26.5 % in the simulated New European Driving Cycle (NEDC). This is a very good value when measured against the current state of the art. However, there is certainly room for improvement. The latest estimates from Schaeffler in cooperation with IAV assume an optimisation potential to achieve an average efficiency of over 30 % in the NEDC.

In addition to reducing friction – for example through highly efficient coating processes in the valvetrain, through switching from plain to roller bearings or through efficient tension systems and decoupling systems in the front end accessory drive to reduce the required preload force – Schaeffler is also working on a wide range of technical solutions aimed at achieving a variable operating point adjustment:

AUTHORS



Uwe Wagner

is Senior Vice President R&D Automotive and Member of the Management Automotive at the Schaeffler Technologies AG & Co. KG in Herzogenaurach (Germany).



Dr. Hartmut Faust

is Senior Vice President R&D Transmission Systems at the LuK GmbH & Co. KG in Bühl (Germany).



Dr. Martin Scheidt

is Senior Vice President R&D Engine Systems Division at the Schaeffler Technologies AG & Co. KG in Herzogenaurach (Germany).



Dr. Manfred Kraus

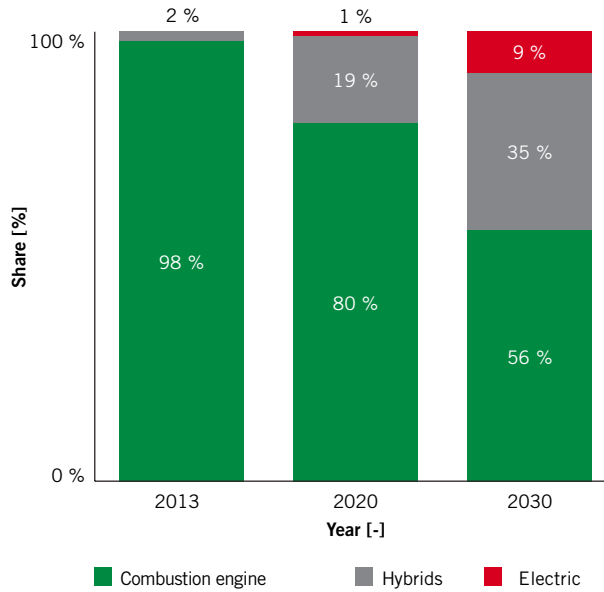
is Senior Vice President R&D Chassis Systems at the Schaeffler Technologies AG & Co. KG in Herzogenaurach (Germany).

- optimisation of thermal operating point and enhanced warm-up through intelligent thermal management
- optimisation of pumping losses, charge motion and combustion through a complete range of variable valve control systems, from cam phasers and switchable finger followers to the fully variable valve control system UniAir. These systems enable various operating strategies like early or late intake valve closing at part load and full load (Miller cycle), cylinder deactivation and internal exhaust gas recirculation or retention
- further optimisation of the combustion process by variable adjustment of the compression ratio.

The size of such technologies' potential has been exemplified by the simulation work, performed in cooperation with IAV, to optimise valve control strategies on a charged 1.4 l petrol engine. Through a combination of early and late intake valve closing, a high-grade downsizing ($p_{me, max} = 29 \text{ bar}$) with consumption advantages of 11.7 % was achieved in the NEDC. It was possible to enhance consumption potential by a further 3.6 % through an intelligent partial load strategy [1].

TORSIONAL VIBRATION DAMPING

Start-stop operation, downsizing and turbocharging of the engine all lead to the attainment of increasingly high peak combustion pressures and thus resulting also in increased rotational irregularity. In addition, the intrinsic damping of the transmission is permanently diminished by reduced friction, which increases sensitivity to rattling. In recent years, that has led to the torsional vibration dampers having a key function in increasing the efficiency of the drivetrain, as they eventually enable the consumption potential of the engine or transmission to be exploited without significant loss of comfort. In the process, the vibration isolation itself must not be achieved through actual physical damping and thus through the dissipation of drive energy, but rather it must primarily be achieved through intermediate storage of the enormous energy spikes in rotating masses and springs. In the course of consumption optimisation and the increasing dynamic requirements of the turbocharged



Source: IHS 2013; University of Duisburg-Essen 2012

FIGURE 1 Development of drivetrain concepts worldwide up to 2030 (© Schaeffler)

engines, a further increase in the inertias was no option, meaning new solutions were required.

Schaeffler has therefore developed high-performance damping concepts based on rotational speed-adaptive damper systems in the form of centrifugal pendulum-type absorbers for use in dual-mass flywheels, clutch discs and torque converters with exceptional

damping properties. When used in torque converters, for example, it was possible to achieve consumption reductions of 3 % through the resulting decrease in lock-up speed [2].

But even with dampers, there are variable systems. For example, for engines with cylinder deactivation, centrifugal pendulum-type absorbers with different orders are used [3]. In the case of suit-

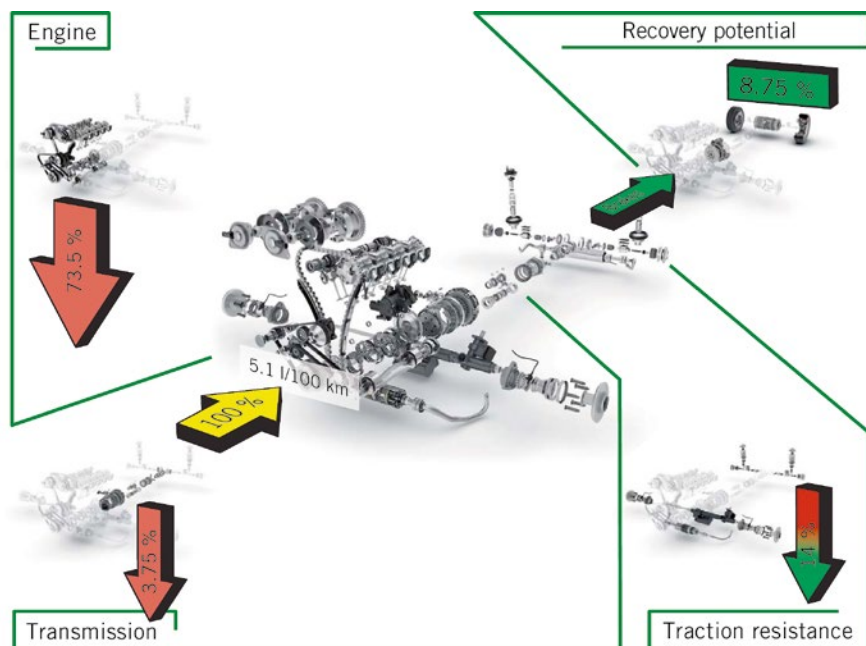


FIGURE 2 Energy balance for a C-segment vehicle with 1.0-l petrol engine in NEDC, acceleration resistance shown as recuperation potential (© Schaeffler)

able hybrid systems, the vibration isolation can be supported by strategies for active damping of the e-motor, **FIGURE 3**.

TRANSMISSION

Although significant progress has been made in transmissions over recent years through the growing use of automation, enhanced efficiency and the increase in usable ratio spread, Schaeffler is still working on optimising efficiency in this area:

- reduction in bearing friction, for example through suitable bearing concepts (fixed/floating bearings instead of preloaded bearing arrangements) or the use of rolling bearings instead of thrust washers on planet gears
- reduction in mounting space and weight, for example through the use of synchronisation units with integrated detents (each synchronisation unit results in an axial mounting space reduction of approximately 10 mm as well as a shifting travel reduction of 1.5 mm)
- development of NVH-optimised chain variators with high efficiency and high ratio spread for use in continuously variable transmissions (CVT)
- reduction of the average parasitic power of the electro-mechanical clutch and gearshift actuation for double

clutch transmissions in the NEDC to less than 20 W.

These actuator systems can also be used to actuate the clutch in manual transmissions. As well as enhanced comfort, these E-clutch systems enable to implement sailing strategies, which makes it possible to save more than 5 % fuel consumption, depending on the driving cycle [4]. In conclusion, the transmission can still be significantly improved in terms of efficiency, weight, mounting space, auxiliary energy requirements and operation point optimisation through adapted variability.

CHASSIS

Schaeffler is also working on measures towards increasing efficiency of chassis. Starting points exist in traction resistance and electrical power consumption for the actuating mechanism, which is necessary for intelligent chassis:

- reduction of bearing friction by more than 25 % through three-row ball bearings with a driving-situation-dependent bearing row load, as well as reduction of the seal friction by up to 50 % on wheel bearings through low-friction seals
- reduction of auxiliary energy for chassis actuation by implementing the power-on-demand concept; this

means electro-mechanical actuator systems used as anti-roll systems can replace the hydraulic systems currently in use.

Additional potential for chassis systems exists in aerodynamic measures like electro-mechanical ride height adjustment. In this concept, the vehicle can be lifted up or lowered via electro-mechanically actuated ball screw drives, depending on the driving condition. The reduction in aerodynamic drag enabled by this concept results in a potential fuel saving of 0.5 to 1.5 % in the NEDC, depending on the vehicle.

ELECTRIFICATION

The hybridisation of drivetrains offers considerable potential in addition to the above measures. It is estimated that by 2030, nearly half of all vehicles worldwide will have an electric motor as a drive source. Approximately 9 % of all vehicles are expected to be driven exclusively by an e-motor, **FIGURE 1**.

One of the key criteria in hybrid concepts is the arrangement of the e-motor in the drivetrain. In this area, Schaeffler is focusing on parallel hybrids. This arrangement of the e-motor builds on existing powertrain technologies. It requires only one e-motor and covers the widest spectrum of electrified drivetrain concepts, from mild hybrids to range extenders. It therefore offers a seamless transition to purely electric vehicles.

The maximum available voltage is a major factor when it comes to dimensioning the e-drive. In the course of the transition to the 48 V on-board net system, opportunities exist for mild hybridisation that would enable savings in fuel consumption of between 8 % and over 15 % in the NEDC, depending on the vehicle, concept and electrical power. In addition to components for belt alternator starter systems, Schaeffler is developing concepts for high-performance 48 V P2 hybrid modules in parallel and coaxial designs and even 48 V electric axle systems, which can be expanded on a modular basis into two-speed systems with torque vectoring [5].

Full efficiency, and thus full consumption reduction potential of well over 20 % in the NEDC and WLTC, can only be achieved by the hybrid systems with correspondingly powerful e-motors, and therefore with high-voltage systems. In

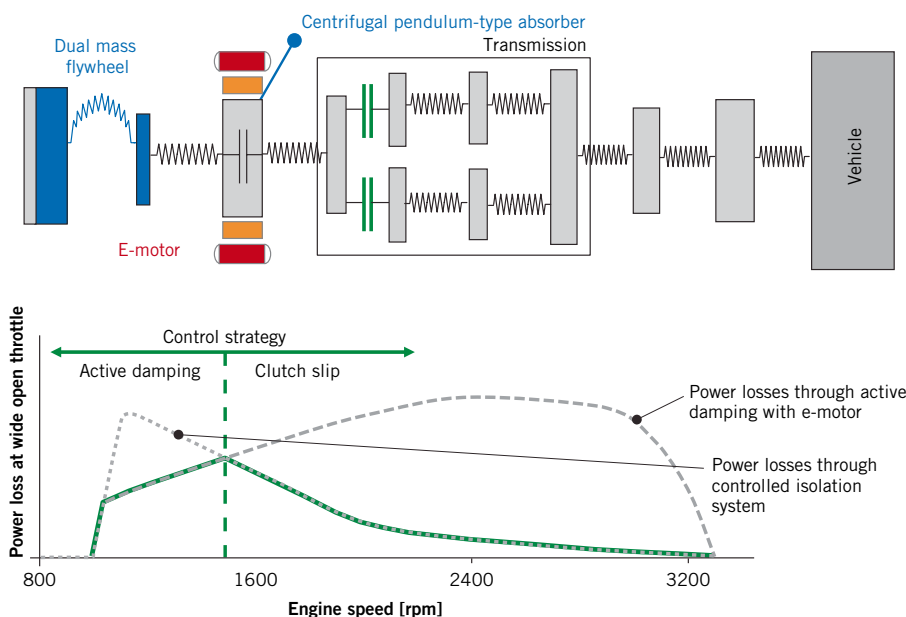


FIGURE 3 System optimisation through a combination of dual-mass flywheel, centrifugal pendulum-type absorber, active damping through the e-motor and controlled slip in the double clutch (© Schaeffler)

this area too, Schaeffler provides solutions for modular designs of hybrid modules and electric axle systems as well as electric wheel hub drives built into the wheel rims, **FIGURE 4**.

SYSTEMIC APPROACH

When considered in full, the above areas of potential to increase efficiency in the drivetrain for the individual assembly areas are strongly dependent on the cycle in which they are measured. In this regard, the WLTC (Worldwide Harmonised Light Duty Vehicle Test Cycle) in particular will lead to another significant change. In addition, practically all of these measures display strong interactions and multiple conflicting aims with regard to comfort, efficiency and harmful emissions. In determining a complete concept, the Total Cost of Ownership (TCO), which decides the purchase for the end customer, must be taken into consideration – the lower fuel costs resulting from one measure must be weighed up against the acquisition costs.

It is therefore clear that, in future, drivetrain technologies must be evaluated and defined at the drivetrain level, and not only at engine or transmission level. As a result, Schaeffler is increasingly evaluating technologies from this perspective. For example, when developing cylinder deactivation, the engine and transmission are regarded as a system,

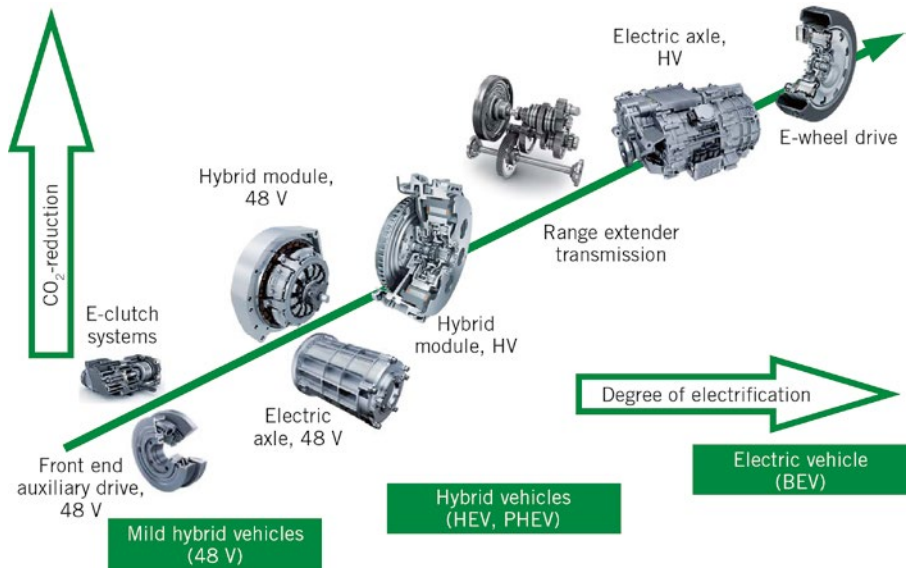


FIGURE 4 Modular solutions and system solutions for all areas of electrification (© Schaeffler)

so that solutions can be provided for a deactivation strategy with the corresponding damping technology [3, 6]. On hybrid or purely electric drives, transmission spread design and number of gears must be re-evaluated [7].

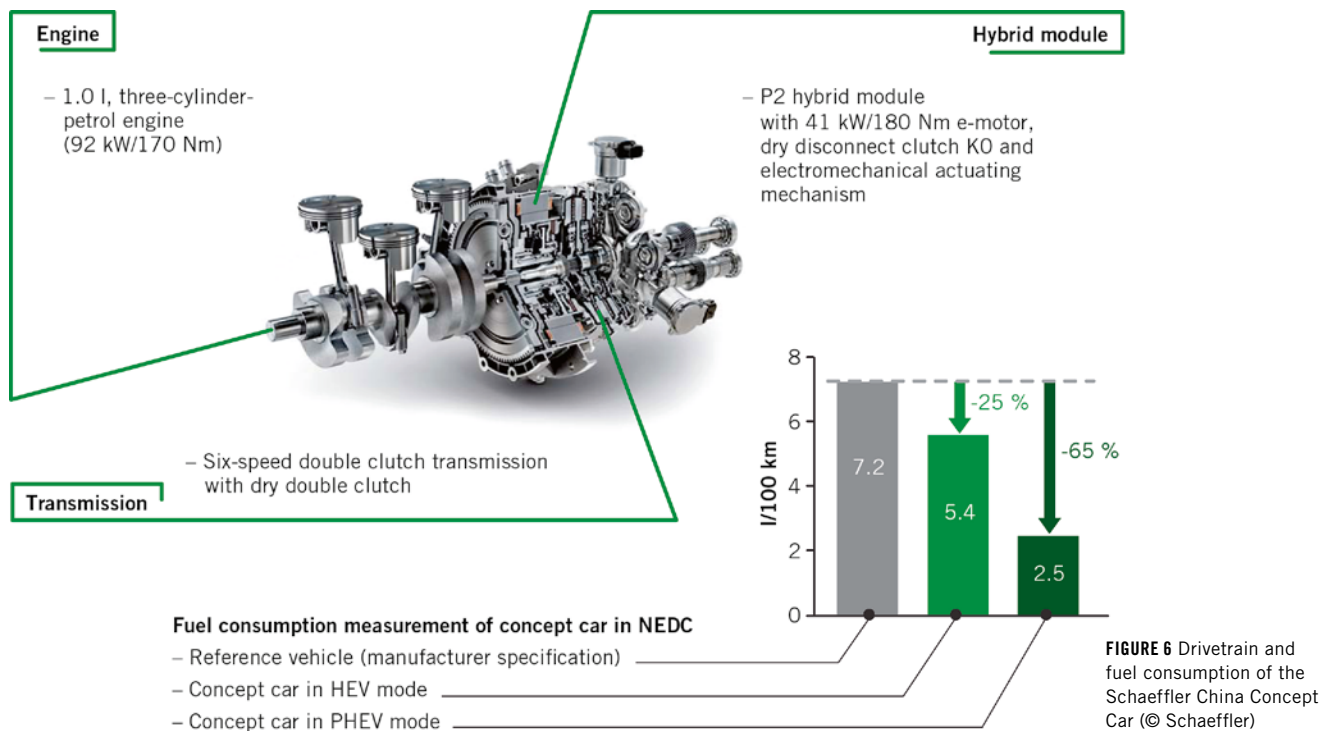
In addition, complete drive concepts are also simulated for the purpose of defining development strategies and evaluating components and subsystems in the drivetrain. For the drivetrain shown in **FIGURE 2**, consumption was reduced from 5.1 to 3.6 l/100 km by combining a mild 48 V P2 hybridisation

with the application of corresponding measures to the engine, transmission and chassis.

For the purpose of verifying the simulations, different concept cars are being constructed, **FIGURE 5**. These are often focused on specific markets and regions in their conception and design, such as the Efficient Future Mobility China Car. The drivetrain in this vehicle was completely converted to a 1-l petrol engine with a powerful Schaeffler high-voltage hybrid module and double clutch transmission with dry double clutch. This



FIGURE 5 Schaeffler concept cars (© Schaeffler)



means that in the chosen configuration, savings in consumption of up to 65 % can be achieved in the NEDC, with an electric range of approximately 30 km in plug-in mode, **FIGURE 6**.

SUMMARY AND OUTLOOK

In the coming years, the demand for reduced fuel consumption and emissions will be the dominant trend in drivetrains. Targets will increasingly be based on real driving emissions (RDE). Approaches to technical solutions are highly diverse and range from friction reduction to increased variability, electro-mobility and alternative fuels.

It must also be taken into account that when purchasing a car, customers are primarily concerned with the life cycle costs, and less so with environmental aspects. Although reduced consumption leads to lower running costs, this can eventually be cancelled out by the higher acquisition costs, depending on the development of oil prices [7]. Consequently, the cost factor will be a key differentiator in the selection of technological solutions.

Against the backdrop of these increasingly stringent requirements on the one hand, and increasing technical complexity on the other, it is no longer enough

for system providers to work at only one level above the system level of their own products. System suppliers must increasingly develop expertise on a drivetrain level. On top of the technical demands, methodical expansion of the development processes will also be necessary, for example regarding functional safety.

With the Mobility for Tomorrow strategy, Schaeffler has optimally positioned itself in recent years and will continue to develop these skills so that these complex demands can be met through expertise from systems down to the last detail.

REFERENCES

- [1] Scheidt, M.; Brands, C.; Kratzsch, M.; Günther, M.: Kombinierte Miller-Atkinson-Strategie für Downsizing-Konzepte [Combined Miller-Atkinson Strategy for Downsizing Concepts], International Engine Congress, Baden-Baden (Germany), 2014
- [2] Dorfschmid, J.; Döpper, W.; Jäggle, G.; Heukelbach, K.: Evolution zum Siebengang-Automatikgetriebe 7G-Tronic Plus [Evolution towards the 7G-Tronic Plus Seven-Speed Automatic Transmission], ATZ 112 (2010), No. 12, pp. 900-907
- [3] Faust, H.: Antriebsysteme der Zukunft – Motor-, Getriebe- und Dämpfersysteme für Downsizing, Downsizing und Zylinderabschaltung [Drivetrain Systems of the Future – Engine, Transmission and Damper Systems for Downsizing, Downsizing, and Cylinder Deactivation], 10th Schaeffler Symposium, Baden-Baden (Germany), 2014
- [4] Müller, N.; Strauß, S.; Tumbach, S.; Christ, A.: Segeln – Start/ Stopp-Systeme der nächsten Generation [Coasting – the Next Generation of Start-Stop Systems], MTZ 72 (2011), No. 9, pp. 644-649

- [5] Smetana, T.: Wer hat Angst vor 48 V? Der Minihybrid mit E-Achse nicht! [Who's Afraid of 48 V? Not the Mini-Hybrid with E-Axle!], 10th Schaeffler Symposium, Baden-Baden (Germany), 2014
- [6] Schamel, A.; Scheidt, M.; Weber, C.; Faust, H.: Zylinderabschaltung für aufgeladene 3-Zylinder-Motoren – machbar und sinnvoll? [Cylinder Deactivation for Charged Three-Cylinder Engines – Feasible and Sensible?], 36th International Vienna Motor Symposium (Austria), 2015
- [7] Gutzmer, P.: Die Zukunft des Motors kommt über das Getriebe [The Future of the Engine Lies in the Transmission], 36th International Vienna Motor Symposium (Austria), 2015
- [8] CO₂-Emissionsreduktion bei Pkw und leichten Nutzfahrzeugen nach 2020, Dienstleistungsprojekt 59/12 [Reduction of CO₂ Emissions from PCs and Light Commercial Vehicles beyond 2020], study commissioned by the Federal Ministry for Economic Affairs and Energy

THANKS

The authors would like to sincerely thank Tobias Eckl and Dr. Christian Gabriel, Schaeffler Technologies AG & Co. KG, for their support in developing the valuable contributions to this publication.



© Continental

AUTHORS



Dipl.-Ing. Friedrich Graf
is Director of Development,
Strategy & Technology, Technology &
Innovation at Continental Powertrain
in Regensburg (Germany).



Dipl.-Ing. Siegmund Deinhard
is Technology & Innovation Team
Leader at Continental Powertrain
in Regensburg (Germany).



Christian Bottke, M. Sc.
is Technology & Innovation System
Developer at Continental Powertrain
in Regensburg (Germany).



Dipl.-Ing. Stefan Grubwinkler
is Technology & Innovation System
Developer at Continental Powertrain
in Regensburg (Germany).



Connected Energy Management with a Backend-based Driving Strategy as an Example

A predictive operating strategy for the powertrain uses data about the surrounding area to allow for proactive action instead of a purely reactive control system. Using a 48 V mild hybrid demo vehicle as an example, Continental shows what saving effects are possible with Connected Energy Management (cEM) on a real route if sensed information about the surrounding area is kept constantly up to date by means of a backend connection.

EXTENDING THE ADVANTAGES OF A MILD HYBRID

Current strategies to minimise energy consumption successfully build on numerous parameters in the vehicle itself. To this end, the overall vehicle and its components are systematically further developed to ensure the greatest possible efficiency. Electrification in hybrid vehicles is one of these strategic steps. This makes driving strategies such as regenerative braking, coasting (decoupling and deactivating the internal combustion engine), eBoost (support from the electric motor for the internal combustion engine), load point shifting, and extended start/stop operation possible. For example, with a mild hybrid based on the 48 V Eco Drive [1], savings of between 8 % (cross-country driving only) and 21 % (in urban traffic) [2]

can be achieved, using an integration-friendly P0 architecture. This consumption saving forms part of the attractive cost-benefit ratio of the 48 V system. By means of predictive driving strategies, sensed information about the vehicle environment, and an online connection to a backend with dynamic map information, it can be used even more efficiently.

USE OF MAP DATA

Predictive driving strategies use static map data [3] that has already been introduced in series production [4] so that efficiency-enhancing hybrid functions can be used even more effectively. Restricting the efficiency of the predictive strategy constitutes the individual driving behaviour that leads to consumption fluctuations of up to 25 % in conventional vehicles [5]. In relevant situa-

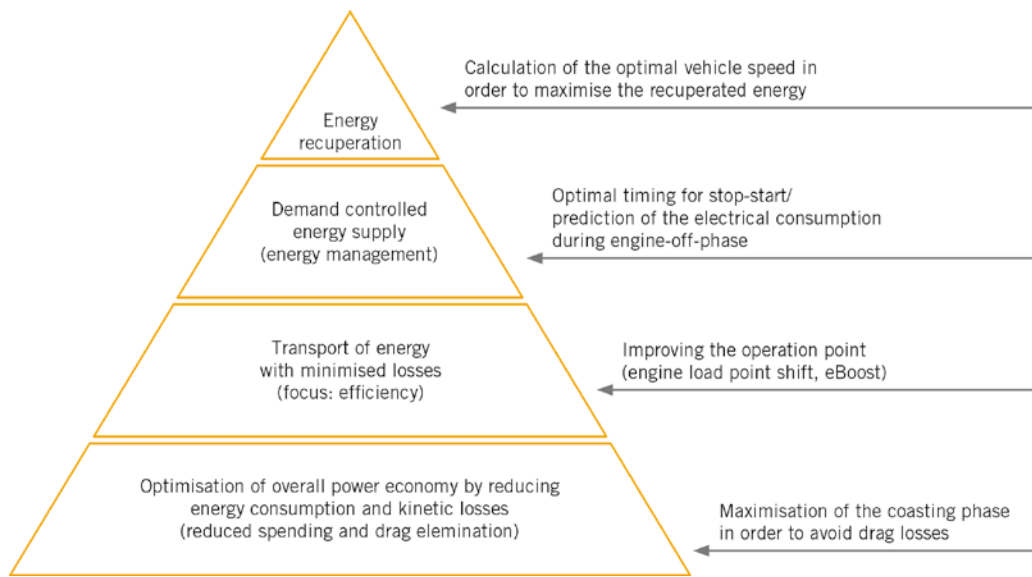


FIGURE 1 Methods to increase the CO₂ savings potential by means of intelligent energy management (© Continental)

tions, comprehensive energy management that not only activates the powertrain components optimally but also supports the driver in selecting an energy-optimum speed trajectory by means of a haptic pedal is therefore beneficial. Intelligent energy management thus reduces energy consumption by means of numerous methods, **FIGURE 1**.

In an initial step, energy consumption was reduced by 3 % during cross-country driving with the 48 V system by using static map information. For further, energy-based optimisation of the speed trajectory, up-to-date, dynamic route information is useful, particularly

for urban driving where conditions change rapidly. Suitable data is provided by means of a vehicle connection to the backend with the dynamic electronic horizon (eHorizon). This means that traffic signs, dynamic speed limits, expected traffic light phases, and current traffic data is available. To complement the dynamic map information, suitable sensors scan and record the area around the vehicle. **TABLE 1** shows the relationship between hybrid functionality, driving situation, and required information. Due to the interconnectivity within the vehicle and with the backend, Continental's cross-vehicle optimisation strategy

goes by the name of Connected Energy Management (cEM). To develop this energy management, the capabilities of the three Continental divisions Chassis & Safety, Interior, and Powertrain can be used at Continental, **FIGURE 2**.

MODE OF OPERATION AND INFLUENCE ON THE POWERTRAIN

In cEM, the expanded data basis of the dynamic eHorizon in conjunction with information about the surrounding area is used to determine an energy-optimum speed trajectory for consumption-relevant driving situations. This makes it

Driving situation	Longitudinal speed	Altitude	Hybrid functionalities								Radar	Required eHorizon information	
			eBoost	Engine load point shift	Coasting	Regenerative braking	Start-stop	SOC conditioning	Electric drive mode (P2-architecture)	Driver involvement (haptic pedal)			
Approaching traffic light, speed limit, slower vehicle ahead	↓	=			×	×	×	×		✓	✓	Dynamic, in real time	
Acceleration due to higher speed limit	↑	=	×	×					×	✓	✓	Dynamic, in real time	
Uphill, hold speed	=	↑	×	×					×			Static	
Downhill, hold speed	=	↓			×	×			×	✓		Static	
Creep mode, (low speed zone, stop and go in slow-moving traffic)	(Very low)	=							×	×	✓	✓	Dynamic, in real time

TABLE 1 Relationship between required information, hybrid function, and driving situation (© Continental)

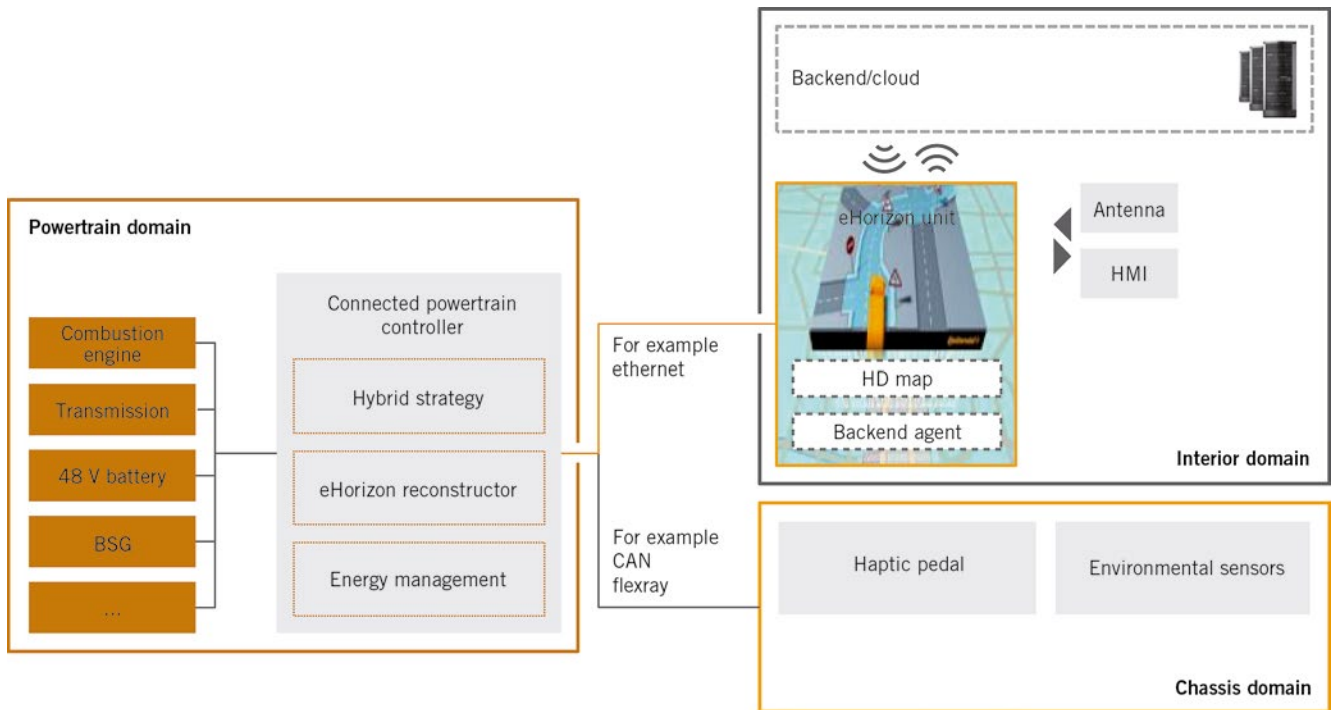


FIGURE 2 Interfaces of an exemplary system architecture (© Continental)

possible to extend the duration of coasting, switch off the internal combustion earlier, and to decelerate during braking phases in such a way that the entire deceleration energy can be used for regenerative braking. The driver feels a haptic signal on the active accelerator (accelerator force feedback pedal, AFFP). After the driver releases the accelerator, cEM initiates the energy-optimum driving profile for the upcoming driving situation. By pressing the accelerator or brake pedal, the driver can override the cEM's input at any time.

To estimate the savings potential of the cEM functions, the focus in the examination conducted is on deceleration phases that are of particular relevance to hybrid vehicles. As assistance

functions for these phases, the advanced driver assistance systems Smart Traffic Light Assist, Smart Curve Speed Assist, and Intelligent Deceleration Assist were initially developed and implemented in the demo vehicle.

CEM POTENTIAL ANALYSIS AND INITIAL FINDINGS

To analyse the energy saving potential, the additional consumption saving made by the cEM compared with the 48-V-Eco-Drive vehicle without cEM was to be calculated. In both cases, the analysis used a Golf VI 1.2 TSI with an automatic transmission. The belt starter generator (BSG) has a power output of between 6 kW (continuous power) and 10 kW

(temporary maximum power) [1]. The analysis used a constant 12 V on-board power supply load of 400 W as its basis.

To calculate the consumption saving, a typically urban driving cycle, 12.5 km in length, in Regensburg city (Regensburg City Cycle, RCC) was used, FIGURE 3. This RCC contains 4.1 km of city freeway (a maximum of 80 km/h), 7.1 km of urban traffic (a maximum of 50 km/h), and 1.3 km at a reduced maximum speed of 30 km/h. Within the selected driving cycle, relevant situations were identified in which an additional consumption saving is possible thanks to cEM by adjusting the speed trajectory. The individual situations were clustered depending on the traffic sign (traffic lights or speed limit), the speed at the start of

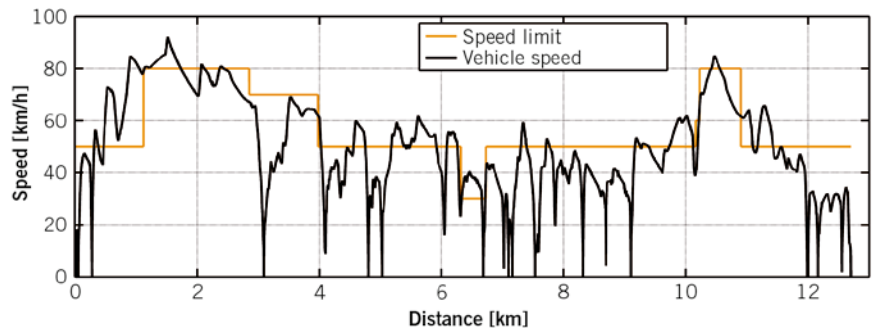
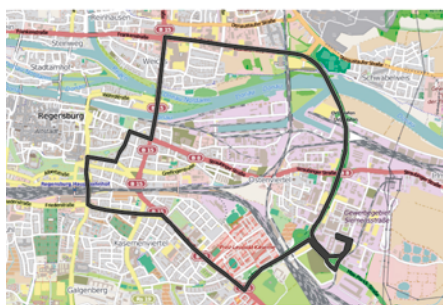


FIGURE 3 Calculation of the fuel saving with the Regensburg City Cycle (RCC) as an example (© Continental)

CO ₂ savings		Real driving	
		Driving cycle non-urban	Driving cycle urban (RCC)
48 V Eco Drive VW Golf VI 1.2 TSI	Basis system	-8.0 %	-21.0 %
	cEM with static eHorizon	-2.8 %	
	cEM with dynamic eHorizon		-0.7 %
			-2.7 %
Total CO₂ economy		-12.8 %	-24.4 %

TABLE 2 Consumption saving thanks to Connected Energy Management (© Continental)

deceleration, and the gradient. The initial value for the speed trajectory, which is adjusted by means of cEM, was determined for each clustered situation on the basis of 29 real RCC test drives with the basic 48 V system. The 29 real drives were also used to determine the expected probability that the situation would arise, for example the frequency of stopping at traffic lights.

By way of example for all situations, the effect of an anticipatory “intelligent” control system is shown by the Smart Traffic Light Assist while the vehicle is approaching a red light at vehicle speed of 50 km/h. The type and expected duration of the current traffic light’s colour are transmitted online by means of cEM. The stopping point at the traffic lights is necessary for an energy-optimum calculation of the speed trajectory. To estimate the potential, this study assumes that the distance from a possible vehicle in front is known thanks to the evaluation of radar information. The course of the gray curve in the schematic diagram in FIGURE 4 reflects the speed curve for the 48 V Eco Drive vehicle without cEM. The average deceleration during the braking

phase as well as the average duration of the coasting phase were calculated for the situation on the basis of the 29 test drives in fluent traffic conditions. The yellow line shows the change in driving strategy when cEM is used: deceleration is limited to maximise regenerative braking energy. In addition, the haptic pedal lengthens the coasting phase by acting on the driver in such a way that the internal combustion engine switches off earlier. When the coasting phase is extended, the fact that the driver accepts only certain lengthening of the coasting phase is taken into consideration. Since the vehicle is approaching a red light in this situation, the longer overall duration of coasting and regenerative braking of 4 s does not lead to an increase in total driving time. This also allows for comparability with the non-connective strategy without cEM.

The CO₂ saving for each situation was calculated using a validated simulation model, and the total CO₂ saving in the RCC was calculated using the expected frequency of occurrence. Depending on the type of deceleration situation, fuel savings of between 0.8 ml (stopping at

traffic lights from 35 km/h) and 6.3 ml (stopping at traffic lights from 70 km/h with a gradient of between -1 % and -2 %) were achieved in some cases. It is assumed that, in 25 % of cases, the driving trajectory calculated by means of cEM cannot be implemented as the traffic situation will not allow it or the area around the vehicle has not been completely scanned and recorded. This results in a total CO₂ reduction of 4.8 g/km for the RCC thanks to cEM. Given average consumption of the conventional 48 V system of 6.1 l/100 km, this corresponds to a further consumption saving of 3.4 %. Of this, 2.7 % can be attributed to the Smart Traffic Light Assist with dynamic map information and 0.7 % to the Intelligent Deceleration Assist in the case of static speed limits, TABLE 2.

SUMMARY AND OUTLOOK

Taking into consideration the dynamic eHorizon data, hybrid driving strategies can be used more effectively through energy-efficient adjustments to the deceleration trajectory. While calculations on the basis of the RCC were being made,

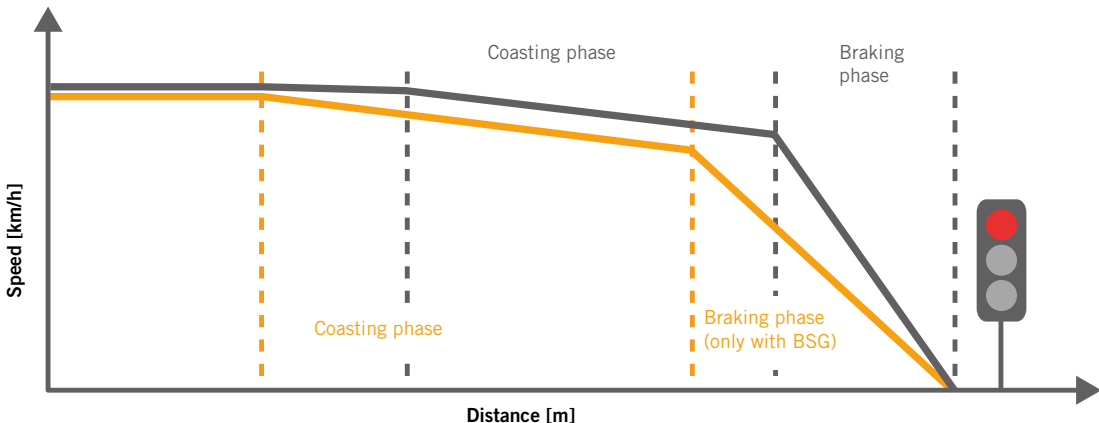


FIGURE 4 Adjustment of the speed trajectory during a deceleration phase (schematic) (© Continental)

cEM revealed potential of an additional 3.4 % fuel saving compared with the already very efficient 48 V Eco Drive demo vehicle. Particularly through the use of the dynamic eHorizon data, total energy consumption was once again reduced considerably with no change to the vehicle components. Particularly in urban traffic, dynamic and up-to-date data supplied by a backend can be used for this purpose. Connectivity can thus make a significant contribution toward reducing CO₂. These improved functions as a result can be achieved in all hybrids, even in vehicles with a conventional powertrain to lengthen the overrun fuel cut-off phases [6]. In light of the fact that the 48 V hybrid system is becoming very widespread, cEM offers an additional method for achieving challenging CO₂ targets in a cost-effective manner.

REFERENCES

- [1] Graf, F.; Knorr, T.; Jehle, M.; Huber, T.: Antriebsstrangmanagement in Hybridfahrzeugen mit 48-V-Bordnetz (Powertrain Management in Hybrid Vehicles with a 48 V On-Board Power Supply). In: MTZ 74 (2013), No. 9, pp. 658-662
- [2] VO X television: "auto mobil." Television program on November 6, 2014, at 5 p.m.
- [3] Raubitschek, C.; Schütze, N.; Kozlov, E.; Bäker, B.: Predictive Driving Strategies under Urban Conditions for Reducing Fuel Consumption based on Vehicle Environment Information, IEEE Forum on Integrated and Sustainable Transportation, Vienna, 2011
- [4] Handelsblatt: Gang runter vor der Kurve (Slowing Down Before Taking a Bend). Handelsblatt online, May 13, 2014
- [5] Dorrer, C.: Effizienzbestimmung von Fahrweisen und Fahrerassistenz zur Reduzierung des Kraftstoffverbrauchs unter Nutzung telematischer Informationen (Determining the Efficiency of Driving Styles and Advanced Driver Assistance Systems to Reduce Fuel Consumption Using Telematic Information). Stuttgart, University of Stuttgart, Dissertation, 2004
- [6] Dornieden, B.; Lutz, J.; Pascheka, P.: Vorausschauende Energieeffiziente Fahrzeuglängsregelung (Anticipatory Energy-Efficient Longitudinal Vehicle Control). In: ATZ 114 (2012), No. 3, pp. 230-235

Influencing Parameters in Emissions Measurement of Plug-in Hybrid Vehicles



© Horiba

The increasingly complex powertrains of hybrid vehicles pose new questions and sources of error. For example, the mass transport and the emission measurement accuracy can be affected if the vehicles use the electric motor during the driving cycle or the engine is switched off when idling. To avoid measurement errors Horiba has developed an alternative measurement method.

AUTHOR



Matthias Schröder
is Manager Emission Engineering
Global Product Planning Group
at the Horiba Europe GmbH
in Oberursel (Germany).

BACKGROUND

A Plug-in Hybrid Electric Vehicle (PHEV) uses an electric motor with an externally chargeable battery and a fuel operated internal combustion engine (ICE). The described investigations shall identify influences on standard measurement procedures and occurring deviations between real-world and test-site operations while testing PHEV's on a chassis

dynamometer. Challenging is the fact, that measurement accuracy is influenced by the continuous decreasing amount of exhaust emissions during driving cycles, since the high electrical range allows a Plug-In Hybrid Electric Vehicle to drive large parts of a cycle all electrical. Furthermore the feasibility to operate the engine at more efficient map points, to shut the engine down while the vehicle

stops and to charge the battery during deceleration, reduces the exhaust volume.

While testing Hybrid Electric Vehicles a particular phenomenon occurs: the exhaust emission mass transport from the transfer tube to the dilution tunnel continues during ICE-off phases. This phenomenon was observed with the measurement results from the diluted modal sampling system. The physical effect of this mass transport can be based on diffusion, natural convection or extraction. These three phenomena were investigated with the help of driving cycles and propane tracer tests. In order to reduce the emission measurement errors while testing PHEVs the measurement accuracy of the gas analyser can be increased or an alternative measurement procedure can be used. This article focuses on the investigation of an alternative procedure named "During Test Top Off" (DTTO). DTTO results will be compared to the conventional method regarding the New European Driving Cycle (NEDC).

TEST EQUIPMENT

For the test all PHEVs are driven on a four wheel drive (4WD) chassis dynamometer. The vehicle's tailpipe is connected to a heated transfer tube and the entire exhaust flow is diluted by the constant volume sampler (CVS) system (dilution tunnel), with critical flow ven-

turis (CFV) assuring a constant diluted exhaust flow, **FIGURE 1**. A sample of diluted exhaust is drawn into the bags for post-test analysis. The modal sampling lines, connected directly to the exhaust gas analyser system, allow modal diluted exhaust measurement during driving cycles. For the investigation of DTTO three two-way valves between the sampling-venturis and batches are used to switch according to ICE operation: When the combustion engine is operating the valves open to the bags, when the combustion engine stops the valves switch to the bypass where the sample is dismissed. Yet this entire system configuration is the same as a conventional CVS system. The two PHEVs used for this study are a Diesel parallel hybrid vehicle and an Otto range extender vehicle.

INVESTIGATION OF MASS TRANSPORT

Mass transport of exhaust emissions from the transfer tube into the dilution tunnel during ICE-off can be based on three physical processes. These are diffusion, natural-convection and extraction:

- Diffusion occurs due to the much higher CO₂ and pollutant emissions in the exhaust pipe and transfer tube compared to concentrations in the dilution tunnel.

- Natural convection means the difference of density which is caused by different temperatures and might cause an unforced gas flow through the transfer tube into the higher-mounted dilution tunnel.
- Extraction describes the mass transport caused by an external driving force such as pressure differences.

FIGURE 2 points out the process of natural convection for better understanding.

There are different approaches, how the three phenomena responsible for the mass transport could be detected. First there is a phenomenological based investigation during driving cycles. The effect of diffusion is insignificant since despite the high CO₂ concentrations in the transfer tube there is no more mass transport after a certain time following the first engine operation. The effect of natural convection appears to be higher than the one of diffusion due to the correlating oxy catalyst temperature and mass transport effect. With every engine operation phase during the test the temperature behind the oxy catalyst rises. The obviously high mass transport at the end suggests that the mass transport is not only influenced by natural convection but could also be by extraction since the CVS flow was increased during the test, **FIGURE 3**. The effect of extraction seems to be negligible since extraction hardly

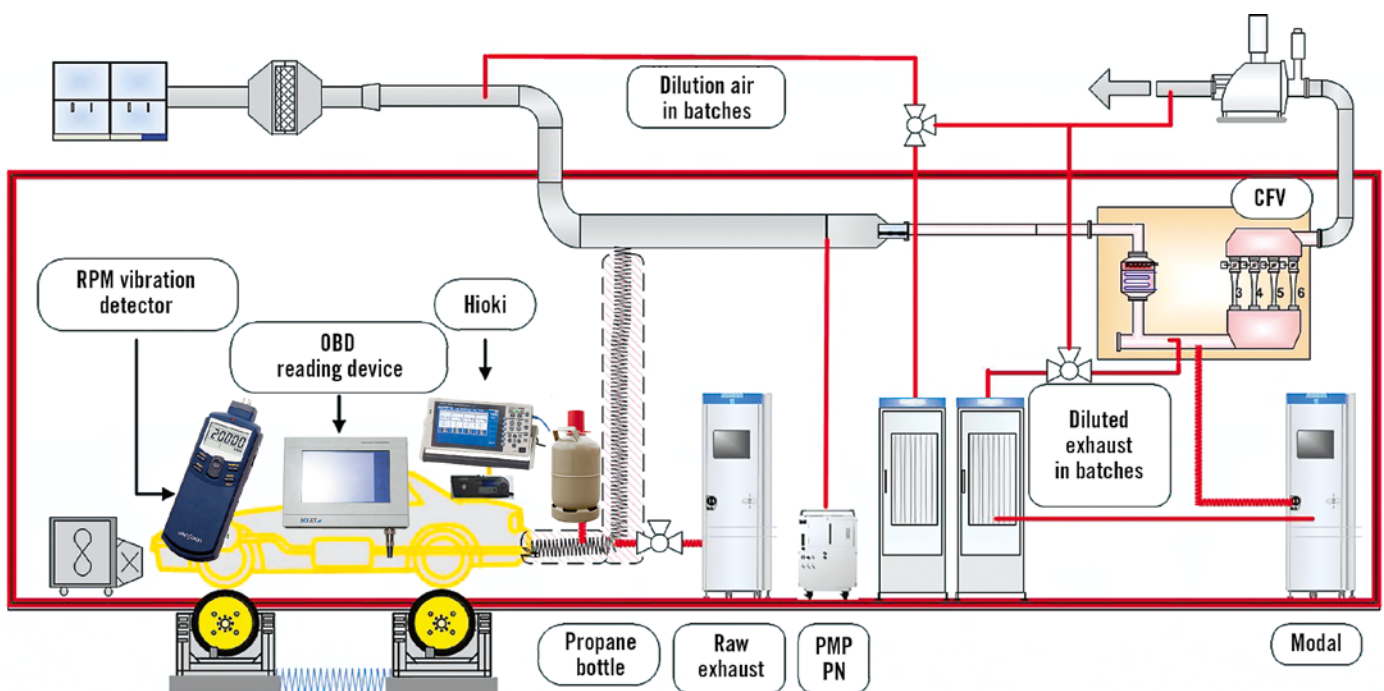


FIGURE 1 Exhaust measurement chassis dynamometer set-up (© Horiba)

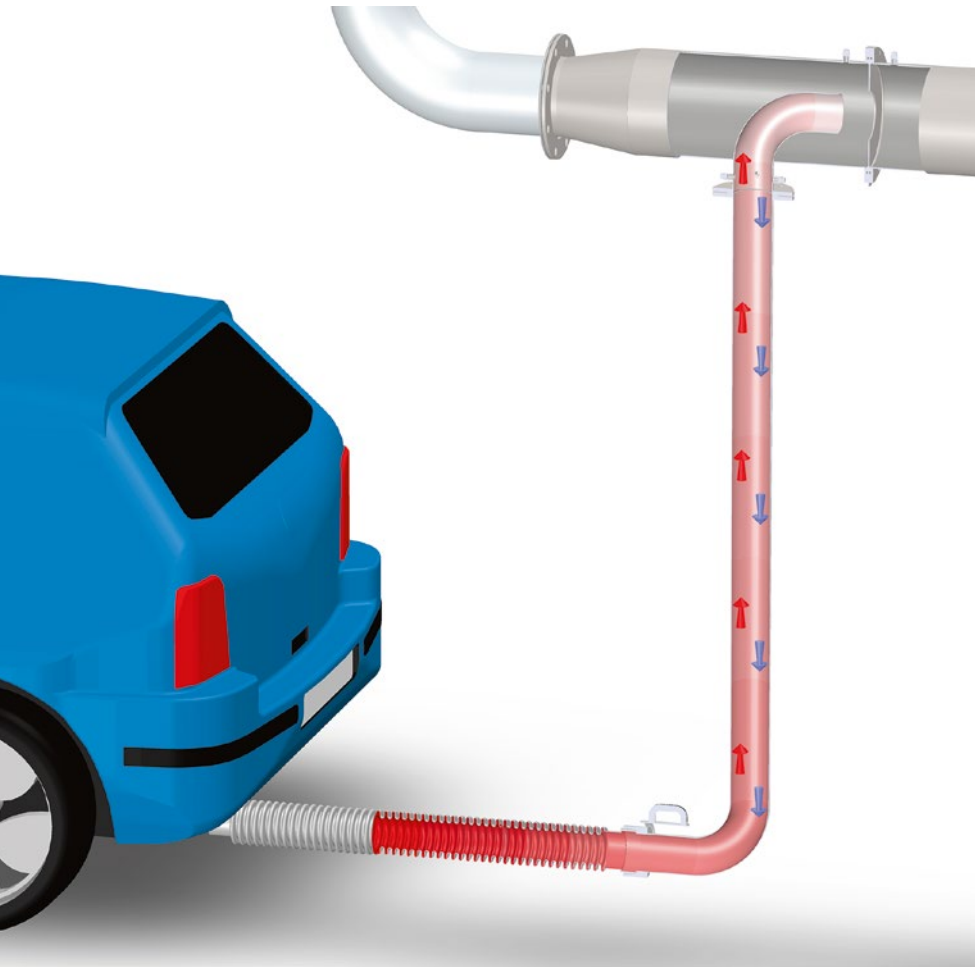


FIGURE 2 Illustration of natural convection in a transfer tube (© Horiba)

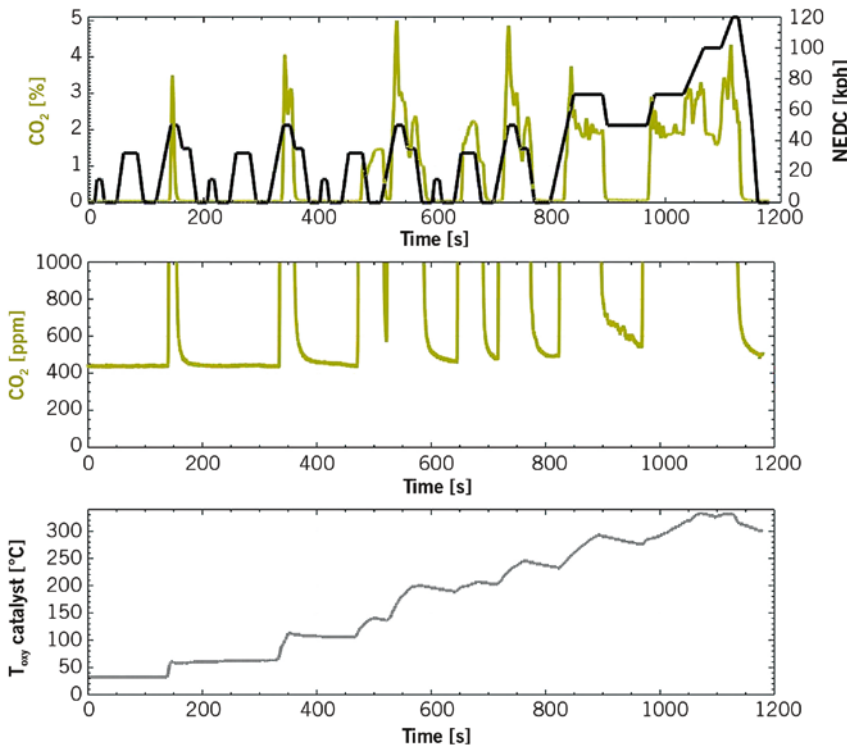


FIGURE 3 Mass transport analysis – observed CO₂ characteristics (© Horiba)

has an effect on mass transport from the beginning of the cycle up to the CVS flow change. Afterwards, due to higher tunnel underpressure, the influence of extraction on mass transport cannot be analysed. For further investigation propane tracer tests and catalyst cooling were performed.

INVESTIGATION OF MASS TRANSPORT WITH PROPANE GAS

To investigate the mass transport within the propane tracer tests the propane bottle was connected to the transfer tube close to the vehicle’s tailpipe. For all propane tests the Diesel-PHEV was placed on the chassis dynamometer with the transfer tube tightly connected to the tailpipe, without engine operation. For repeatability a small defined volume was filled with a defined pressure of propane and released into the transfer tube afterwards, FIGURE 4.

The first propane test was performed with an unheated transfer tube in order to investigate the effect of diffusion. When the transfer tube is disconnected from the tailpipe at the end of the test about 99 % propane is still left in the transfer tube and sucked into the dilution tunnel after the disconnection. This confirms the assumption from above: the influence of diffusion on mass transport is not significant.

For the second test the transfer tube and tailpipe were heated. 1000 s after this test started the transfer tube was disconnected in order to detect the remaining propane in the transfer tube for the investigation of natural convection with the result that most of the propane (85 %) was still left in the transfer tube, FIGURE 5.

To investigate the phenomenon of extraction an unheated transfer tube was used and the connection between the propane gas bottle and the transfer tube was opened. In the first half of the test the Total Hydro Carbons (THC) concentration raised roughly and it increased rapidly short after opening the gas bottle. About 1100 s into the driving cycle the concentration levelled out.

These propane tests prove that when the transfer tube is thoroughly connected to the tailpipe and not heated externally or internally – with exhaust gas – there is no significant mass transport.



FIGURE 4 Test set-up to investigate mass transport with propane gas (© Horiba)

INVESTIGATION OF CATALYST COOLING

Catalyst cooling particularly means the risk of catalyst temperature being cooled below the light-off temperature during a driving cycle, which can also be pushed artificial by test side conditions. Cooling can occur on basis of radiation and convection on the outside of the catalyst and from the inside due to a potential extraction of exhaust gas by the CVS underpres-

sure. If catalyst cooling during ICE-off phases occurs, the pollutant emissions can be increased with the next engine start until the catalyst temperature rises above the light-off temperature again. For the evaluation of catalyst cooling the measurement results from temperature sensors or the diluted modal measurement results, in particular the CO, THC and NO_x emissions have been investigated with no significant results regarding the three mass transport phenomena.

ALTERNATIVE MEASUREMENT PROCEDURE DTTO

The special operation of PHEV engines requires an alternative approach to the investigation of mass transport. During the measurement procedure DTTO, the exhaust gas and dilution air are only filled into the bags while operating the combustion engine and thus reduces high dilution factors due to mere dilu-

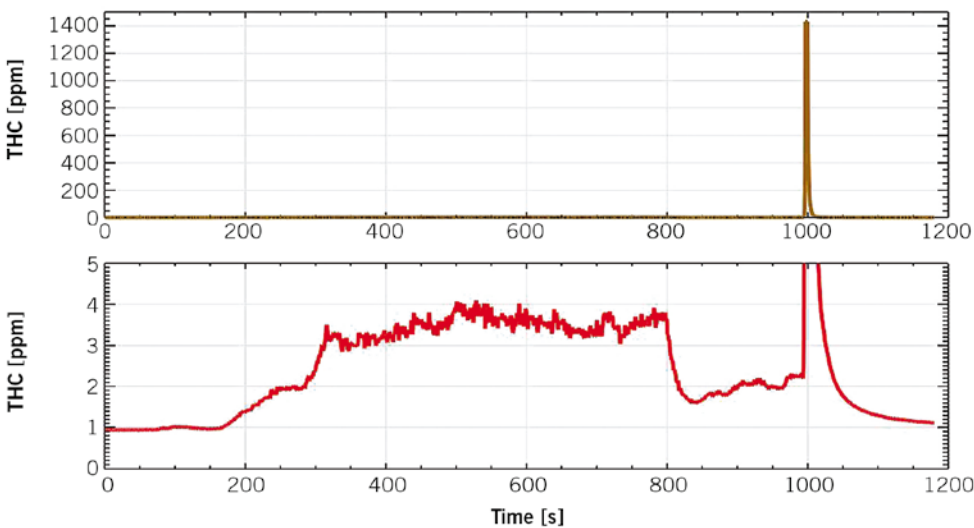


FIGURE 5 Propane test with heated transfer tube; investigation of natural convection (© Horiba)

	Urban exhaust gas batch		Extra-urban exhaust gas batch	
	DTTO	Conventional	DTTO	Conventional
Sample probe venturi flow [l/min]	6	6	13	12
Bag filling time [s]	400	780	269	400
Fuel consumption [l/100 km]	5.9	6.1	6.3	6.1
CO ₂ mass [g]	623	650	1178	1141
CO ₂ [ppm]	6140	3471	16,539	10,891
CO [ppm]	13.95	10.08	0.57	0.94
THC [ppm]	1.48	1.75	0.88	0.95
NO _x [ppm]	5.97	3.23	15.98	9.96

TABLE 1 Comparison of measurement data of DTTO and conventional procedure (© Horiba)

ent sampling. Considering minimum bag sampling time for a proper analysis volume, top-off sampling will be (re-) started approaching the end of each phase even without engine operation.

An Ono Sokki FT-7200 tachometer in combination with its vibration detector is attached on top of the engine to detect its operation. This value is the input for the automation system's decision of DTTO sampling phases. The CVS flows are manually chosen for both phases of the NEDC according to the expected maximum exhaust flows before the driving cycle. During each phase of a NEDC the size of the exhaust gas and dilution air sample venturis is chosen automatically by the system at first engine start to gain a maximised sample volume without exceeding the maximum batch volume on worst-case (no following engine shut-off).

When the combustion engine is not operating, the three two-way valves between the sample venturis and the batches switch to bypass the batches and the sample flows are dismissed. As soon as combustion engine operation is detected the valves switch again and the batches are filled with diluted exhaust gas and dilution air. The filling of the batches continues for 5 s after the ICE stops in order to sample the diluted exhaust gas delayed by the volume of the system piping.

If the minimum batch volume for an accurate analysis has not been reached close to the end of a sampling phase due to very few ICE operations, the three two-way valves open continuously to the batches. This continuous batch filling lasts until the end of the current phase.

Two separate, homologation compliant NEDCs were driven with the Diesel-PHEV, one applying DTTO and the other one using the conventional method. In both tests the state of charge (SOC) of the traction battery was logged during the test in order to verify that the vehicle operates similarly in both tests. Due to the preconditioning of the vehicle before each NEDC, the SOC of the traction battery was reproduced also resulting in the identical engine operation. The CVS flows in both tests and all phases were 9 m³/min.

TABLE 1 summarises the sample probe venturi flows, bag filling time, fuel consumption, CO₂ mass and CO₂, CO, THC and NO_x concentrations for the urban and extra-urban exhaust gas batches of the DTTO and the conventional method.

It is clear that in the exhaust batches the CO₂ concentrations are higher with the DTTO procedure than they are with the conventional procedure. The difference of measurement error accounts to 1.93 % and could be much higher with less engine operation.

Besides the advantage of decreased sensor errors analysing higher bag concentrations, the overall emission mass determination gains accuracy due to lower effective CVS volume multiplied with sensor readings – and its errors. This can also be interpreted as reaching a lower effective dilution factor without risking under-dilution during engine operation.

SUMMARY

First, the physical process of mass transport from the transfer tube into the CVS dilution tunnel during ICE-off phases

has been researched. From the investigation with driving cycles and propane tracer tests it was derived that mass transport based on natural convection will occur due to high exhaust gas temperatures. With rising exhaust and transfer tube temperatures the mass transport increases steadily.

Second, catalyst cooling, which means the risk of high pollutant emissions after long ICE-off phases, has been investigated with the help of a temperature sensor installed downstream of the oxy catalyst in the Diesel-PHEV. From examining pollutant emissions after ICE-off phases in driving cycles and a calculation of the worst case, it is clear, that catalyst cooling did not occur due to heat losses nor did it happen by CVS suction. However, catalyst position concerning air flow and valve-overlapping engine designs could be influencing factors.

Furthermore, during driving cycles it happens that Plug-in Hybrid Electric Vehicles drive the majority of the cycle pure electrical and therefore only few combustion-engine emissions are sampled in the diluted exhaust gas batches, with the rest being only diluent sampled. One investigated solution is an alternative measurement procedure where the dilution air and diluted exhaust gas batches are only filled when the combustion engine is operated. Moreover, bag volume is topped-off approaching the end of the phase for sufficient analysing volume but on the same time not increasing test length. The method increases the emission concentrations in the diluted exhaust gas batches.

3RD INTERNATIONAL ENGINE CONGRESS 2016

ENGINE TECHNOLOGY IN THE VEHICLE

WITH ACCOMPANYING TRADE EXHIBITION

23 and 24 February 2016
Baden-Baden | Germany

REGISTER NOW!

Passenger Car Engine Technology

Commercial Vehicle Engine Technology

(separately bookable)

Alternative Fuels and New Lubricants

(for passenger cars and commercial vehicles)

MEETING PLACE OF THE ENGINE COMMUNITY

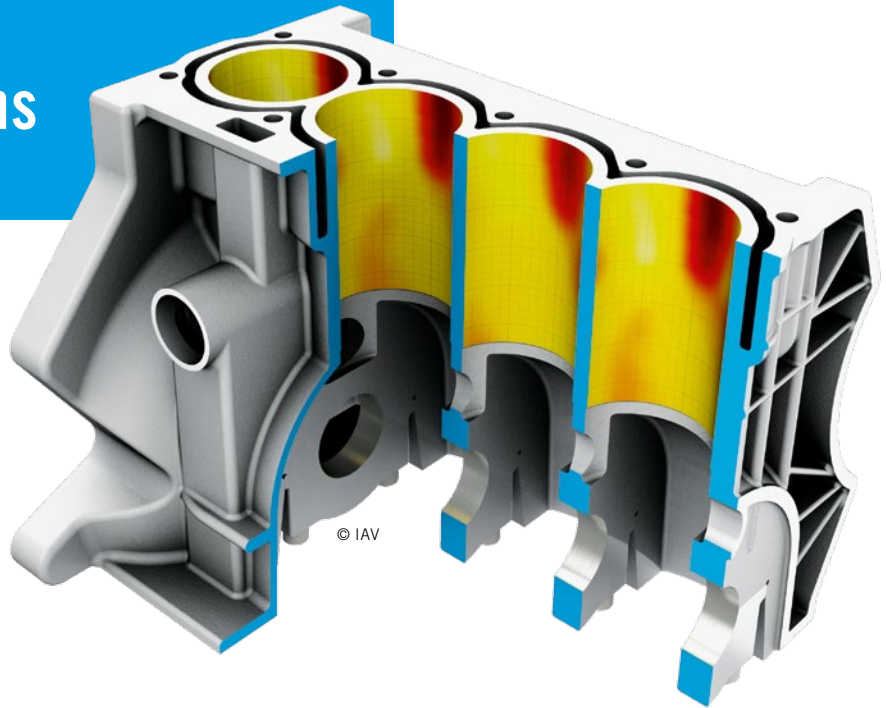
MAIN SUBJECT AREAS

Mechanical Components | Charge Exchange | Combustion |
Emission Concepts | Electrification | Commercial Vehicle Gas Engines |
NVH and Thermal Management



Modern Methods for Optimising Cylinder Distortions

Forthcoming RDE legislation will require a greater level of reliability in keeping emissions in check, also beyond the present driving cycles. As a result of higher demands on load and dynamics, phenomena such as oil input into the combustion chamber may also have a negative impact on emission behaviour. This will put an ever greater focus on the piston/cylinder system and on optimising cylinder distortions throughout the development process. The following paper examines the possibilities of using innovative IAV tools and methods to assist systematic steps targeted at reducing cylinder distortion.



ONLY SLIGHT CYLINDER DISTORTION IN TORQUED OPERATING STATE

Engine development activities are being driven forward primarily by the challenge of continuing to reduce CO₂ and exhaust emissions. At the same time, the measures that are needed to do this, such as downsizing, supercharging and mass reduction, are exposing all engine components to ever increasing strain. Under these boundary conditions, the tribologi-

cal systems of an engine are moving more and more into the focus of attention, with the piston/cylinder system being the most important one. It has the greatest influence on oil consumption and blow-by and, at approximately 30 %, accounts for the largest share of an engine's mechanical losses. It has a major impact on fuel consumption and exhaust gas emission.

In addition to many other factors, cylinder variance from the ideal shape also has a major influence on the operation of the piston/cylinder system. Reducing cylinder

AUTHORS



Dr.-Ing. Michael Berg
is Senior Vice President
Base Engine/Transmission,
Powertrain Development Division,
at the IAV GmbH in Chemnitz
(Germany).



Dr.-Ing. Hubert Schultheiß
is Technical Consultant in
Powertrain Tribology,
Powertrain Development Division,
at the IAV GmbH in Chemnitz
(Germany).



Dipl.-Ing. David Musch
is Design Engineer, Powertrain
Development Division,
at the IAV GmbH in Chemnitz
(Germany).



Dipl.-Wirt.-Inf. Thomas Hilbert
is Software and Database Developer,
Powertrain Development Division,
at the IAV GmbH in Chemnitz
(Germany).

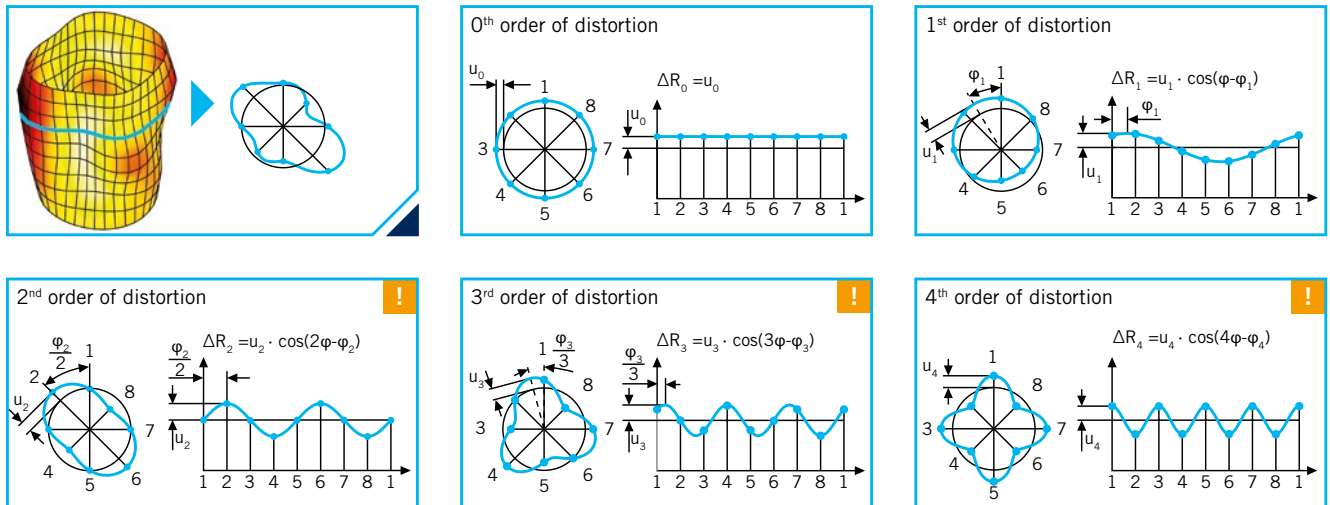


FIGURE 1 Analysing cylinder distortion order by means of Fourier decomposition (© IAV)

distortion is particularly promising from the aspect of optimisation: Whereas a compromise always needs to be found for other influencing parameters, reducing cylinder distortion has nothing but a positive influence on all target variables.

Apart from demands to guarantee problem-free engine assembly, cylinder distortion is of particular relevance to the way the piston/cylinder system works under real-life operating conditions. Above all, this is influenced by the torquing between cylinder crankcase and cylinder head and by thermal and dynamic stress induced on the cylinder crankcase while the engine is running.

Today, honing plates (torque plates) are often used to set this torqued state as early as the honing process so that after honing the cylinder crankcase exhibits no cylinder distortion when it is torqued with the cylinder head in a cold static state or, better still, in the warm operating state. The use of honing plates, however significantly increases the work involved in production. In the context of volume production, this means that the scope for plate honing is always limited. An innovative albeit equally time-consuming alternative is form honing in which geometric deviations are selectively introduced into the cylinder while honing by applying a complex process to control the honing tool. These deviations equate to the negative shape of the cylinder in the operating state and have the purpose of compensating for the distortions that occur during operation.

Consequently, this makes it all the more important to configure the cylinder crankcase as well as adjoining components, such as cylinder head and gasket, in a way that, wherever possible, only slight and non-critical cylinder distortions are produced in the torqued operating state.

BASIC THEORY

In evaluating cylinder distortions, it has generally proven worthwhile to look at the shape of each individual contour level of a cylinder and, by means of Fourier decomposition, divide them up in terms of individual distortion orders which are each characterised by amplitude and phase angle, **FIGURE 1**.

Many years of experience have shown that the amplitude size of the 2nd to 5th distortion order in particular has an influence on oil consumption, blow-by, friction and wear. Lower orders are less relevant as their distortions can easily be compensated for by the piston rings; in practice, the amplitudes of higher orders are so small that they usually have no notable influence on the functional system. In publications (e.g., [1]), various reference or limit values are given for the amplitudes of the 2nd to 5th order. These are mostly based on experience and empirical findings obtained from developing and analysing existing production engines.

Apart from these empirical values, analytical methods are also used which make it possible to determine the con-

formability of the piston rings to the real deviation in cylinder shape [2, 3]. These methods also provide order-specific limit values for each particular application case.

The limit values derived in this way show the distortions up to which the piston ring envisaged in each case can conform to the deformed cylinder contour without producing an excessive leakage gap between both bodies.

Today, analysing and displaying cylinder distortions is virtually inconceivable without complex software solutions. For this purpose, IAV uses a tool called IAV Engine::Analyzer which was developed in-house. Its “liner distortion” module provides functions for data processing as well as extensive methods of analysis, such as computing concentricity and cylindricity deviation, Fourier order analysis or evaluating the order-specific piston-ring conformability. The user is also provided with functions for offsetting datasets (e.g. difference between cold and warm, untorqued and torqued) and analysing piston ring conformability by FE simulation. Given the many capabilities of importing, filtering and comparing data, the tool IAV::Analyzer can be used at every stage of the development process chain for analyses and comparisons.

OPTIMISING CYLINDER DISTORTION IN THE ENGINE DEVELOPMENT PROCESS

Today, cylinder distortion plays an important part throughout the engine development process, **FIGURE 2**, from the concept

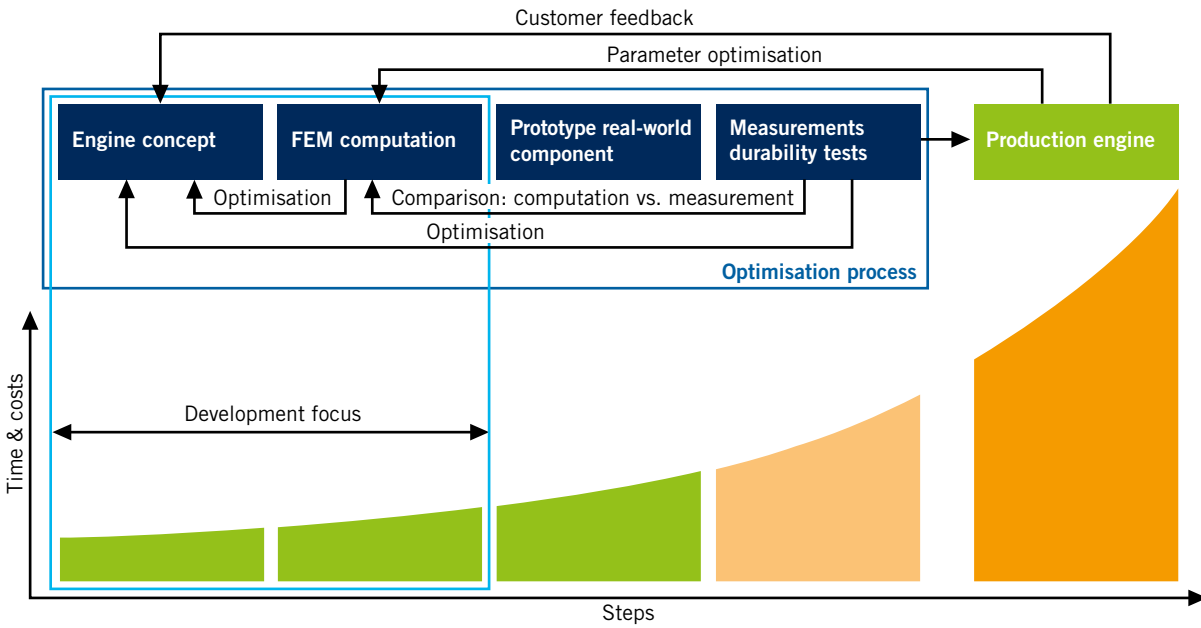


FIGURE 2 Engine development process (© IAV)



FIGURE 3 Influencing parameters and effects of cylinder distortion (© IAV)

phase, further detailed engineering, FEM computation, optimisation, measurements in engine testing to release for volume production and monitoring production [4]. In developing an engine, however, all-new designs are only rare. Frequently, existing designs are adapted to meet new requirements. In the remaining individual stages of the development process too, consideration must always be given to the influence of cylinder distortion.

The initial stages of development can only be geared towards the expected magnitude of cylinder distortion. However, once the first prototypes have been produced, evaluation is based not only on

the measured cylinder distortions but, in particular, on the parameters influenced by cylinder distortion, **FIGURE 3**. In most cases, exceeding a limit value for one of these parameters can be compensated for with other measures, although this often has drawbacks elsewhere. For optimisation to be effective, it is therefore important to channel the findings of engine investigations as quickly as possible into further optimising the design.

Costs and process time increase with every development step. For this reason, developing an engine should always focus on the initial stages of the process chain. Not only the components themselves, but also the FE mod-

els are continually optimised by subsequent measurements.

DESIGN MEASURES FOR OPTIMISING CYLINDER DISTORTIONS

Design parameters with a significant influence on the type and magnitude of cylinder distortion must be taken into consideration as early as the concept phase. In practice, the many possible influences, **FIGURE 3**, make this a complex task.

The main characteristic of cylinder distortion in an engine is determined by the material that is selected, by the method chosen for casting the cylinder

crankcase and by the ultimate basic design concept. For example, selecting the high-pressure die-casting method for reasons of economy limits choice to an open-deck design, producing relatively large cylinder distortions in the upper region of the cylinder.

The design of the cylinder crankcase, skirt design and, associated with this, the choice of bearing tunnel design in terms of individual bearing caps or bed-plate have a major influence on an engine block's stiffness. Usually, these decisions are made at the start of the development activity and leave hardly any room for changes later on in the process to scheduling, production technologies and assembly technologies.

Optimisations then chiefly take place in relation to the geometry of webs, the water jacket or the length and connection of the cylinder head bolts. In addition to this, an attempt can be made to reduce severely deformed areas by adding ribs or modifying wall thicknesses. It must be remembered here that the regions of a cylinder exposed to the highest loads need not necessarily show the greatest deviations in geometry.

FAST SIMULATION TOOL FOR OPTIMISING CYLINDER DISTORTIONS

Today, optimising cylinder distortion is hardly conceivable any more without computations. If these are only made at an advanced stage of the project and necessitate additional loops, major costs and high costs must be expected which

can put development stages at risk or threaten volume production launches. By assessing geometry early on, existing potentials can be exploited better and the development process can be speeded up and made more cost-effective. To do this, IAV has created a fast and straightforward simulation tool that is used by the designer as early as the concept phase. This simplified simulation has the aim of analysing a large number of variants and of identifying parameter sets that produce the desired result.

The key advantage lies in the speed with which modifications can be introduced into the simplified model and then evaluated because only one software tool is needed to cover the entire process. The results are sufficiently accurate in direct comparison with a complex computation (provided the level of design detailing is sufficient) and provide an early and reliable basis for reaching design decisions. It must be remembered that greater convergence with real-life component behaviour involves greater model detailing, which automatically lengthens computing time.

FIGURE 4 illustrates the process cycle. The basic dimensions of the crankcase being optimised are imported into a CAD control model, known as the "skeleton". From this, an assembly, which works fully parametrically within appropriate process limits, automatically regenerates a basic model – comprising cylinder crankcase with bearing caps and bolt connections as well as cylinder head with gasket and bolt connections. The dataset generated from this forms the

basic variant for FE analysis. After this first computation run, all changes are controlled by parameter modifications on the skeleton. Here, variants can be computed one after the other without any supervision.

This way, parameter fields with a large number of computed geometries are produced for specific boundary conditions. Result data can be imported into IAV::Analyzer and then easily processed and compared in a clearly structured manner. This provides the capability of evaluating influences on cylinder distortions and carrying out optimisations.

As a further advantage, this process can also be used for components that are already in volume production. Owing to the degree of data detailing with the methods used to date, a considerable amount of work is involved in entering the changes into a crankcase for just a few variants. With the approach pursued here, it is now only necessary to finish designing those variants with the greatest potential for detailed analysis. The best variants from the simplified simulation can then be channeled into the full-fledged CAD model and verified by means of a complex FE simulation.

COMPLEX SIMULATION OF CYLINDER DISTORTION UNDER REAL-LIFE OPERATING CONDITIONS

Apart from the detailed geometry, complex simulation also involves taking other input variables into account even more accurately than with the above-mentioned

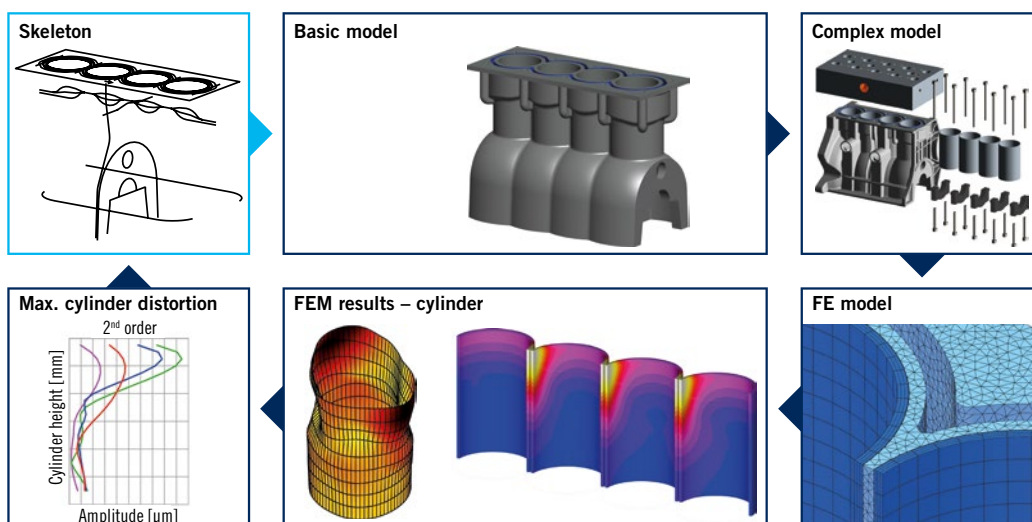


FIGURE 4 Process for optimising cylinder distortion (© IAV)

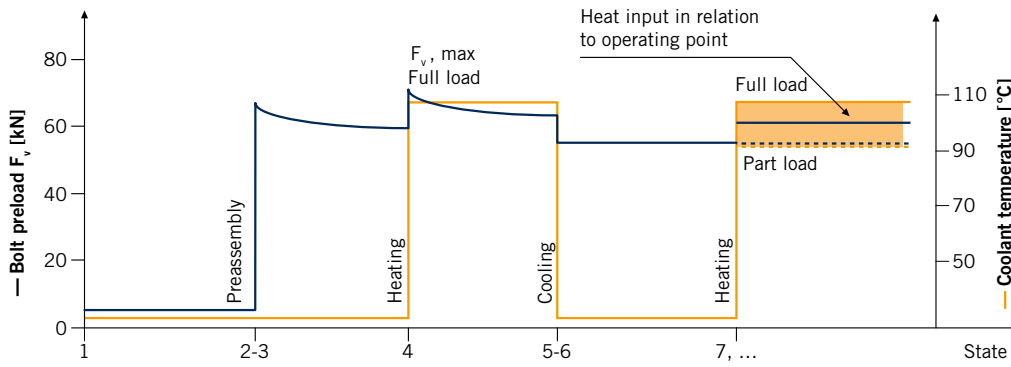


FIGURE 5 Complex distortion simulation: schematic diagram showing key influencing parameters (© IAV)

method. For example, these include bolt preloads, material properties, behaviour in the region of the cylinder head gasket, time-related temperature fields, the assembly process and engine “aging”. In most cases today, complex CFD simulations are carried out to take account of heat input on the combustion chamber side and heat transfer on the coolant side. **FIGURE 5** illustrates the impact of the load history on bolt preload force factored in. The factored-in reduction in bolt force is based on experience from statistically evaluating bolt force measurements. It is also possible to simulate residual bolt forces in engines with material data and with assumptions on material settlement

and creep behaviour. **FIGURE 5** shows that distortion simulations are not only carried out for the nominal output point but also for other operating points. In the subsequent computations of blow-by and oil consumption, this means it is not only possible to take into account the real-life combustion pressures and temperatures but also the distortions occurring at a specific operating point.

MEASUREMENT OF CYLINDER DISTORTION DURING FIRED ENGINE OPERATION

In most cases, only the cold static torquing state has been used in the past

to evaluate the design of cylinder crank-cases. Reproducing and analysing the influence of thermal and dynamic stress on cylinder distortion has only been possible with major effort and therefore often neglected.

As a result of constantly rising demands and better computation capabilities, cylinder distortions are also being computed in a warm operating state, producing the necessity to verify the results of this simulation.

Using a measuring method developed by IAV and already tried out on gasoline and diesel engines, cylinder distortions can be sensed in a fired combustion engine with a high level of accuracy.

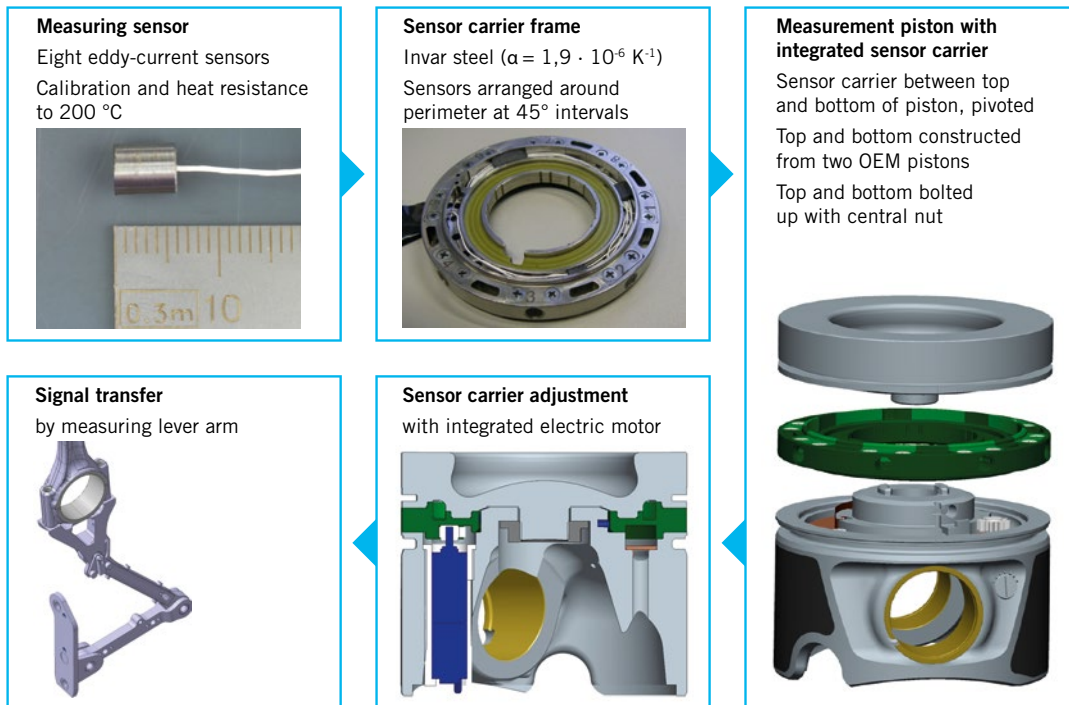


FIGURE 6 Measurement piston for measuring cylinder distortion during fired engine operation (© IAV)

The contour of the cylinder liner is measured directly from the piston. The piston is a special measurement piston with integrated sensor carrier frame. The eight eddy-current sensors used for measurement are staggered at 45° intervals around the perimeter of the sensor carrier which is positioned at the level of the second piston ring, **FIGURE 6**.

The sensor carrier can be rotated by an electric motor integrated in the measurement piston and a specially developed adjustment and positioning facility while the engine is running. As a result, the same points on the cylinder surface are measured by different sensors in direct succession. This makes it possible to determine any sensor errors in relation to each other and allow for these in evaluation.

While the engine is running, the lifting movement of the piston measures the entire part of the cylinder liner relevant to the function of the piston rings. The data measured are transferred by cable from the oscillating piston to the static crankcase via a lever arm. On integrating the measuring equipment into the engine, it is important to make sure that the cylinder crankcase and all other relevant components remain largely unchanged so as not to influence the cylinder distortions that occur. The data measured are evaluated using a special mathematical method [5] which has been integrated into the IAV::Analyzer evaluation tool.

Besides identifying and allowing for sensor errors, the key advantages of the new method also include compensating for sensor failure without any notable loss of accuracy as well as the ability to meas-

ure at intermediate positions as the sensor carrier turns. These advantages make IAV's method far superior to other measuring techniques in terms of resolution, measuring accuracy and reproducibility. It was possible to prove that variance between several measurements is less than $\pm 1 \mu\text{m}$ under identical testing conditions. Measurement results are delivered in a previously unattained quality and provide an excellent basis for validating simulation results.

FE-MODEL-BASED ANALYSIS OF PISTON-RING CONFORMABILITY

Evaluating the ability of piston rings to conform to a distorted liner has so far been based primarily on equations for approximating order-specific conformability in accordance with Goetze or Dunaevsky. These deliver limit values for the maximum permissible amplitudes of individual distortion orders. In comparing these approaches, major differences are in some cases revealed in the permissible limit values. These methods also only evaluate Fourier orders on their own. They make no allowance for any superimposing of these orders or their angular position. These effects, however, are important in obtaining information of the greatest possible accuracy on conformability or on critical areas, and consequently also in defining specific measures for optimising cylinder distortion.

Therefore, IAV has developed a calculation method based on an FE model. Piston-ring modelling uses Bernoulli beam elements which are pressed against the

distortion profile with a linear load. Computation is done quasi-statically at contour levels which are analysed individually.

The IAV::Analyzer tool supports multiple-core processors which means it can quickly deliver a large number of results and parameters. The high computing speed of each computation also permits interactive parameter studies. The results are presented in diagrams as well as in a 3-D model, **FIGURE 7**. Computation delivers results, such as gap width, area and volume, bending energy as well as the stress of the piston ring. It is also possible to determine the contact frequencies between piston ring and liner around the circumference or the energy-related preferred position of the ring gap at each contour level. Studies of characteristic gap areas and gap volumes in relation to individually analysed Fourier amplitudes have shown that results of IAV's new methodology and the computations to Goetze and Dunaevsky deliver limit values of an equal order of magnitude for these simple cases.

However, the new approach focuses on analysis based on real-life deformation, **FIGURE 8**, with superimposed Fourier orders. This method is very accurate in locating those regions of the cylinder in which the piston ring cannot sufficiently conform to the cylinder surface, **FIGURE 9**. From this, it is possible to derive appropriate measures for optimising cylinder distortions and the entire piston ring/cylinder system. In further research work, IAV will analyse the correlation of conformability, friction loss, blow-by as well as oil emissions measured online and on a cylinder-selective basis in order to enhance the accuracy and relevance of the new method and limit values.

SUMMARY AND OUTLOOK

This article describes the interaction of specialists from the areas of design, simulation, measurement engineering and mechanical testing with a view to solving a very complex task in a targeted and fast way. A particular focus was placed on validating the different approaches. To this end, a unique process was used for precision-measuring of the cylinder shape during engine operation. The sealing capacity of the piston ring/cylinder contact was derived from the real-life cylinder form and the elastic behaviour of the rings, providing

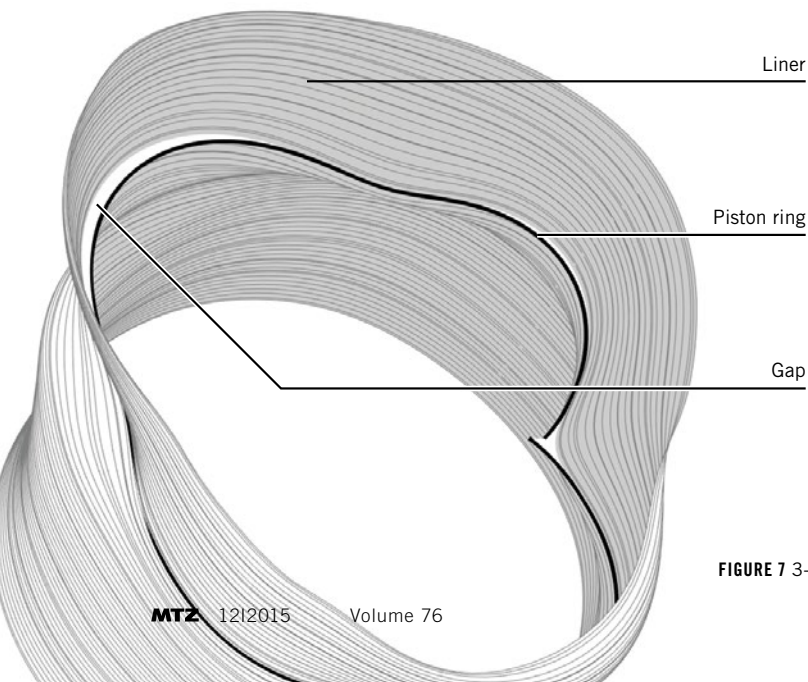
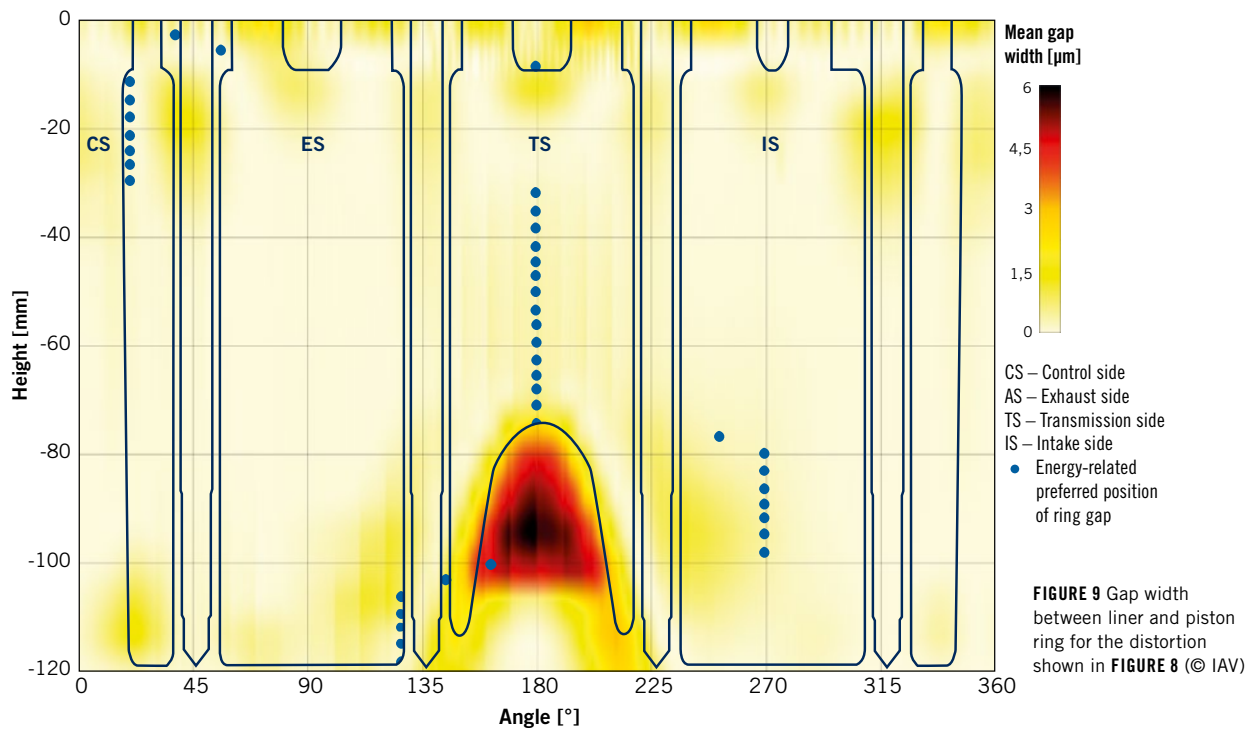
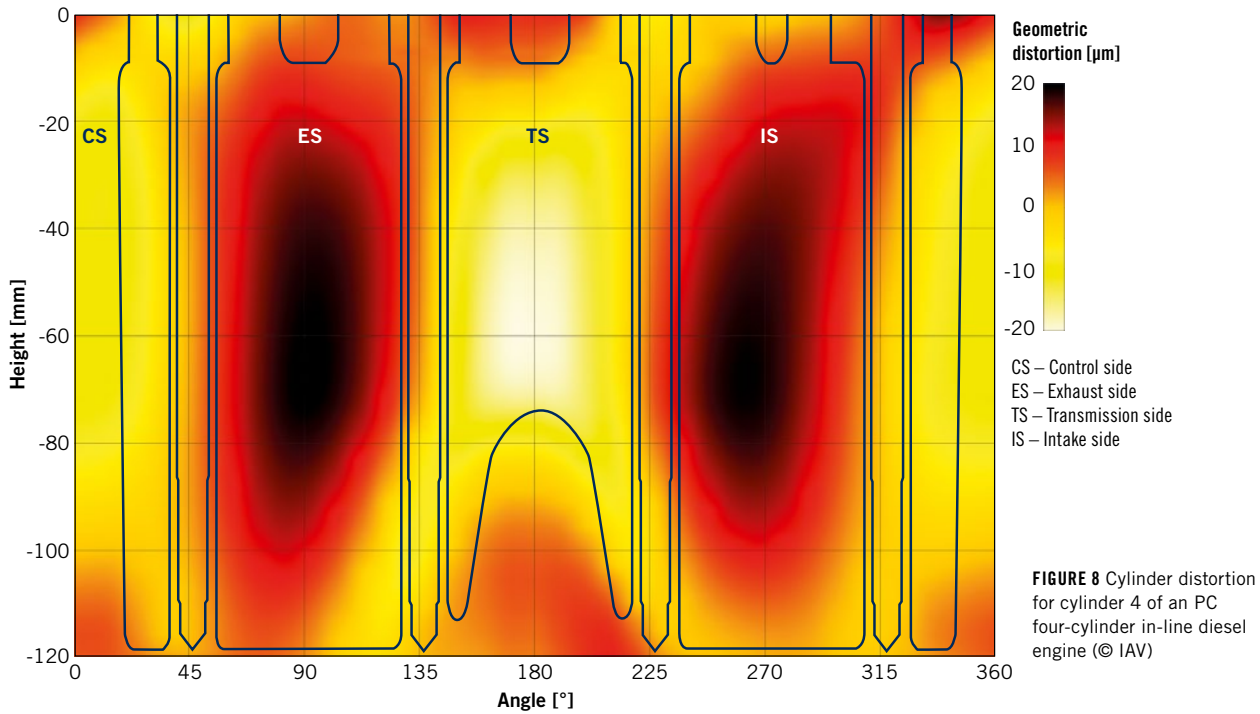


FIGURE 7 3-D model (© IAV)



much more accurate information than established approaches. This offers the basis for a systematic optimisation of the system. Further work serves the purpose of validating and enhancing the informative value of the new method and deriving limit values in order to meet defined target values for friction,

oil emission and blow-by with less development input.

REFERENCES

- [1] Küntscher, V.; Hoffmann, W. (publisher): Kraftfahrzeugmotoren. Auslegung und Konstruktion. Vogel publishing, 2006
- [2] Goetze AG (publisher): Piston Ring Manual. Burscheid, 1989

- [3] Dunaevsky, V.: Analysis of distortions of cylinder and conformability of piston rings. In: Tribology Transactions 33 (1990), No. 1, pp. 33-40

- [4] Schultheiß, H.; Musch, D.; Hilbert, T.: Optimierung von Zylinderverzügen im Rahmen des Motorenentwicklungsprozesses. VDI report 2230, 2014
- [5] Busse, T.; Schultheiß, H.: Patent application DE 10 2004 057 462.6: Verfahren zur Auswertung von Messdaten. IAV GmbH, Chemnitz, 2004

ATZ live

Spotlight on Powertrain and Vehicle Engineering.



ATZlive Conferences for Vehicle and Engine Specialists

- G** **DER ANTRIEB VON MORGEN**
MTZ-Fachtagung
- INTERNATIONAL ENGINE CONGRESS**
Engine Technology in the Vehicle
- DRIVER ASSISTANCE SYSTEMS**
International ATZ Conference
- G** **KAROSSERIEBAUTAGE HAMBURG**
ATZ-Fachtagung
- CHASSIS.TECH PLUS**
International Munich Chassis Symposium
- G** **VPC – SIMULATION UND TEST**
MTZ-Fachtagung
- G** **LADUNGSWECHSEL IM VERBRENNUNGSMOTOR**
MTZ-Fachtagung
- G** **WERKSTOFFTECHNIK IM AUTOMOBILBAU**
ATZ-Fachtagung
- HEAVY-DUTY, ON- AND OFF-HIGHWAY ENGINES**
International MTZ Conference
- AUTOMOTIVE ACOUSTICS CONFERENCE**
International ATZ Conference
- G** **REIBUNGSMINIMIERUNG IM ANTRIEBSSTRANG**
ATZ-Fachtagung

/// CONFERENCES MARKED WITH A **G** WILL BE HELD IN GERMAN

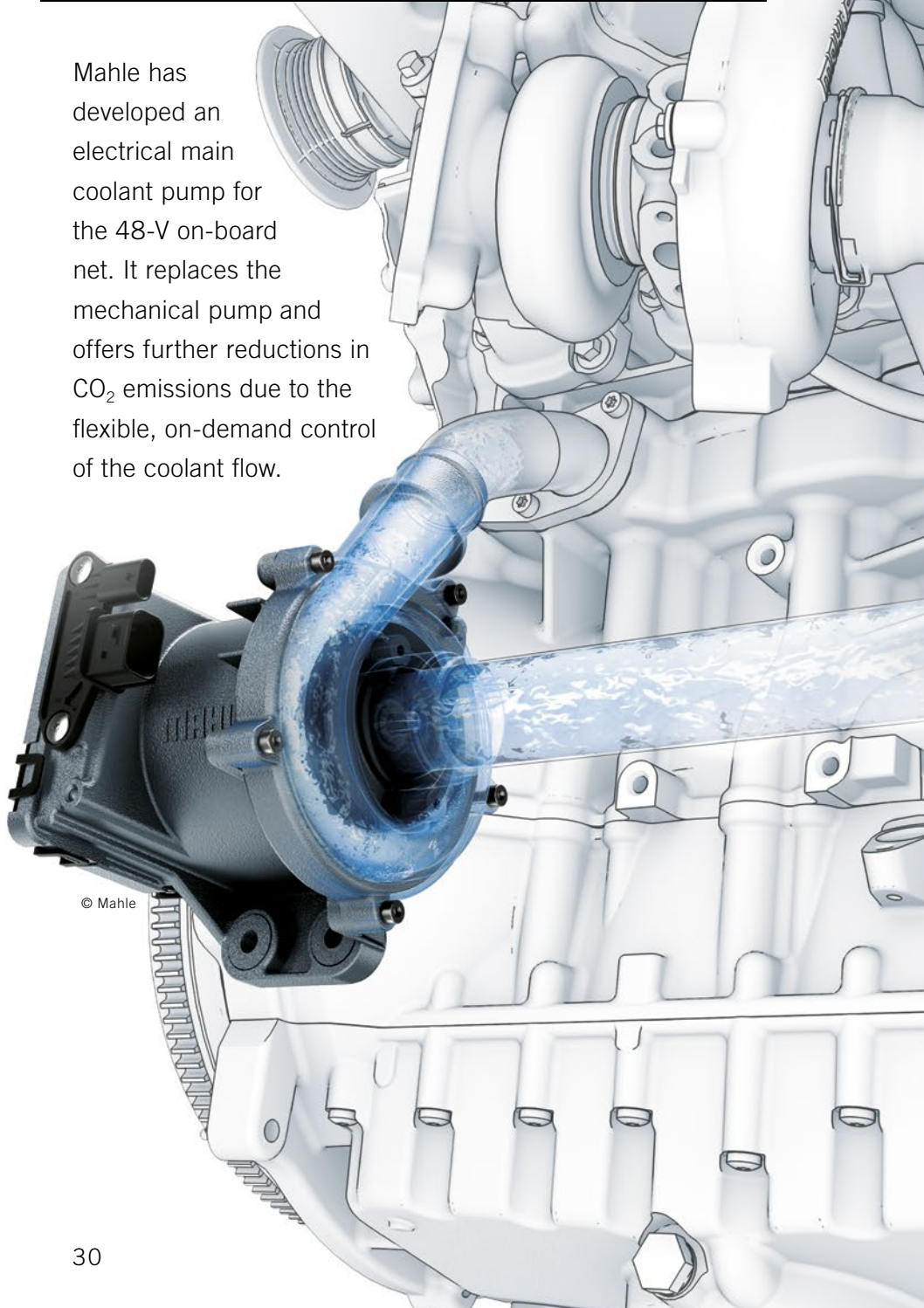
ATZ live
Abraham-Lincoln-Straße 46
65189 Wiesbaden | Germany

Phone +49 611 7878 131
Fax +49 611 7878 452
ATZlive@springer.com

PROGRAM AND REGISTRATION
www.ATZlive.de

Electrical 48-V Main Coolant Pump to Reduce CO₂ Emissions

Mahle has developed an electrical main coolant pump for the 48-V on-board net. It replaces the mechanical pump and offers further reductions in CO₂ emissions due to the flexible, on-demand control of the coolant flow.



© Mahle

AUTHORS



Karl-Martin Fritsch
is Development Engineer in
Corporate Advanced Engineering
of the Mahle International GmbH
in Stuttgart (Germany).



Stephan Weber
is Development Engineer in
Corporate Advanced
Engineering of the Mahle
International GmbH
in Stuttgart (Germany).



Michael Krappel
is Project Leader in
Corporate Advanced
Engineering of the Mahle
International GmbH
in Stuttgart (Germany).



Dr. Alfred Elsäber
is Head of Testing in Corporate
Advanced Engineering of the
Mahle International GmbH
in Stuttgart (Germany).

REDUCING CO₂ EMISSIONS WITH ELECTRICAL AUXILIARY COMPONENTS

As a result of the trend toward reducing CO₂ emissions caused by traffic, it becomes increasingly crucial to hybridise or electrify vehicle powertrains. According to statutory requirements, a reduction of CO₂ output to 95 g/km should already be implemented by the year 2020. This is applicable not only to Europe, as the future targets in other regions of the world are also below 100 g/km. In order to reach these levels, it is necessary to implement new drive concepts and to continuously rethink existing concepts. One possibility lies in the electrification of auxiliaries in motor vehicles. By operating on demand, this results in consumption savings. Thanks to the electrification of the oil, power steering, and coolant pumps as well as the radiator fan, these can be decoupled from the engine speed. By decoupling these components, it is possible to control their power consumption according to their requirements. **FIGURE 1** shows the schematic diagram of a coolant circuit and its components.

For the application shown here for the electrical main coolant pump, a concrete benefit emerges in that the cooling performance can be adapted to the operating point by means of the volume flow at a particular coolant temperature. **FIGURE 2** (left) shows a simulation of operation in the New European Driving Cycle (NEDC). When the cooling requirement is low, the coolant pump is run variably at a minimal speed. Switching it off entirely and thus saving additional drive energy brings additional consumption savings, especially because the engine compo-

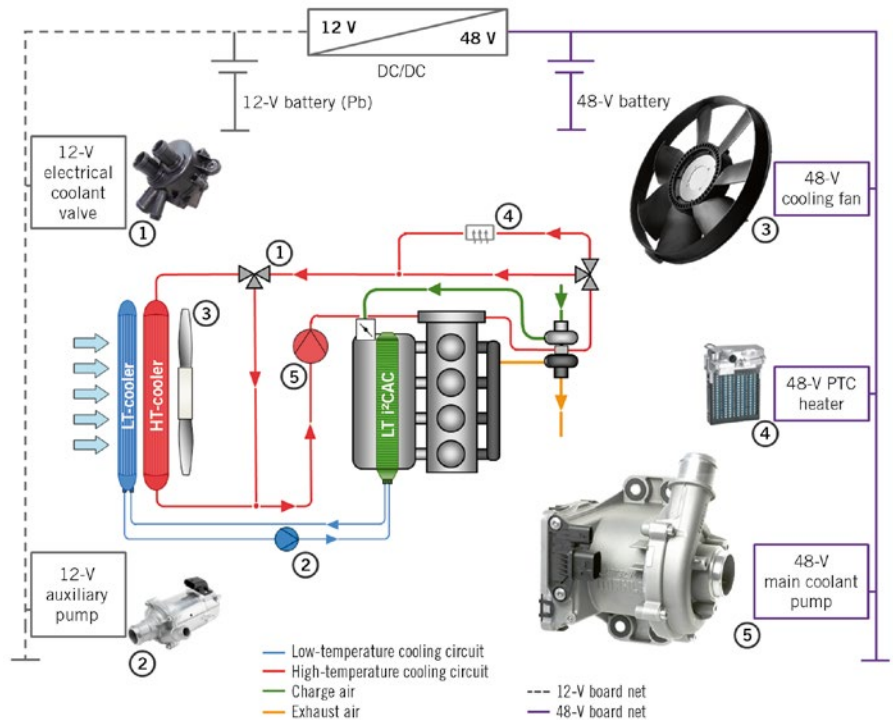


FIGURE 1 Cooling circuit with potential 12- and 48-V technologies: electrical coolant pump, radiator fan, electric heater, and electric coolant valve (e-valve) (© Mahle)

nents heat up more quickly during warm-up. For this simulation, only the fuel consumption-relevant vehicle components were represented: the combustion engine with transmission, the driving resistances, the cooling system at ambient temperature, and the vehicle speed. Previous simulations show a reduction in CO₂ emissions by 1.8 g/km in comparison with a switchable mechanical coolant pump. [1] When compared with a non-switchable mechanical pump, this can even result in potential fuel savings of 3 to 5 % [2]. This is dependent on the use of intelligent thermal management functions in the cooling circuit.

At high ambient temperatures or under high loads, the cooling performance is increased by applying the maximum pump speed, thus ensuring maximum protection of the engine components. By adding a postcooling phase, this can take place when the engine is stopped as well. Additional electrical auxiliary pumps used to this end are thus no longer needed. Depending on the power density of the combustion engine, hydraulic pump performance of up to 1000 W may be necessary. At the conventional voltage level of 12 V, this results in very high currents that require large cable cross sections and thus in an unfavorable package and

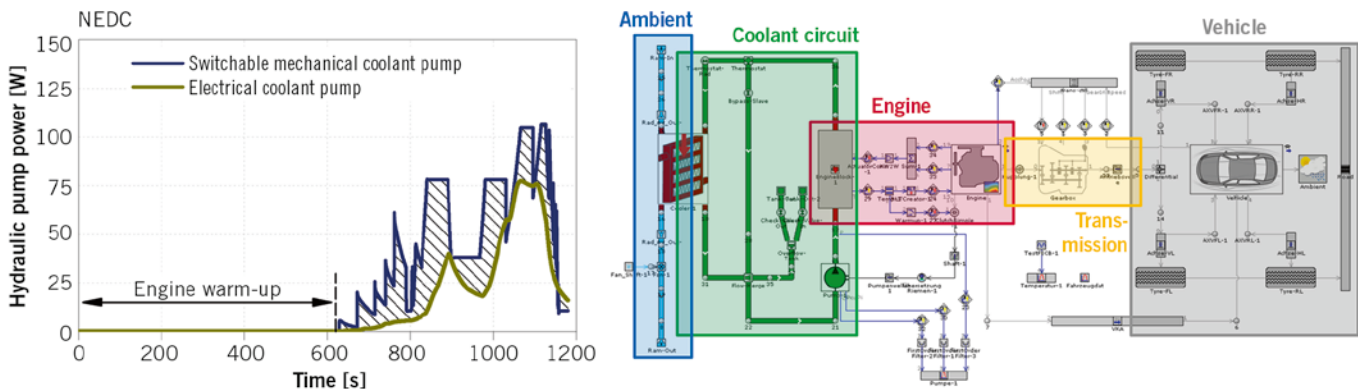


FIGURE 2 Power requirement for a main coolant pump in the NEDC and the simulation model used (© Mahle)

DEVELOPMENT COOLING

weight. In addition, the power electronics quickly reach their thermal limits. The introduction of the new 48-V level can prevent these problems. The currents in a 48-V electrical system are lower by a factor of four at the same power level. The recuperation of energy for hybrid applications and the integration of components can be achieved more easily.

CHALLENGES AND DESIGN STRATEGY

The development goal for an electrical coolant pump is to provide hydraulic power with the highest possible power density. Package and weight should be minimised and the available package constraint is used as efficiently as possible. Due to the area of application, however, this gives rise to a conflict of interests. The coolant pump encounters fluid temperatures of up to 130 °C. When installed close to the engine, possibly on the exhaust side, this component is subjected to even higher ambient temperatures. This means that the power loss to be minimised cannot always be reliably dissipated to the environment. In order to guarantee reliable operation under all environmental influences and full load of the coolant pump, it is essential to know the thermal loads on individual components, and to adjust them precisely to the

specific area of application at hand. For a coolant pump, one of the parameters that determines its size is the speed at which the maximum volume flow is reached. In pump theory, the circumferential speed u_2 of the hydraulic system at the outlet defines the energy transferred swirl-free to the medium for incident flow, or in this case the specific vane work Y_{sch} [3]:

Eq. 1	$Y_{sch} = u_2 \cdot c_{u2}$
--------------	------------------------------

It decreases as the rotational speed increases for a constant circumferential speed u_2 of the outer diameter of the hydraulic system. This results in changes to the power composition of the individual components. As design speed increases, the torque required for the hydraulic system decreases for a constant level of hydraulic power output. The electric motor can thus be smaller or the copper losses can decrease. However, this also leads to increased parasitic losses in the system. Therefore,

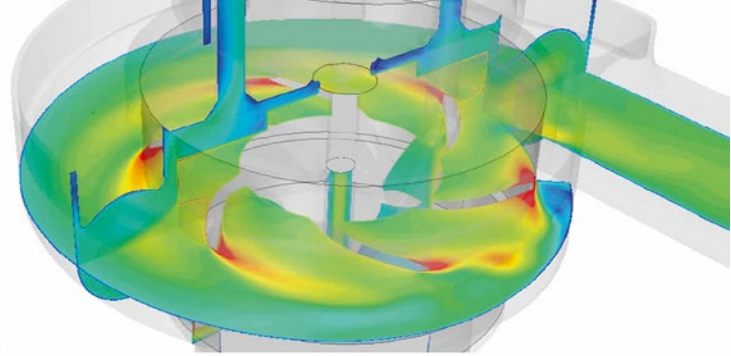


FIGURE 3 Simulation of the hydraulic system (© Mahle)

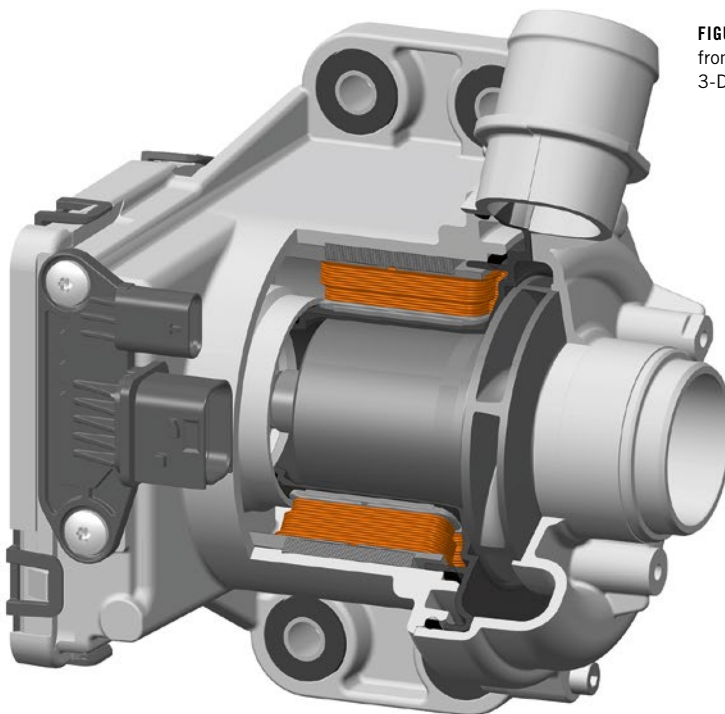
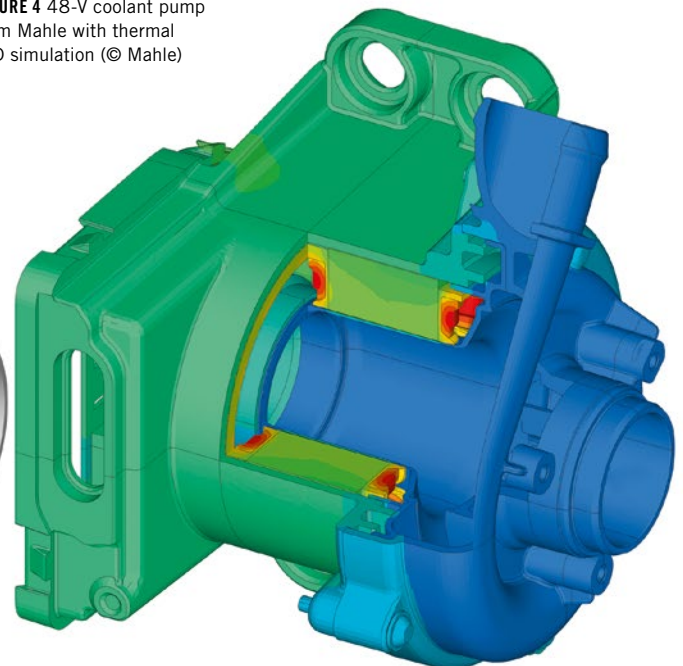


FIGURE 4 48-V coolant pump from Mahle with thermal 3-D simulation (© Mahle)



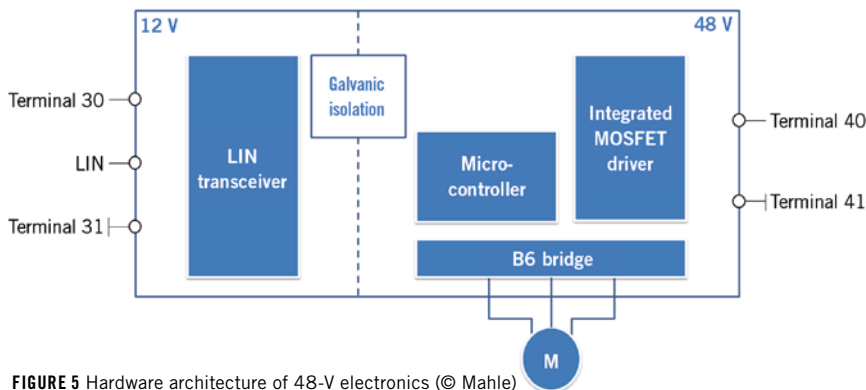


FIGURE 5 Hardware architecture of 48-V electronics (© Mahle)

there is a minimum of power loss at a given speed that represents a global optimum.

To achieve this optimum, analytical modules are used for the design which simulate and combine the physical properties of the individual components of the coolant pump. The models are validated with sample experiments for their individual range of validity. The detailed development of the components uses simulation software. For the hydraulic system development, CFD (Computational Fluid Dynamics) simulations are performed, FIGURE 3. This explores various customer requirements, such as good partial-load behaviour, a specific installation space situation, or production requirements, and their effects on operation are evaluated.

Finite element analyses (FE) can be used to develop different concepts for the electric motor and compare them with each other. It is thus possible to use ferrite magnet materials for permanent rotor excitation in a brushless DC (BLDC) motor. The advantages include cheaper procurement and lower price volatility. For high power densities, however, magnets made from rare earth elements are currently used. The motor design must therefore be coupled to the thermal 3-D simulation in order to achieve low system package and weight. The interaction of software, electronics, and motor allows various controls and functions to be compared for the corresponding application.

The use of analytical models in conjunction with targeted application of simulation software shortens development times and reduces prototype and validation costs.

IMPLEMENTATION OF COMPONENTS

The coolant pump design is shown in FIGURE 4 (left). The system is divided up in three areas: the hydraulics, the electric motor, and the control electronics. Owing to the design speed and the required hydraulic power, the hydraulic system consists of an impeller with three-dimensional vanes. With an innovative and easy-to-assemble bearing concept, high efficiencies can be achieved. This is made possible by tight sealing gaps thanks to short tolerance chains.

The rotor is a wet running design with no seals. The media are partitioned by a separation can. The thermal 3-D simulation, FIGURE 4 (right), sets the heat transfer path for power loss from the electric motor in the direction of the fluid in the spiral housing. Power loss can be dissipated reliably, even under extreme environmental and operating conditions.

FIGURE 5 shows a schematic diagram of the electronics integrated in the coolant pump. The hardware architecture includes the power semiconductors on the 48-V side in the form of a B6 bridge, as well as the logic for actuating the electric motor and regulating its speed. The 12-V electrical system is necessary for LIN communications. The two voltage levels are connected to each other via galvanic insulation in order to meet the requirements of VDA recommendation 320. Due to high ambient temperatures, all components used here must be able to withstand temperatures of up to 150 °C. The thermal connection of the components with high specific power loss presents a special challenge. They are also coupled to the fluid via

calculated heat conduction paths in order to ensure reliable operation over the entire service life, even at high ambient temperatures. With analytical modelling and simulation, it is possible to implement modular systems with different vehicle system voltages, e.g., for the conventional 12-V electrical system as well.

VALIDATION

Various test benches are used to test the coolant pump under real operating conditions. Each assembly is validated against the simulation and design by means of component testing. The efficiency and influence of all main components can thus be investigated in a targeted manner and evaluated individually. Testing at the systems level validates the overall set-up and is compared with the preceding component tests. Potential additional losses and deviations are thereby clearly identified. The integration of individual components is rapidly analysed and optimised.

It is only at the systems level that the coolant pump can be subjected to all the required boundary conditions simultaneously. Testing equipment is available in order to produce wide temperature variations. In close cooperation with the customer, the service life of components can be evaluated on an endurance test bench with realistic operating scenarios. Mobile coolant circuits, as depicted in FIGURE 6 (top), allow operation under various environmental influences, such as salt and splashing water, moist and warm surroundings, or even high accelerations. The EMV and noise emissions are also evaluated in Mahle in-house labs.

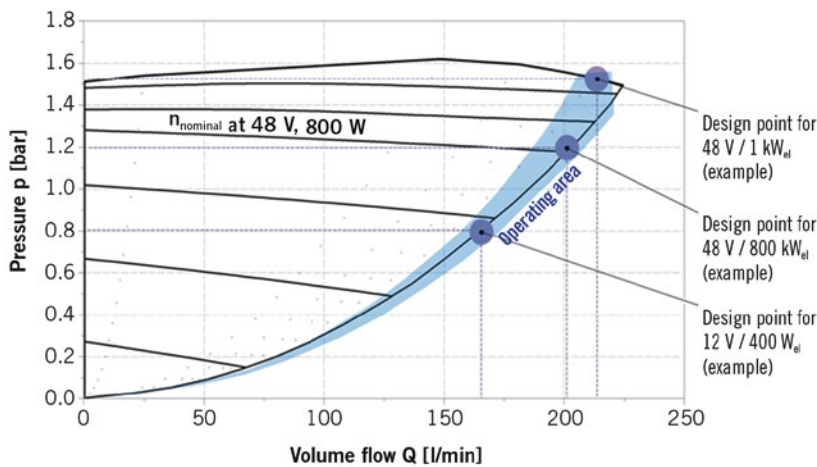


FIGURE 6 Flexible testing equipment and operating map of the electrical coolant pump (© Mahle)

SUMMARY

On-demand operation of the Mahle electrical coolant pump reduces the CO₂ emissions of a vehicle. A high power density, and thus favorable package and weight, conflicts with the required operation at high coolant and ambient temperatures. Precise design and optimisation of the thermal balance can, however, solve this conflict at the best. Using analytical models, the optimum design can be determined and investigated in simulations. The validation tests, performed first at the component level, are compared with the simulation. Based on these information a physical model is created, which helps to understand the complete system “electri-

cal coolant pump” accurately. Systems tests under real operating conditions ensure that the electrical coolant pump completely fulfill all customer requirements. With the electrification of components in and around the combustion engine, Mahle is making a contribution toward complying with even tighter targets for CO₂ reduction in the future.

REFERENCES

- [1] Krappel, M.; Heidecker, C.; Streng, S.; Elsäßer, A.: Electrical 48V coolant pump for highest thermal management requirements. 15th Stuttgart International Symposium, 2015
- [2] Lunanova, M.: Optimierung von Nebenaggregaten. Wiesbaden: Vieweg+Teubner, 2009
- [3] Güllich, J.: Kreiselpumpen. Heidelberg: Springer, 2010

IT'S TIME FOR EXPERT KNOWLEDGE WITH MORE FLEXIBILITY.



ATZ eMAGAZINE.

© creativa republic 2015

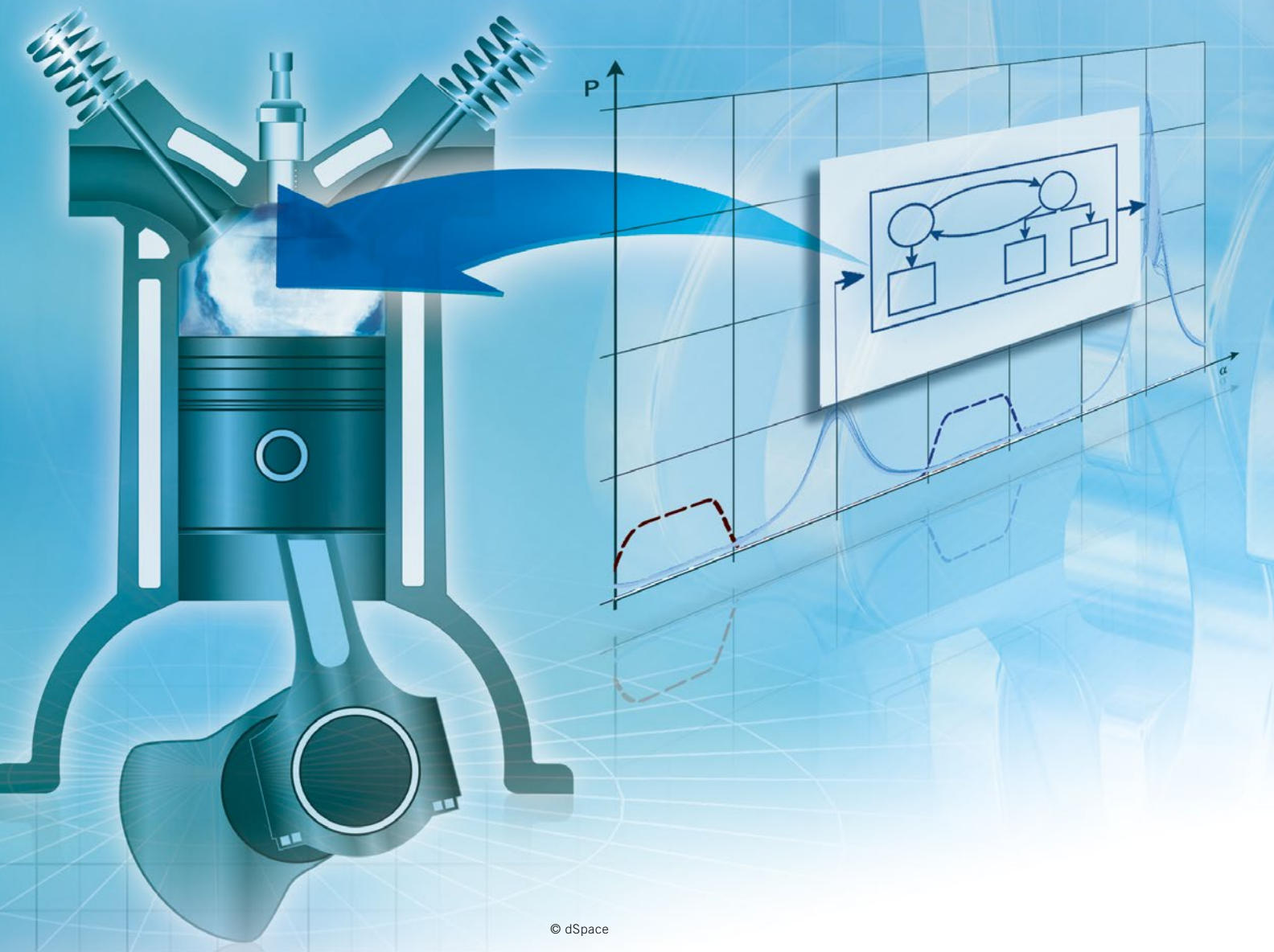


THE FASTEST INFORMATION IS DIGITAL.

The **ATZ eMagazine** for the technology-oriented management in the automotive industry is loaded with the latest findings in research, development and production – for every aspect of passenger car and commercial vehicle engineering, for every branch and specialty. The **ATZ eMagazine** is fast and up-to-date: easily find topics with keyword searches, read up on feature articles in the online archives or create a PDF with extracted information.

www.my-specialized-knowledge.com/ATZworldwide

ATZ



© dSpace

In-cycle Control Offers High Potential for New Combustion Concepts

Rapid control prototyping systems are established tools for developing and optimising new combustion processes. Using a closed loop control with the indicated combustion chamber pressure as the input value has proved to be particularly promising. The direct analysis of the thermodynamic state makes it possible to use fast closed loops within a running combustion cycle. This enabled the Institute for Combustion Engines of RWTH Aachen University to develop and successfully implement an in-cycle control for stabilising the gasoline controlled autoignition.

AUTHORS



Dipl.-Ing. Bastian Lehrheuer is Research Associate at the Institute for Combustion Engines of the RWTH Aachen University (Germany).



Maximilian Wick, M. Sc. is Research Associate for Mechatronic Systems for Combustion Engines at the RWTH Aachen University (Germany).



Dipl.-Ing. Jesse Lakemeier is Application Engineer for Rapid Control Prototyping at the dSpace GmbH in Paderborn (Germany).



Prof. Dr. Jakob Andert is Junior Professor for Mechatronic Systems for Combustion Engines at the RWTH Aachen University (Germany).

BASICS AND SYSTEM SETUP

Gasoline controlled autoignition (GCAI) offers a great potential for reducing CO₂ emissions, comparable to current lean-burn stratified engines [1, 2]. The low-temperature combustion of the GCAI process requires nearly no exhaust gas aftertreatment because almost no nitrogen oxide is emitted [3]. Factors hindering the broad application of this combustion process include a limited stable operating area, high sensitivity towards changing conditions, and the resulting need for fast closed loop control algorithms [4, 5]. The most promising

approaches are based on the implementation of cycle-based controllers using FPGAs (Field Programmable Gate Arrays) for indication analysis and low-latency controllers [6].

A broadly practiced method for initiating and controlling gasoline autoignition is internal exhaust gas recirculation (EGR), which is possible through a variable valvetrain. The Institute for Combustion Engines of RWTH Aachen University uses a research engine with an electromechanical valvetrain (EMVT) for this purpose, **FIGURE 1** (left). It is a direct-injection single-cylinder engine with an outward-opening piezoelectrically

actuated hollow cone nozzle in a central position. Because the valvetrain is mechanically decoupled from the crank drive, the valve might hit the piston. To avoid this, the piston has valve pockets to ensure completely unhindered valve movement. Still, the engine achieves a compression ratio of $\epsilon = 12$.

The engine is fueled with conventional RON95-E10 fuel and is used in a conditioned environment on the thermodynamics test bench. For example, in the experiments described in this article, an intake manifold temperature of $T_{\text{air}} = 50 \text{ }^\circ\text{C}$ and an engine temperature (oil and coolant) of $T_{\text{oil}} = T_{\text{coolant}} = 90 \text{ }^\circ\text{C}$ are

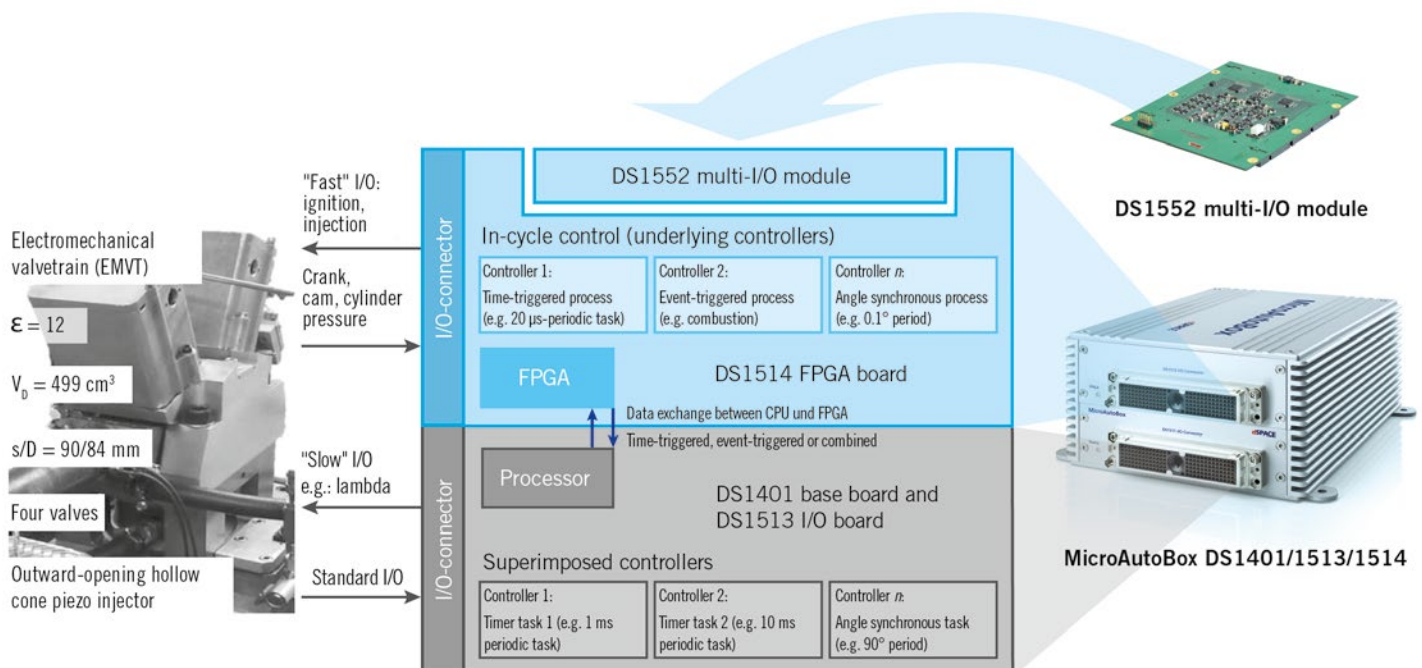


FIGURE 1 Single-cylinder research engine with electromechanical valvetrain (left) and development ECU MicroAutoBox II with Kintex-7 FPGA (right) © dSpace

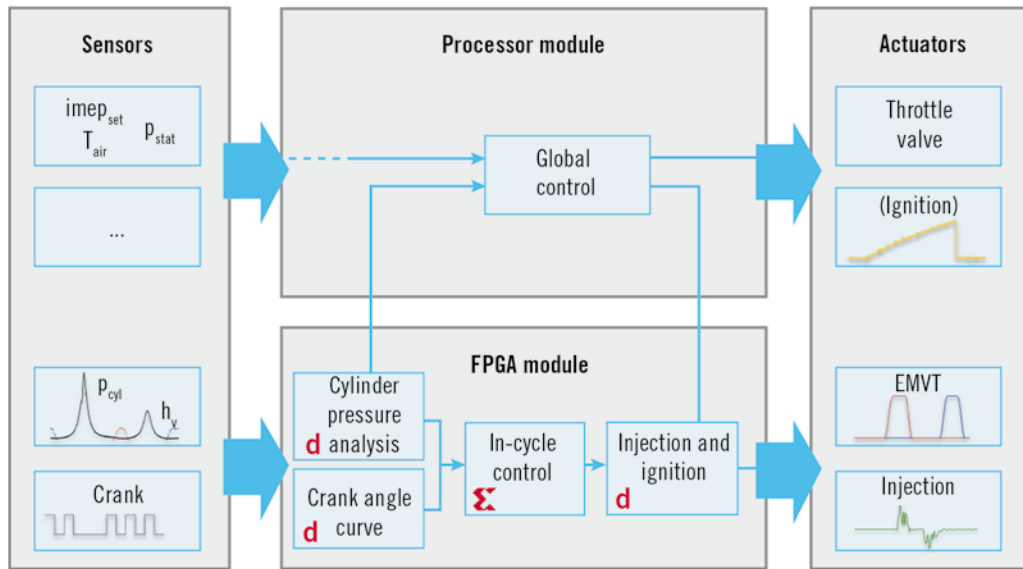


FIGURE 2 Schematic signal flow of the in-cycle control on the processor and FPGA of the MicroAutoBox II (© dSpace)

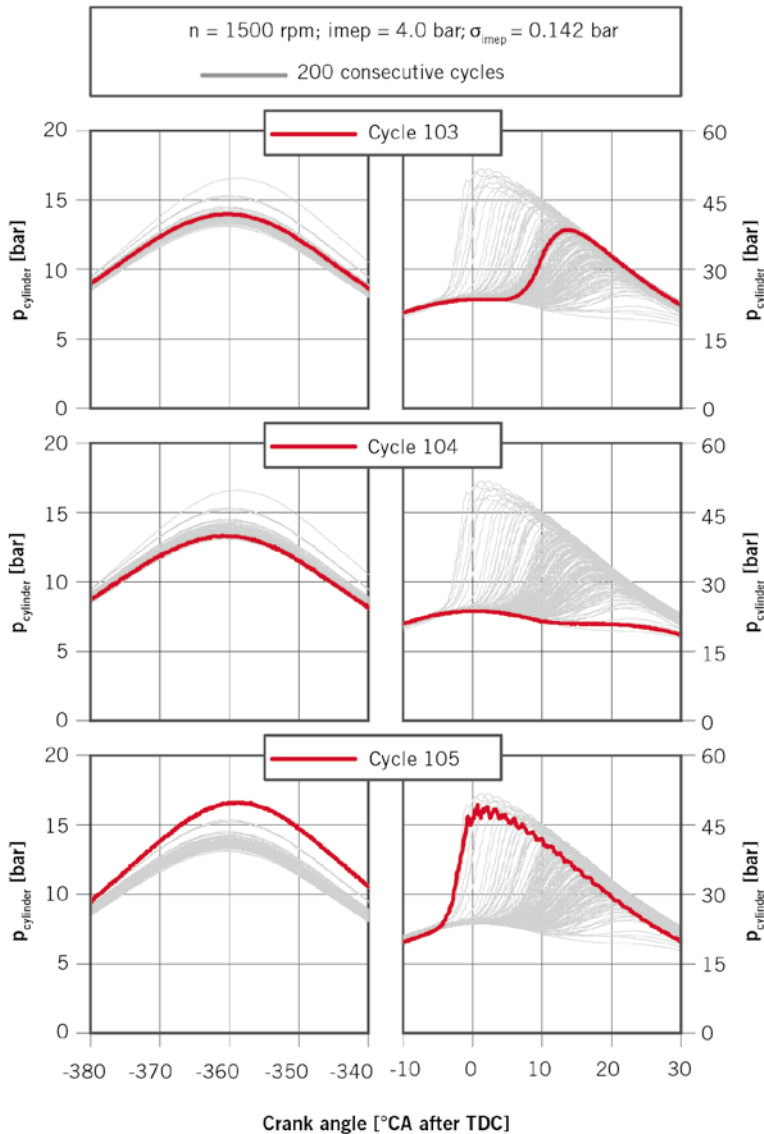


FIGURE 3 Consecutive combustion cycles of GCAI operation via CCR at $n = 1500$ rpm and $\text{imep} = 4$ bar: intermediate compression (left) and combustion (right) (© dSpace)

set. The engine has piezoelectric and piezoresistive quartz pressure transducers in the combustion chamber and on the intake and output sides, respectively.

In addition to the well-established evaluation of the pressure signals via a CAS indication system (Combustion Analyzer System), the pressure signals are also passed to the I/O of a development ECU (dSpace MicroAutoBox II), where they are evaluated in real time by a user-programmable Kintex-7 FPGA from Xilinx. For this purpose, dSpace's new so-called Advanced Engine Control Solution [7] is used. The solution consists of an open library for model-based FPGA design in Simulink, based on System Generator from Xilinx (XSG). As one of its features, this library contains real-time-capable cylinder pressure indication. This indication provides the parameters required by a controller in one cycle. The fast actuators (EMVT, fuel injection) are also controlled via components of the Advanced Engine Control Solution inside the FPGA, which lets developers intervene in the closed loop control in a few nanoseconds. This control intervention can occur within one combustion cycle and is a correction variable in the slow, global, closed loop control, **FIGURE 2**.

COMBUSTION CHARACTERISTICS

In the experiments described here, the amount of residual gas needed for auto-ignition is controlled by combustion

chamber recirculation (CCR). In CCR, the outlet valve is closed early to keep the residual gas of the previous cycle in the combustion chamber. The gas is then compressed until the top dead centre of the gas exchange is reached.

For lower loads, a higher amount of residual gas is needed to compensate the low exhaust gas enthalpy. On the one hand, this increases efficiency by 30 % compared to conventionally throttled, spark ignition operation. On the other hand, it can decrease stability. As [1] shows, the operating range for low loads can be expanded by means of multiple injections and additional spark ignition. The high exhaust gas recirculation rates lead to a strong connection between consecutive cycles, which in turn causes high fluctuation in the state of combustion and thus stability [4, 8].

For high engine loads, the steep pressure increase in particular is the limiting variable. The high exhaust gas enthalpy and the high combustion chamber temperature are beneficial for autoignition. To counter these effects, the combustion duration has to be increased by means of charge dilution (forced induction/external EGR) or decreasing the actual compression ratio via late intake valve timings. During this process, the centre of combustion is also delayed, which in turn has a negative effect on stability.

FIGURE 3 shows the pressure curve of 200 consecutive combustion cycles at a rotational speed of 1500 rpm and a load of indicated mean effective pressure $imep = 4$ bar. The high standard deviation of $\sigma_{imep} = 0.142$ bar also becomes clear when looking at the high fluctuation of the cylinder pressure traces during combustion, **FIGURE 3** (right). A recurring sequence of combustions, as illustrated in **FIGURE 3** for the cycles 103 and following, is responsible for this instability. A regular combustion of good efficiency (cycle 103) is followed by an exceptionally bad, incomplete combustion (cycle 104). From the low cylinder pressure during the intermediate compression, **FIGURE 3** (middle left), a low enthalpy of the residual gas can be derived, which causes adverse autoignition conditions and thus an incomplete combustion, **FIGURE 3** (middle right). The ignitable mixture in the exhaust gas that results from incomplete combustion is beneficial for autoignition in the following cycle, which causes a significant amount of heat to be released in the intermediate compression, and a particularly early combustion follows, **FIGURE 3** (bottom right). The pressure oscillates near the top dead centre, which is similar to knocking. The relations shown in the figure are typical for GCAI and lead to characteristic sequences of high standard deviations

of the indicated mean effective pressure $imep$ and the centre of combustion α_{50} . An in-cycle control seeks to predict and actively stabilise these sequences.

IN-CYCLE CONTROL

A first control strategy can be derived from the sequence of consecutive cycles shown above. This strategy is based on the observation that a low pressure level during intermediate compression results in a particularly late, incomplete combustion, and vice versa. The entire sequence can be avoided by preventing the first incomplete combustion.

The control variable is the crankshaft angle at which the intake valve closes (IVC). If this event is delayed, the actual compression ratio is reduced, and the conditions for autoignition and thus the combustion takes place later. If this event occurs earlier, autoignition is supported and combustion also takes place earlier. If the dSpace Advanced Engine Control Solution's real-time analysis of the cylinder pressure finds a low peak pressure at the top dead centre of the gas exchange during the intermediate compression, IVC is brought forward in the same cycle to prevent a late centre of combustion.

FIGURE 4 shows the result of the described in-cycle control for 1000 consecutive combustion cycles, where the

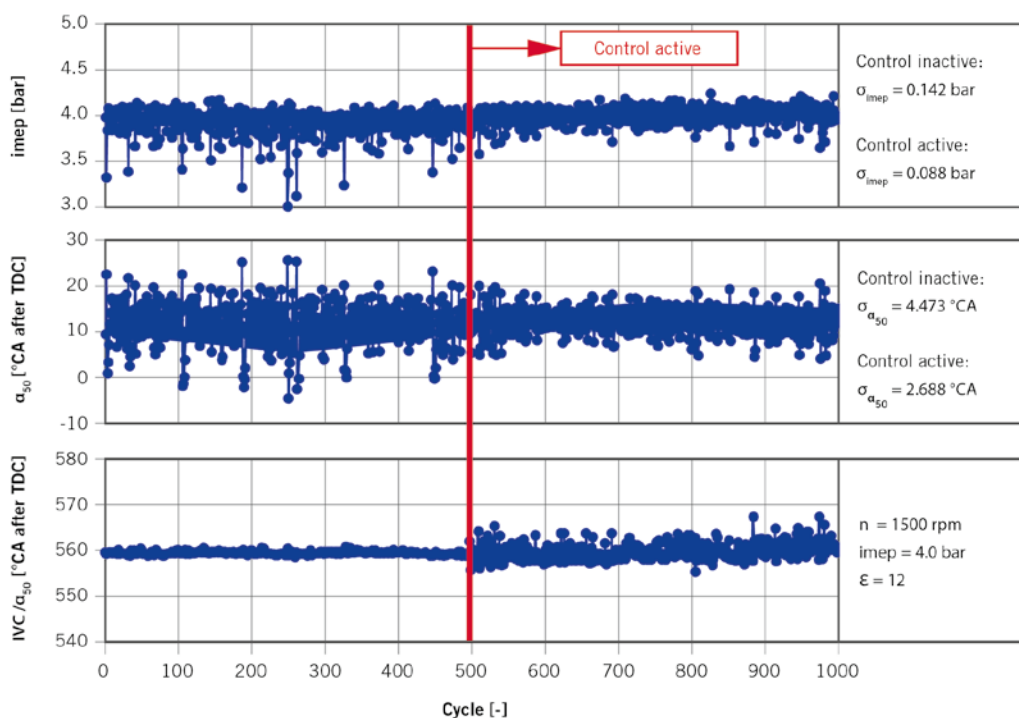


FIGURE 4 Load $imep$, centre of combustion α_{50} , IVC for 1000 consecutive cycles without and with active in-cycle control in the FPGA of the MicroAutoBox II (© dSpace)

control is activated after approximately 500 cycles. It can be seen that the particularly high load deviations can be prevented by means of active control, which decreases the standard deviation of the indicated mean pressure pronouncedly from $\sigma_{imep} = 0.142$ to 0.088 bar, **FIGURE 4** (top). The centre of combustion also clearly improves; particularly early and late positions can be avoided, **FIGURE 4** (bottom).

SUMMARY AND OUTLOOK

It has been shown that FPGA-based real-time cylinder pressure analysis enables in-cycle control interventions, making it possible to avoid critical sequences in stationary GCAI operation. Combustion stability was significantly increased. By using the correlation between intermediate compression and subsequent combustion, it was possible to implement an in-cycle control and demonstrate it on the single-cylinder research engine. This highlights the potential of fast control interventions. The in-cycle control inside the FPGA was implemented using the Advanced Engine Control Solution from dSpace and the System Generator from Xilinx.

It is furthermore intended to optimise the prediction of the combustion process via real-time cylinder pressure analysis within a cycle. The growing number of characteristic combustion variables and their correlation detected when analysing the individual cycles in detail, instead of using mean values, require new methods for efficiently analysing large amounts of data. The large and powerful Kintex-7 FPGA from Xilinx of MicroAutoBox II provides the perfect conditions for realising even computation-intensive control algorithms with minimal latencies. But further control variables for in-cycle control intervention have to be identified. This is why the Institute for Combustion Engines of RWTH Aachen University is researching multiple-injection strategies and water injection.

REFERENCES

[1] Brassat, A.: Betriebsstrategien der kontrollierten Selbstzündung am aufgeladenen direkteinspritzenden Ottomotor. Dissertation, RWTH Aachen University, 2013
 [2] Kulzer, A.; Fischer, W.; Karrelmeyer, R.; Sauer, C.; Wintrich T.; Benninger, K.: Kontrollierte Selbstzündung beim Ottomotor – CO₂-Einsparpotenziale. In: MTZ 70 (2009), No. 1, pp. 50-57
 [3] Zhao, H.: HCCI and CAI engines for the automotive industry. Cambridge, England: Woodhead Publishing, 2007

[4] Andert, J.: Modellbasierte Echtzeitoptimierung der ottomotorischen Selbstzündung. Dissertation, RWTH Aachen University, 2012
 [5] Hoffmann, K.; Drews, P.; Seebach, D.; Stapf, K.-D.; Pischinger, S.: Optimized closed loop control of controlled auto ignition CAI. Fisita World Automotive Congress, Munich, 2008
 [6] Pfluger, J.; Andert, J.; Ross, H.; Mertens, F.: Rapid Control Prototyping für Zylinderdruckindizierung. In: MTZ 73 (2012), No. 11
 [7] Juhász, L.; Schütte, F.; Berneck, D.; Lakemeier, J.: Advanced RCP Solutions for In-Cycle Control of Combustion Engines. Symposium for Combustion Control, Aachen, 2015
 [8] Koch, M.; Shahbakhti, C. R.: Characterizing the cyclic variability of ignition timing in a homogeneous charge compression ignition engine fuelled with n-heptane/iso-octane blend fuels. In: International Journal of Engine Research 2008, No. 9, pp. 361-397

THANKS

The authors are grateful to the German Research Foundation (DFG) for its financial support in the Collaborative Research Centre SFB 686 "Model-Based Control of Homogenized Low-Temperature Combustion".

chassis.tech_{plus}

6th International Munich Chassis Symposium

16 and 17 June 2015

Munich | Germany

NEW CHASSIS SYSTEMS

Requirements for the chassis of tomorrow

ENERGY EFFICIENCY AND SAFETY

Innovations and requirements

DRIVER ASSISTANCE SYSTEMS

Lateral control and lane keeping

/// PLENARY LECTURES

BMW Group | Daimler AG |
Robert Bosch GmbH |
ADAC e. V. Technik Zentrum |
AVL List GmbH | Continental
Teves AG & Co. oHG |
TÜV SÜD AG

/// ONE FOR ALL

**Four congresses
in one event**



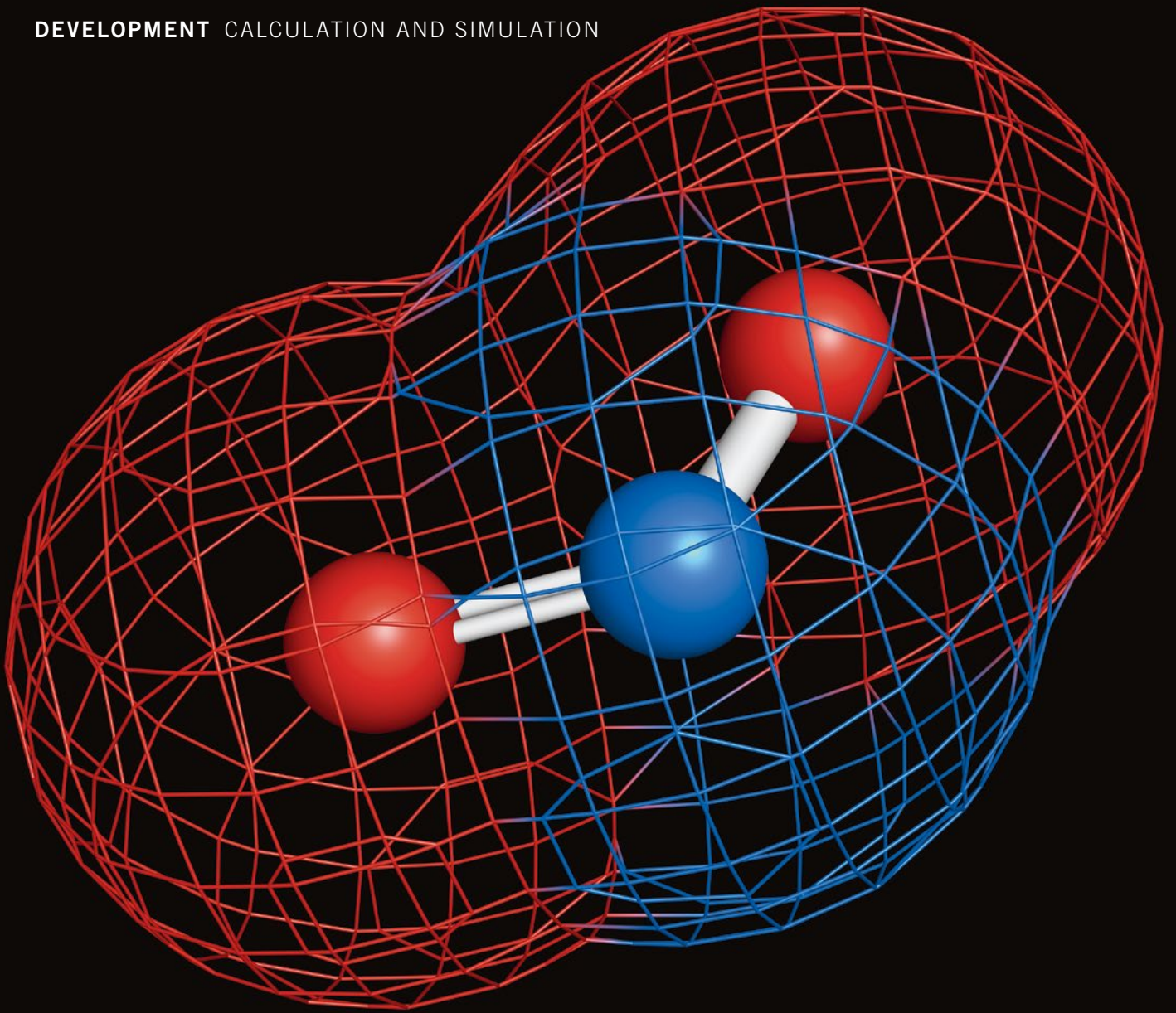
/// KINDLY SUPPORTED BY



ATZ live
Abraham-Lincoln-Straße 46
65189 Wiesbaden | Germany

Phone +49 611 7878-131
Fax +49 611 7878-452
ATZlive@springer.com

PROGRAM AND REGISTRATION
www.ATZlive.com



© molekuul.be | Fotolia

A New Global Algebraic NO_x Emissions Formation Model for Natural Gas Engines

Engineers from Ricardo developed a new global NO_x emissions formation model. It is formulated by a single analytically derived algebraic equation, applicable to both stoichiometric and lean burn natural gas combustion systems for use in 1-D and 3-D simulation codes as well as for direct post-processing of engine test data.

AUTHORS



Dr. Georgios Bikas

was Chief Engineer Large Engines till September 2014 at the Ricardo Deutschland GmbH in Schwäbisch Gmünd (Germany) and is now Engineering Manager at the Delphi Deutschland GmbH in Flechtorf (Germany).



Dr. Konstantinos Michos

was Senior Research Engineer (till May 2015) at the Ricardo Deutschland GmbH in Schwäbisch Gmünd (Germany).



Dr. Ioannis Vlaskos

is Director Engines Business Unit and Director of the Global Market Sector Marine at the Ricardo Deutschland GmbH in Schwäbisch Gmünd (Germany).

CHALLENGING LIMIT VALUES FOR NO_x

NO_x emissions compliance is a boundary condition for almost all engine developments and has a direct relationship to engine design and operating parameters that engineers are required to optimise in order to achieve performance and fuel efficiency targets. For this reason, it is especially important for any simulation code to incorporate a generic and fully predictive NO_x formation model that is capable not only to capture the effect of engine operating and design parameters, but also to provide in a reliable way quantitatively accurate results.

The main weakness of the commonly used NO_x emissions models, which are historically based on the extended Zeldovich mechanism as proposed by Lavoie et al. [1], is their inability to predict NO_x emissions under very lean, high pressure and low to moderate temperature conditions (case of highly boosted, lean burn large gas engines). This is due to the fact that not all possible chemical pathways for NO_x formation are taken into account [2] and also because of the large uncertainties of the rate constants of the relevant reactions [3]. Furthermore, these models are usually first calibrated against measured NO_x data and then

used to predict NO_x emissions at other operating points. However, such a procedure limits the applicability of the models in a narrow range around the point of calibration, making their use uncertain at a wide range of operating parameters. If higher accuracy is needed, detailed chemical reaction schemes can be used [4]. However, their use in reactive 3-D CFD codes results in unacceptable computational costs [5], while, in 1-D codes, the increased complexity and the requirement for experienced users with programming skills render this approach unattractive.

In the present article, a newly developed, simple and quick to implement and run, global algebraic NO_x emissions model, applicable to both stoichiometric and lean burn combustion systems, is briefly described. The model takes into account both the thermal and the N₂O pathway mechanisms, which are considered to be the most relevant ones especially under the lean burn combustion conditions of large high-boost turbocharged gas engines, and is applicable to all such engines without need for tuning of model constants. The developed model practically consists of a single algebraic expression which is the analytical solution of a set of differential equations that describe the temporal evolution of NO concentration.

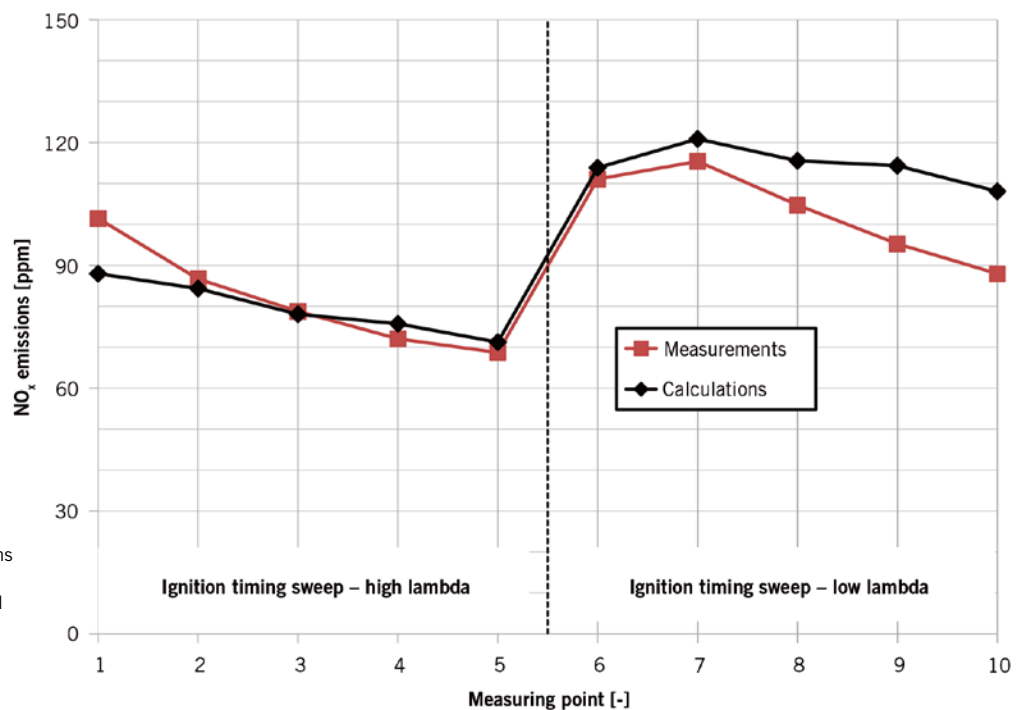


FIGURE 1 Comparison between measured and calculated NO_x emissions of the stationary engine at the two ignition timing sweeps of the high and low lambda values (© Ricardo)

No.	Reaction	A	n	E	Re	
Extended Zeldovich mechanism						
1	$N_2 + O \rightarrow NO + N$	1.80×10^{14}	0	319008	[3]	
2	$N + O_2 \rightarrow NO + O$	1.80×10^{10}	1	38909	[3]	
3	$N + OH \rightarrow NO + H$	7.10×10^{13}	0	3741	[3]	
N₂O pathway mechanism						
4	$N_2O + O \rightarrow N_2 + O_2$	1.40×10^2	0	45230	[6]	
5	$N_2O + O \rightarrow 2NO$	2.90×10^{13}	0	96870	[6]	
6	$N_2O + H \rightarrow N_2 + OH$	3.87×10^{14}	0	79000	[6]	
7	$N_2O + OH \rightarrow N_2 + HO_2$	2.00×10^{12}	0	88120	[6]	
8 ^a	$N_2O (+M) \rightarrow N_2 + O (+M)$	k_0	6.37x10 ¹⁴	0	237000	[6]
		k_∞	7.91x10 ¹⁰	0	234410	[6]

^a Third body, pressure-dependent reaction. Third body efficiencies are equal to 1 for all species of the mixture. The rate constant at any pressure is given (by the Lindemann form) as a combination of the rate constants at the low- and high-pressure limits.

TABLE 1 Extended Zeldovich mechanism and N₂O pathway mechanism; rate constants are written as $AT^n \exp(-E/R_m T)$; units are: mol, cm³, s, K, J (© Ricardo)

The validity of this NO_x emissions model is then demonstrated by comparison against experimental data of both a stationary gas engine and a truck engine, both CNG fuelled and operating under lean burn conditions. Its predictive capability against basic operating parameters, such as lambda value, ignition timing and engine speed, is tested and proven satisfactory. The value of the model as a promising alternative tool for

modelling NO_x emissions is then highlighted by comparing its characteristics to those of the extended Zeldovich mechanism and detailed chemical kinetics approaches.

BRIEF DESCRIPTION OF GLOBAL ALGEBRAIC NO_x EMISSIONS MODEL

In this section the model for the calculation of the kinetically controlled NO con-

centration in the postflame gases of the combustion chamber, as determined by the simultaneous effect of the thermal and the N₂O pathway mechanisms, is briefly presented. Basic feature of this new model is the derivation of a global analytical solution for the temporal development of NO concentration, starting from subsets of detailed chemical kinetic schemes for the description of the two mechanisms.

Regarding thermal NO, which is dominant under high temperature and close to stoichiometric conditions, the well-established extended Zeldovich mechanism is adopted. At the same time, NO production via the N₂O route, which becomes significant at low combustion temperatures, high pressures and for very lean mixtures, is modelled using a relevant subset of elementary reactions taken from the detailed kinetic mechanism GRI-Mech 3.0 [6], which concerns methane combustion with NO_x formation reactions also included. The relevant chemical reactions of the two mechanisms, along with their associated rate constants, are given in **TABLE 1**.

Assuming steady-state approximations for N and N₂O due to their very low concentrations in the burned gas mixture and after extensive mathematical manipulations, the following single global algebraic expression is analytically derived, which describes the temporal

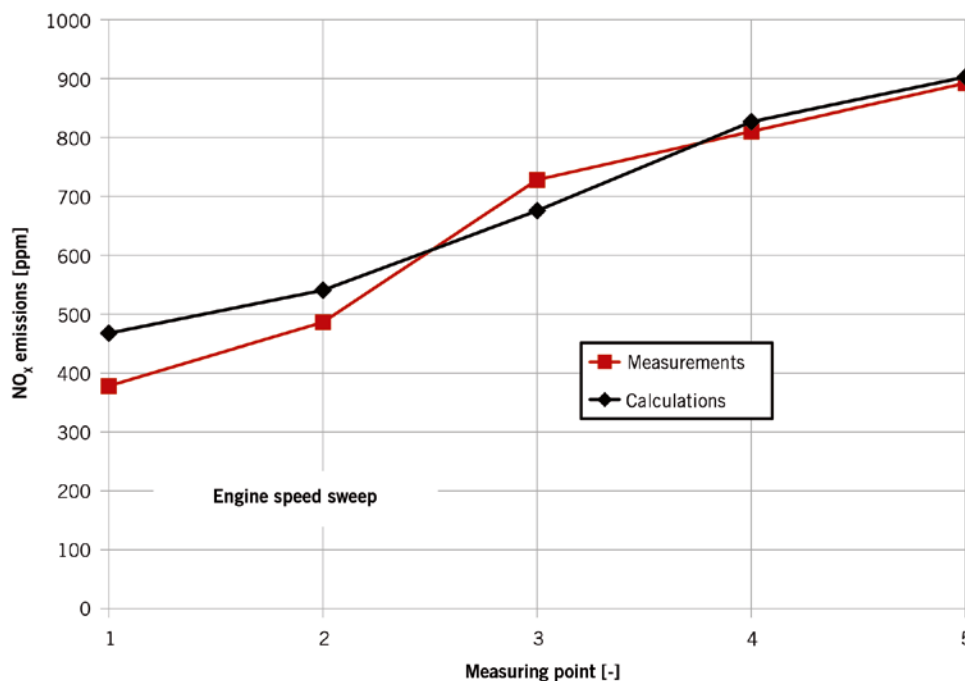


FIGURE 2 Comparison between measured and calculated NO_x emissions of the truck engine at various engine speeds (© Ricardo)

evolution of the NO concentration towards its equilibrium value, including the simultaneous contributions of the thermal and N₂O pathway mechanisms:

Eq. 1	$t - t_0 = B \cdot \ln(1 + a) - A \cdot \ln(1 - a) + (A - B) \cdot \ln(D \cdot a + 1)$
--------------	--

Where $t - t_0$ is the time elapsed from the initiation of the combustion event and a can be interpreted as the NO progress variable, defined as the ratio of the instantaneous NO concentration to its equilibrium value:

Eq. 2	$\alpha = \frac{[\text{NO}]}{[\text{NO}]_e}$
--------------	--

During the combustion event, the value of a gets from 0 to 1. At any time t this practically indicates the percentage of the equilibrium NO that has been formed so far. For example, a solution of Eq. 1 with $a = 0.3$ means that 30 % of the theoretically maximum (equilibrium) NO has been created. Recognising that the maximum concentration NO can reach during a combustion event is its equilibrium value (at least in a lambda range between 1 and 2,3) and taking

also into consideration that practically equilibrium can never be fully reached due to the limited combustion duration, during a cycle simulation Eq. 1 needs to be iteratively solved for within an equilibrium calculation scheme on a time (or equivalently crank angle) basis in order for the engine-out NO_x emissions to be calculated.

At this point, it is worth mentioning that the mathematical expression of Eq. 1 itself is of great interest, since it includes parameters directly related to the description of the physics that govern the formation of NO_x through the involved mechanisms. This is accomplished through the introduction of the characteristic timescales of the thermal and N₂O pathway mechanisms in the expressions of the variables A and B , which have dimensions of time and are defined as:

Eq. 3	$A = \left(\frac{1}{\tau_{NO}^{th} (1 + \kappa)} + \frac{1}{\tau_{NO}^{nit}} \right)^{-1}$
--------------	---

and

Eq. 4	$B = \left(\frac{1}{\tau_{NO}^{th} (1 - \kappa)} + \frac{1}{\tau_{NO}^{nit}} \right)^{-1}$
--------------	---

respectively, as well as in the variable D , which is a nondimensional parameter given as:

Eq. 5	$D = \frac{\kappa}{(\tau_{NO}^{nit}/\tau_{NO}^{th}) + 1}$
--------------	---

In the expressions of A , B and D all involved variables are dependent on the corresponding equilibrium state and they are defined as:

Eq. 6	$\tau_{NO}^{th} = \frac{[\text{NO}]_e}{4R_1}$ $\tau_{NO}^{nit} = \frac{(1 + \lambda) [\text{NO}]_e}{2R_5}$ $\kappa = \frac{R_1}{R_2 + R_3}$ $\lambda = \frac{R_3}{R_4 + R_6 + R_7 + R_8}$
--------------	---

where R_i ($i = 1$ to 8) the equilibrium rates of the 8 reactions of **TABLE 1**.

It is noted that, in the present study, the burned gas mixture is composed of 27 combustion products (species) and its equilibrium composition and adiabatic flame temperature are calculated based on the composition, initial temperature and pressure of the unburned gas mixture. Therefore, through the direct use of Eq. 1, the effect of residence time, the remaining variable affecting NO production, is explicitly accounted for.

VALIDATION OF GLOBAL ALGEBRAIC NO_x EMISSIONS MODEL

The global algebraic NO_x emissions model was validated against experimental NO_x emissions data of two lean burn, CNG fuelled turbocharged gas engines. The first engine was for stationary applications and run under steady-state, full-load conditions. Comparison between calculated and measured data was performed at two sets of ignition timing sweeps of different lambda values within the high efficiency and low NO_x emissions range of the engine. The second engine was a truck engine running at various speeds under full-load conditions at a constant lambda value.

For the calculation of the engine-out NO_x emissions a simplified computational method, based on a multi-zone approach, was also developed. This method is considered as postprocessing of engine test data and uses as input the measured indicated data, lambda and mass flows of air and fuel. A heat release

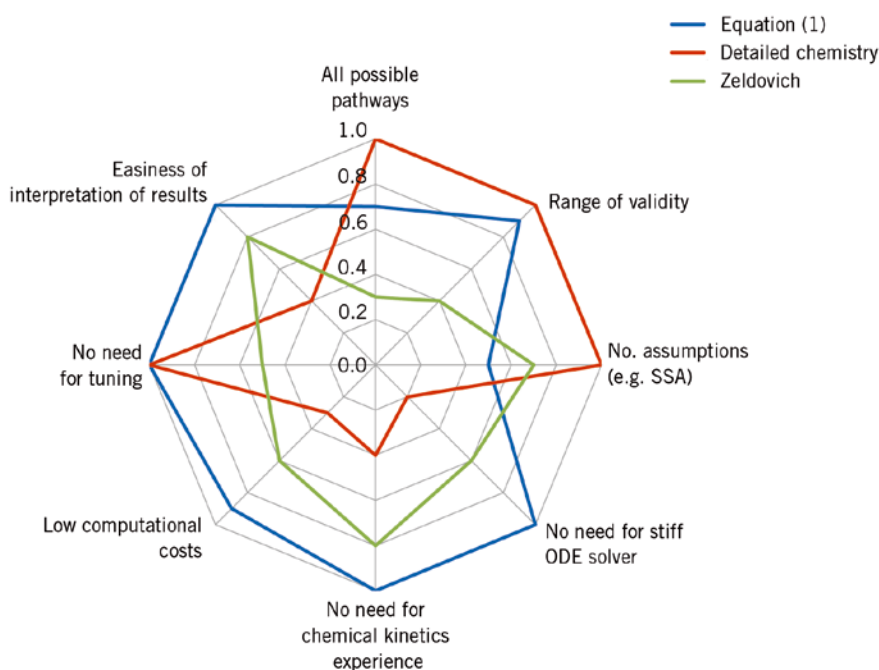


FIGURE 3 Comparison of different NO_x emissions modelling approaches (© Ricardo)

analysis is performed on the measured pressure trace, resulting in an estimation of the unburned gas temperature and mass fraction burned during combustion.

FIGURE 1 presents the comparison between the measured and calculated NO_x emissions of the stationary engine for the ignition timing sweeps at the high and low lambda values. It can be observed that the current NO_x model shows generally a good matching with the measured data, with a maximum deviation of about 20 ppm at the low lambda set. The accuracy of the model in terms of capturing the effect of lambda can be considered even higher, if the mean measured and calculated NO_x emissions of the various ignition timings for each set of lambda value are compared. At the same time, it can be seen

that the experimental trend of NO_x emissions variation with ignition timing is also adequately followed by the model.

The ability of the model in capturing the effect of engine speed variation can be assessed in **FIGURE 2**, where the comparison between the measured and calculated NO_x emissions of the truck engine is shown. Apart from following the trend of NO_x emissions variation with engine speed, the model also presents good quantitative agreement with the measured NO_x emissions, with a maximum deviation of less than 100 ppm at the low engine speed limit.

Overall, the response of the model to all basic operating parameters, such as air/fuel ratio, ignition timing and engine speed, can be considered satisfactory. Thus, the model could be successfully implemented in both 1-D and 3-D CFD codes, presenting the benefits over its commonly used counterparts of taking into consideration both thermal and N₂O pathway NO_x production, absence of any calibration constants, as well as speed of calculation due to the use of a single algebraic expression, Eq. 1.

CONCLUSION

In this paper, a newly developed global algebraic NO_x emissions formation model for stoichiometric and lean burn combustion systems is briefly described, which presents the clear advantages over its commonly used counterparts of taking into account both the thermal and N₂O pathway mechanisms, use of well-validated rate constants, no need for calibration and low computational costs. In **FIGURE 3** comparison of the new algebraic model against the extended

Zeldovich mechanism and detailed chemical kinetics shows the pros and cons of this approach. It is evident that Eq. 1 represents a good compromise between accuracy, computational cost and easiness to implement and use.

The model is then validated on two lean burn turbocharged gas engines for stationary and truck applications, presenting good match with experimental data for variations of lambda, ignition timing and engine speed.

The model is well suited for 1-D, 3-D CFD simulation codes and for direct postprocessing of engine test data as well. It is expected to significantly reduce computational costs, rendering the solution of 3-D turbulent reactive flows accomplishable by avoiding the need for detailed kinetic schemes of NO_x chemistry and numerical solution of additional differential equations.

REFERENCES

[1] Lavoie, G. A.; Heywood, J. B.; Keck, J. C.: Experimental and Theoretical Study of Nitric Oxide Formation in Internal Combustion Engines. In: *Combust. Sci. Technol.* (1970), No. 1, pp. 313-326
 [2] Merker, G. P.; Schwarz, C.; Stiesch, G.; Otto, F.: *Simulating Combustion*. Heidelberg/Berlin: Springer, 2006
 [3] Hanson, R. K.; Salimian, S.: Survey of Rate Constants in the H/N/O System. In: *Combustion Chemistry*: Springer, New York, 1984
 [4] Miller, R.; Davis, G.; Lavoie, G.; Newman, C.; Gardner, T.: A Super-Extended Zeldovich Mechanism for NO_x Modeling and Engine Calibration. SAE Paper No. 980781, 1998
 [5] Löffler, G.; Sieber, R.; Harasek, M.; Hofbauer, H.; Hauss, R.; Landauf, J.: NO_x Formation in Natural Gas Combustion – A New Simplified Reaction Scheme for CFD Calculations. In: *Fuel* (2006), No. 85, pp. 513-523
 [6] Smith, G. P.; Golden, D. M.; Frenklach, M.; Moriarty, N. W.; Eiteneer, B.; Goldenberg, M.; Bowman, C. T.; Hanson, R. K.; Song Jr., S.; Gardiner, W. C.; Lissianski, V. V.; Zhiwei, Q.: available at http://www.me.berkeley.edu/gri_mech

Notation	
<i>A</i>	Preexponential factor
<i>α</i>	NO progress variable
<i>E</i>	Activation energy (J/mol)
<i>k</i>	Reaction rate constant
<i>n</i>	Temperature exponent
<i>R</i>	Equilibrium rate (mol/cm ³ ·s)
<i>R_m</i>	Universal gas constant (8.3143 J/mol·K)
<i>T</i>	Temperature (K)
<i>t</i>	Time (s)
<i>κ</i>	Nondimensional parameter
<i>λ</i>	Nondimensional parameter
<i>τ_{NO}th</i>	Characteristic timescale related to thermal NO (s)
<i>τ_{NO}^{nitr}</i>	Characteristic timescale related to N ₂ O pathway NO (s)
Subscripts	
<i>e</i>	Equilibrium
Abbreviations	
ODE	Ordinary Differential Equation
SSA	Steady-state Approximation

IT'S TIME FOR EXPERT KNOWLEDGE WITH NEW FLEXIBILITY. MTZ eMAGAZINE.



© creativa republic / Rentop Frankfurt - 2010



THE FASTEST INFORMATION IS DIGITAL.

MTZ eMagazine loaded with the newest findings in research and development of automotive engines.

Delivered to your e-mail as PDF. **MTZ eMagazine** is fast and up-to-date.

Easily find topics with keyword searches, read up on feature articles in the online archive or create a PDF with extracted information.

www.my-specialized-knowledge.com/automotive

MTZ

Founded 1939 by Prof. Dr.-Ing. E. h. Heinrich Buschmann and Dr.-Ing. E. h. Prosper L'Orange

Organ of the Fachverband Motoren und Systeme im VDMA, Verband Deutscher Maschinen- und Anlagenbau e.V., Frankfurt/Main, for the areas combustion engines and gas turbines
 Organ of the Forschungsvereinigung Verbrennungskraftmaschinen e.V. (FVV)
 Organ of the Wissenschaftliche Gesellschaft für Kraftfahrzeug- und Motorentechnik e.V. (WKM)
 Organ of the Österreichischer Verein für Kraftfahrzeugtechnik (ÖVK)
 Cooperation with the STG, Schiffbautechnische Gesellschaft e.V., Hamburg, in the area of ship drives by combustion engine

12|2015 _ Volume 76

Springer Vieweg | Springer Fachmedien Wiesbaden GmbH

P. O. Box 15 46 · 65173 Wiesbaden · Germany | Abraham-Lincoln-Straße 46 · 65189 Wiesbaden · Germany

Amtsgericht Wiesbaden, HRB 9754, USt-IdNr. DE811148419

Managing Directors Armin Gross, Joachim Krieger, Dr. Niels Peter Thomas

Managing Director Marketing & Sales Armin Gross | Director Magazines Stefanie Burgmaier | Director Production Dr. Olga Chiarcos

SCIENTIFIC ADVISORY BOARD

Prof. Dr.-Ing. Michael Bargende
 Universität Stuttgart

Prof. Dr. techn. Christian Beidl
 TU Darmstadt

Dr.-Ing. Ulrich Dohle
 Rolls-Royce Power Systems AG

Dipl.-Ing. Markus Duesmann
 BMW AG

Prof. Dr.-Ing. Lutz Eckstein
 WKM

Dr.-Ing. Torsten Eder
 Daimler AG

Dipl.-Ing. Friedrich Eichler
 Volkswagen AG

Dipl.-Ing. Dietmar Goericke
 Forschungsvereinigung
 Verbrennungskraftmaschinen e.V.

Prof. Dr.-Ing. Uwe Dieter Grebe
 AVL List GmbH

Prof. Dr.-Ing. Jens Hadler
 APL

Prof. Dr.-Ing. Jürgen Hammer
 Robert Bosch GmbH

Dr. Thomas Johnen
 Adam Opel AG

Rainer Jückstock
 Federal-Mogul Corporation

Prof. Dr. Hans Peter Lenz
 ÖVK

Prof. Dr. h. c. Helmut List
 AVL List GmbH

Dipl.-Ing. Wolfgang Maus
 Continental Emitec GmbH

Peter Müller-Baum
 VDMA e.V.

Prof. Dr.-Ing. Stefan Pischinger
 FEV GmbH

Wolf-Henning Scheider
 Mahle GmbH

Prof. Dr. Hans-Peter Schmalzl
 Pankl-APC Turbosystems GmbH

Dr. Markus Schwaderlapp
 Deutz AG

Prof. Dr.-Ing. Ulrich Seiffert
 WiTech Engineering GmbH

Dr. Michael Winkler
 Hyundai Motor Europe
 Technical Center GmbH

EDITORIAL STAFF

EDITORS IN CHARGE

Dr. Johannes Liebl, Wolfgang Siebenpfeiffer

EDITOR IN CHIEF

(responsible for editorial content)

Dr. Alexander Heintzel
 phone +49 611 7878-342 · fax +49 611 7878-462
 alexander.heintzel@springer.com

DEPUTY EDITOR IN CHIEF

Dipl.-Journ. (FH) Martin Westerhoff
 phone +49 611 7878-120 · fax +49 611 7878-462
 martin.westerhoff@springer.com

MANAGING EDITOR

Kirsten Beckmann M. A.
 phone +49 611 7878-343 · fax +49 611 7878-462
 kirsten.beckmann@springer.com

EDITORS

Angelina Hofacker
 phone +49 611 7878-121 · fax +49 611 7878-462
 angelina.hofacker@springer.com

Dipl.-Ing. Ulrich Knorra
 phone +49 611 7878-314 · fax +49 611 7878-462
 ulrich.knorra@springer.com

Dipl.-Ing. Michael Reichenbach
 phone +49 611 7878-341 · fax +49 611 7878-462
 michael.reichenbach@springer.com

Markus Schöttle
 phone +49 611 7878-257 · fax +49 611 7878-462
 markus.schoettle@springer.com

FREELANCERS

Dipl.-Ing. (FH) Richard Backhaus,
 Dipl.-Ing. (FH) Andreas Burkert, Dipl.-Ing. (FH)
 Andreas Fuchs, Roland Schedel, Stefan Schlott

ENGLISH LANGUAGE CONSULTANT

Paul Willin

ONLINE | ELECTRONIC MEDIA

Portal Manager Automotive
 Christiane Brünglinghaus
 phone +49 611 7878-136 · fax +49 611 7878-462
 christiane.bruenglinghaus@springer.com

SPECIAL PROJECTS

Managing Editorial Journalist
 Markus Bereszewski
 phone +49 611 7878-122 · fax +49 611 7878-462
 markus.bereszewski@springer.com

Editorial Staff | Coordination

Dipl.-Reg.-Wiss. Caroline Behle
 phone +49 611 7878-393 · fax +49 611 7878-462
 caroline.behle@springer.com
 Christiane Imhof M. A.
 phone +49 611 7878-154 · fax +49 611 7878-462
 christiane.imhof@springer.com

PROJECT MANAGEMENT | ASSISTANCE

Yeliz Konar
 phone +49 611 7878-180 · fax +49 611 7878-462
 yeliz.konar@springer.com
 Martina Schraad
 phone +49 611 7878-276 · fax +49 611 7878-462
 martina.schraad@springer.com

ADDRESS

Abraham-Lincoln-Straße 46 · 65189 Wiesbaden
 P. O. Box 1546 · 65173 Wiesbaden, Germany
 redaktion@ATZonline.de

ADVERTISING

SALES MANAGEMENT

(responsible for advertising)
 Volker Hasedenz
 phone +49 611 7878-269 · fax +49 611 7878-78269
 volker.hasedenz@best-ad-media.de

MEDIA SALES

Frank Nagel
 phone +49 611 7878-395 · fax +49 611 7878-78395
 frank.nagel@best-ad-media.de

KEY ACCOUNT MANAGEMENT

Rouwen Bastian
 phone +49 611 7878-399 · fax +49 611 7878-78399
 rouwen.bastian@best-ad-media.de

DISPLAY AD MANAGER

Nicole Brzank
 tel +49 611 7878-616 · fax +49 611 7878-78164
 nicole.brzank@best-ad-media.de

AD PRICES

Advertising ratecard from October 2014.

MARKETING | OFFPRINTS

HEAD OF MARKETING
 MAGAZINES + EVENTS

Jens Fischer
 phone +49 611 7878-340 · fax +49 611 7878-407
 jens.fischer@springer.com

OFFPRINTS

Martin Leopold
 phone +49 2642 907-596 · fax +49 2642 907-597
 leopold@medien-kontor.de

PRODUCTION | LAYOUT

Heiko Köllner
 phone +49 611 7878-177 · fax +49 611 7878-78177
 heiko.koellner@springer.com

All persons specified may be contacted by post at the publisher's address.

SUBSCRIPTIONS

Springer Customer Service Center GmbH
 Haberstraße 7 · 69126 Heidelberg · Germany
 phone +49 6221 3454-303 · fax +49 6221 3454-229
 Monday to Friday, 8 a.m. to 6 p.m.
 springervieweg-service@springer.com
 www.my-specialized-knowledge.com/automotive

ORDERING OPTIONS

The eMagazine MTZworldwide appears 11 times a year for subscribers. Ordering options and details on the subscription conditions can be found at www.my-specialized-knowledge.com/MTZworldwide.

All rights reserved.

Reproduction: This magazine and all its contents, including all images, graphics and photographs, are protected by copyright. Unless its usage is, in exceptional cases, expressly permitted by copyright law, no part of this magazine may be reproduced without the prior written consent of the publisher. This applies in particular to copies, reprints, adaptations, translations, microfilms, provision of public access and the storage and processing of this magazine in whole or in part in databases and other electronic systems and its distribution or usage via electronic systems.

YOUR HOTLINE
 TO MTZ

- Editorial Staff
- +49 611 7878-120
- Customer Service
- +49 6221 3454-303
- Advertising
- +49 611 7878-395

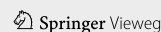
The articles published in MTZworldwide are produced with the greatest possible care and attention. However, the editors do not accept any liability for the correctness, completeness and current accuracy of the content printed. The content of advertisements is the sole responsibility of the advertiser.

Every annual subscription includes access to the online archive at Springer für Professionals. Access is available exclusively to the individual subscriber and is not transferable.

No liability can be accepted for the unsolicited submission of manuscripts, photographs or illustrations.

© Springer Vieweg | Springer Fachmedien Wiesbaden GmbH, Wiesbaden 2015

Springer Vieweg is part of Springer Science+Business Media.



PEER REVIEW

Peer Review Process for Research Articles
in ATZ, MTZ and ATZelektronik

STEERING COMMITTEE

Prof. Dr.-Ing. Lutz Eckstein	RWTH Aachen University	Institut für Kraftfahrzeuge Aachen
Prof. Dipl.-Des. Wolfgang Kraus	HAW Hamburg	Department Fahrzeugtechnik und Flugzeugbau
Prof. Dr.-Ing. Ferit Küçükyay	Technische Universität Braunschweig	Institut für Fahrzeugtechnik
Prof. Dr.-Ing. Stefan Pischinger	RWTH Aachen University	Lehrstuhl für Verbrennungskraftmaschinen
Prof. Dr.-Ing. Hans-Christian Reuss	Universität Stuttgart	Institut für Verbrennungs- motoren und Kraftfahrwesen
Prof. Dr.-Ing. Ulrich Spicher	MOT	
Prof. Dr.-Ing. Hans Zellbeck	Technische Universität Dresden	Lehrstuhl für Verbrennungsmotoren

ADVISORY BOARD

Prof. Dr.-Ing. Klaus Augsburg	Dr. Malte Lewerenz
Prof. Dr.-Ing. Michael Bargende	Prof. Dr.-Ing. Markus Lienkamp
Prof. Dipl.-Ing. Dr. techn. Christian Beidl	Prof. Dr. rer. nat. habil. Ulrich Maas
Prof. Dr. sc. techn. Konstantinos Boulouchos	Prof. Dr.-Ing. Markus Maurer
Prof. Dr. Dr. h.c. Manfred Broy	Prof. Dr.-Ing. Martin Meywerk
Prof. Dr.-Ing. Ralph Bruder	Ao. Univ.-Prof. Dr. Gregor Mori
Dr. Gerhard Bruner	Prof. Dr.-Ing. Klaus D. Müller-Glaser
Prof. Dr. rer. nat. Heiner Bubb	Dr. techn. Reinhard Mundl
Prof. Dr. rer. nat. habil. Olaf Deutschmann	Prof. Dr. rer. nat. Peter Neugebauer
Prof. Dr.-Ing. Klaus Dietmayer	Prof. Dr. rer. nat. Cornelius Neumann
Dr. techn. Arno Eichberger	Prof. Dr.-Ing. Nejila Parspour
Prof. Dr. techn. Helmut Eichseder	Prof. Dr.-Ing. Peter Pelz
Prof. Dr. Wilfried Eichseder	Prof. Dr. techn. Ernst Pucher
Dr.-Ing. Gerald Eifler	Dr. Jochen Rau
Prof. Dr.-Ing. Wolfgang Eifler	Prof. Dr.-Ing. Konrad Reif
Prof. Dr. rer. nat. Frank Gauterin	Prof. Dr.-Ing. Stephan Rinderknecht
Prof. Dr. techn. Bernhard Geringer	Prof. Dr.-Ing. Jörg Roth-Stielow
Prof. Dr.-Ing. Uwe Dieter Grebe	Dr.-Ing. Swen Schaub
Dr. mont. Christoph Guster	Prof. Dr. sc. nat. Christoph Schierz
Prof. Dr.-Ing. Holger Hanselka	Prof. Dr. rer. nat. Christof Schulz
Prof. Dr.-Ing. Horst Harndorf	Prof. Dr. rer. nat. Andy Schürr
Prof. Dr. techn. Wolfgang Hirschberg	Prof. Dr.-Ing. Ulrich Seiffert
Prof. Dr. techn. Peter Hofmann	Prof. Dr.-Ing. Hermann J. Stadtfeld
Prof. Dr. rer. nat. Peter Holstein	Prof. Dr.-Ing. Karsten Stahl
Prof. Dr.-Ing. Volker von Holt	Prof. Dr. techn. Hermann Steffan
Prof. Dr.-Ing. habil. Werner Hufenbach	Prof. Dr.-Ing. Wolfgang Steiger
Prof. Dr.-Ing. Armin Huß	Prof. Dr.-Ing. Peter Steinberg
Dr. techn. Heidelinde Jetzinger	Dr.-Ing. Peter Stommel
Prof. Dr.-Ing. Roland Kasper	Dr.-Ing. Ralph Sundermeier
Prof. Dr.-Ing. Prof. E. h. mult. Rudolf Kawalla	Prof. Dr.-Ing. Wolfgang Thiemann
Prof. Dr.-Ing. Tran Quoc Khanh	Prof. Dr.-Ing. Dr. h.c. Helmut Tschöke
Dr. Philip Köhn	Prof. Dr.-Ing. Georg Wachtmeister
Prof. Dr.-Ing. Ulrich Konigorski	Prof. Dr.-Ing. Jochen Wiedemann
Prof. Dr. Oliver Kröcher	Prof. Dr. rer. nat. Gerhard Wiegler
Prof. Dr.-Ing. Peter Krug	Prof. Dr. techn. Andreas Wimmer
Dr. Christian Krüger	Prof. Dr. rer. nat. Hermann Winner
Prof. Dr. techn. Thomas Lauer	Prof. Dr. med. habil. Hartmut Witte
Prof. Dr. rer. nat. Uli Lemmer	Dr.-Ing. Michael Wittler

Scientific articles of universities in ATZ Automobiltechnische Zeitschrift, MTZ Motortechnische Zeitschrift and ATZelektronik are subject to a proofing method, the so-called peer review process. Articles accepted by the editors are reviewed by experts from research and industry before publication. For the reader, the peer review process further enhances the quality of the magazines' content on a national and international level. For authors in the institutes, it provides a scientifically recognised publication platform.

In the Peer Review Process, once the editors has received an article, it is reviewed by two experts from the Advisory Board. If these experts do not reach a unanimous agreement, a member of the Steering Committee acts as an arbitrator. Following the experts' recommended corrections and subsequent editing by the author, the article is accepted.

In 2008, the peer review process utilised by ATZ and MTZ was presented by the WKM (Wissenschaftliche Gesellschaft für Kraftfahrzeug- und Motorentechnik e. V./ German Professional Association for Automotive and Motor Engineering) to the DFG (Deutsche Forschungsgemeinschaft/German Research Foundation) for official recognition. ATZelektronik participates in the Peer Review since 2011.



Quick Ashing of Particulate Filters

The literature discloses numerous methods for quick ashing of particulate filters. However, it is largely unknown if a combination of these methods is possible and which one is the method of ashing at normal use of particulate filters most likely. As well as the influencing factors are not fully understood at the ash formation, a particulate filter in a defined cycle was ashed of the Institute for Internal Combustion Engine at the TU Braunschweig under a FVV project of several operating points.

AUTHORS



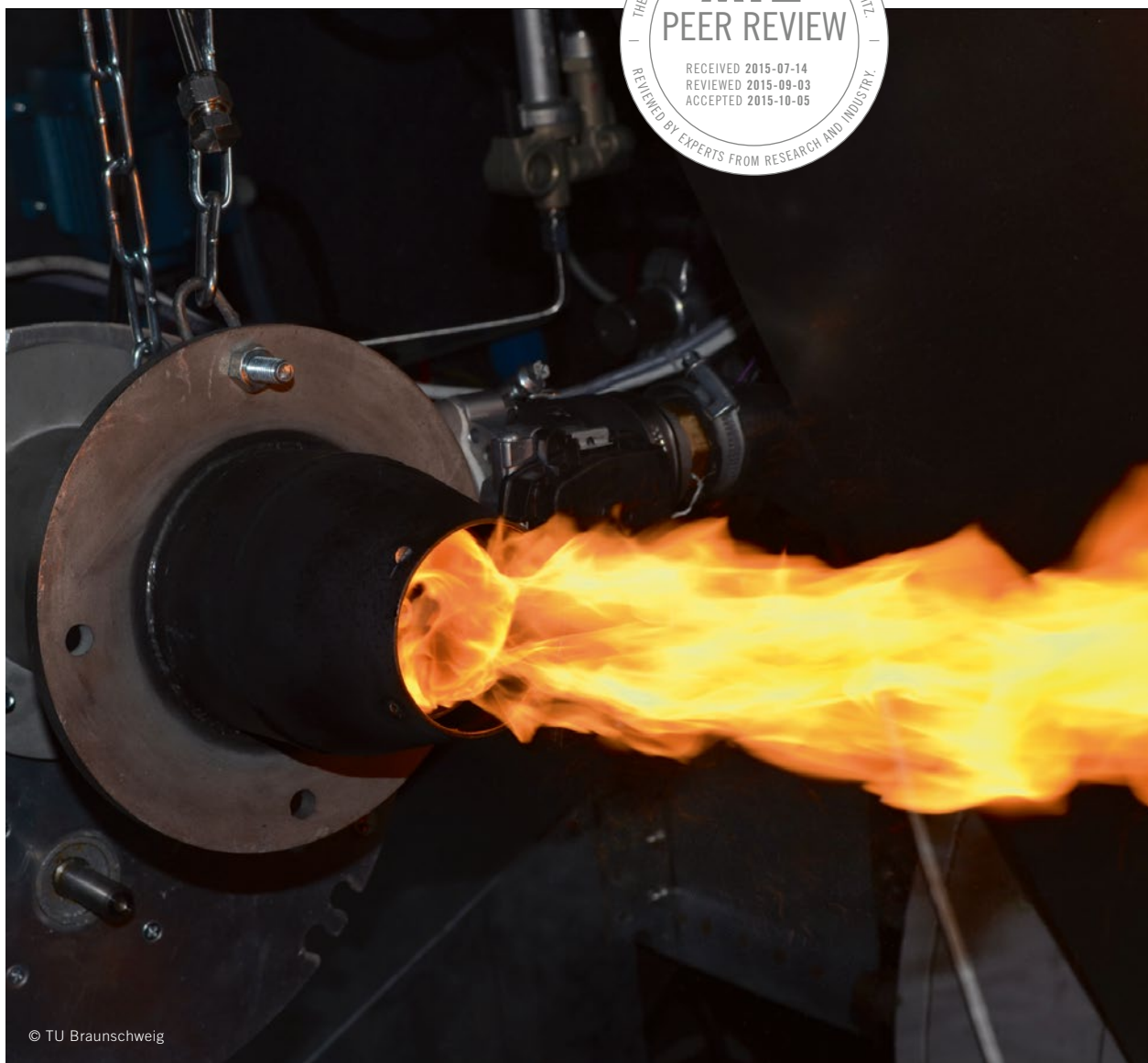
Dipl.-Ing. Fabian Sonntag

was at the time of the research project Research Assistant of the Institute of Internal Combustion Engines (ivb) at the Technische Universität Braunschweig and is now Test Engineer at the IAV GmbH in Gifhorn (Germany).



Prof. Dr.-Ing. Peter Eilts

is Head of the Institute of Internal Combustion Engines (ivb) at the Technische Universität Braunschweig (Germany).



© TU Braunschweig

1	MOTIVATION
2	EXPERIMENTAL SETUP
3	TEST PREPARATION
4	EXPERIMENTAL RESULTS
5	EVALUATION OF RESULTS
6	SUMMARY AND OUTLOOK

1 MOTIVATION

During the lifetime of the filter it accumulates ash. This ash is the inorganic rest of trapped particulate mass which is not regenerative. Depending on the trapping position the ash results in an increased back pressure of the filter. With the use of quick ashing methods a faster generation of ash is possible. Besides, cost savings are attainable by reducing the test bench time and lower fuel consumption. For this the same or at least similar ash qualities are required. Beside the check of the design concerning ash deposition and ash migration the check of new technologies is feasible with a loadable quick ashing method in the context of the particle filter to lower costs.

2 EXPERIMENTAL SETUP

The test engine is a four-cylinder diesel engine with a displacement of 2.0 l and a maximum power of 103 kW. The engine is equipped with a common rail injection system, turbocharger with variable turbine geometry and with closed loop high pressure exhaust recirculation. The standard EGR-system is mechanically closed. **FIGURE 1** shows the general test bench setup. The start of the engine is done with suitable heating actions. Therefore it is ensured that the engine is only started with operating temperature.

Components used for these experiments are taken from passenger cars. The Diameter of all substrates is 5.66". The length of the DOC is 3" and it is coated with platinum and palladium in an proportion of 2:1 with an over all precious metal content of 90 g/ft³. The length of the DPF is nearly 6" and it is coated with the same platinum to palladium proportion like the DOC but the precious metal content is only 25 g/ft³. The substrate of the DPF is silicon carbide with a cell density of 350 cpsi and an asymmetric cell technology. To avoid a potential lost of ash a second DPF is inserted downstream of the first one. This backup DPF has the same geometry like the first DPF and shall trap the ash which passes the main DPF.

The ashing cycle fulfils the requirements for continuously regeneration. According to literature [1], there is a high NO_x/soot-ratio and an exhaust temperature between 300 and 450 °C are necessary. To reach these conditions an ashing cycle similar to the European Stationary Cycle (ESC) has been selected. Deviating from this certifying cycle for heavy duty vehicles the full load operating points and the idle operating point will not be considered. Under idle condition the oil consumption and thereby the ash production rate is very low. At full load conditions the exhaust temperature is so high that an active regeneration could be started. This results in an ash transport within the DPF channels and a deterioration of the catalytic coating. The oil consumption is measured with the drop-off-method.

3 TEST PREPARATION

3.1 INCREASEMENT OF SULPHATED ASH CONTENT

A kind of oil with a low ash content, a so-called low-saps oil with an ash content of 0.9% is used for the reference run. Next to this normal oil, commercial oil with an increased sulphated ash content of 1.7% is taken. The third one is a special oil with an extra high ash content of 2.8%.

3.2 BURNER GENERATED ASH DOSAGE

There are several investigations described in literature, which use an oil burner to generate ash [2]. In contrast to literature the burner exhaust is mixed with the engine exhaust and then streams to the DPF in this investigation. The burner system is a commercial one, which is designated for firing in one-family-houses and small industrial establishments. The maximum firing power of the burner system is 50 kW.

Yellow burner are burning the fuel with a bright yellow diffusion flame and normally they emit soot. Blue burners are a further development in the burning technology. Since they burn with a premixed flame the colour of the flame is transparent to slight blue. The exhaust of blue burners is nearly without soot [3].

FIGURE 2 shows the setup used in these investigations. The oil mass flow is controlled with a mass flow controller, which works according to the Coriolis principle. The ash particle size of the engine is measured with the following set-up: a sample of the engine exhaust is enriched with oxygen and sent through an oven at a temperature of 1000 °C. Ash is the only component of particle size measurement at this temperature.

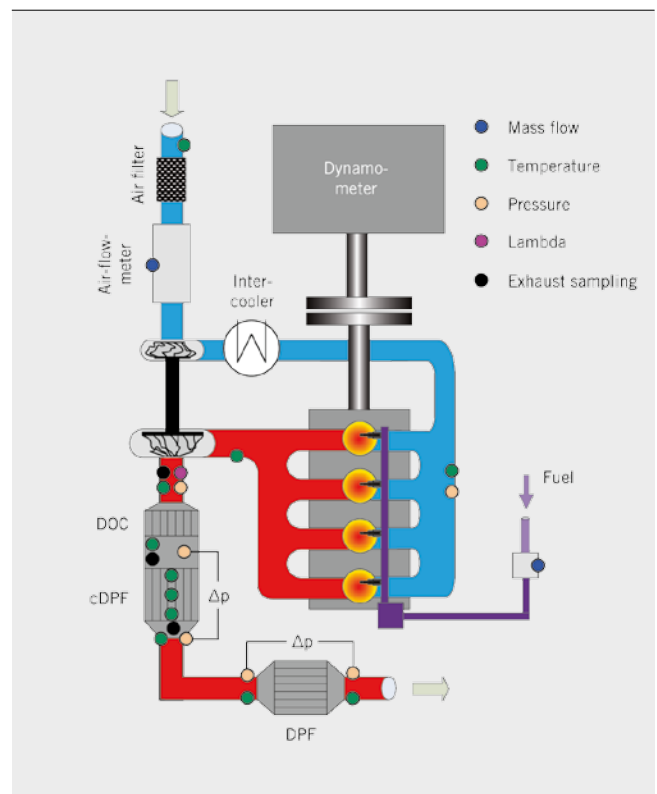


FIGURE 1 Experimental setup and measurement positions of the engine test bench (© TU Braunschweig)

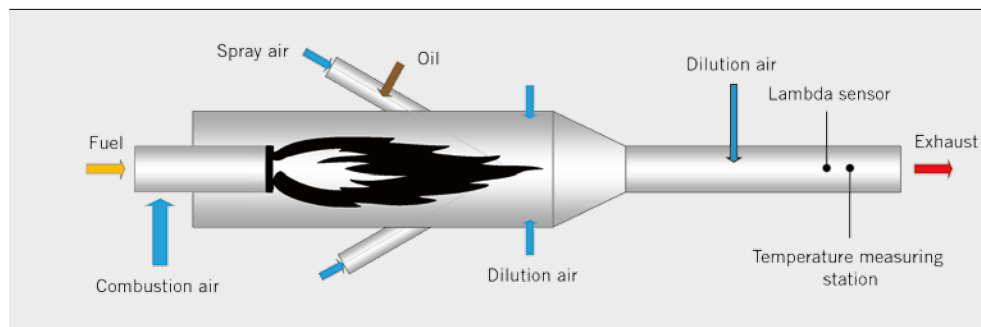


FIGURE 2 Setup burner system © TU Braunschweig

An atomiser close to **FIGURE 3** is used, because it has a high degree of freedom regarding the size of the generated oil droplets. Next to the air-to-oil-mass-flow-ratio a number of other parameters have influence on the droplet size like the distance l and z as well as the angle β . Thus a variation of the inner diameter of the oil-pipe in a range from 0.6 to 1.2 mm at a constant external diameter of 1.6 mm was done. Apart from that the other boundary conditions are taken constant. The more the inner diameter increases, the more the middle diameter of the ash rises. An inner diameter of 0.8 mm turned out to be the most similar to the engine-driven ash emissions. The air-pipe has an external diameter of 6 mm and an internal diameter of 4 mm. The distance l is 10 mm and the dimension z is 0 mm. An angle of slope β of 0° is chosen to simplify the assembly.

3.3 OIL INJECTION INTO INLET MANIFOLD

Common-rail-components, which are set in standard factory model passenger cars, are used for the injection of oil. The high pressure pump is electrically operated and the suction valve is taken in a constant position. An external pressure sensor registers the pressure in the rail. With the help of a pressure control valve a controller adjusts the rail pressure at a constant value of 300 bar. Due to the definite higher viscosity of lubricating oil compared to diesel the injectors are wrapped with a heating string and heated to a temperature of 110°C . One injector for each cylinder is used for the injection of oil. This ensures a good uniformity of the oil going into the cylinders. Single-hole-nozzles are mounted to ensure injection of minimal amounts of oil. With these nozzles the injection time is in normal ranges. The injected spray direction is aligned towards the filling channel.

3.4 FUEL DOPING

The dosage of oil is carried out with the mass flow controller described above. Oil mass flow is adjusted in each operating point to the double of the normal engine oil consumption. The oil is mixed with the fuel upstream the engine. This results to a mass ratio of 0.5% of oil in fuel.

4 EXPERIMENTAL RESULTS

Within this report a small selection of analyses and evaluations only can be shown. So the most important and most characteristic parameters of the ashing process are presented including reached time-lapse factor, difference pressure and ash morphology. For further information see the final report of this project [54].

TABLE 1 shows an overview of the realised quick ashing runs. After having reached an ash mass of 74.4 g in the reference run, it was the goal of further runs to generate this amount of ash. The oil dosage means additional oil whether via oil injection into inlet manifold, burner system or fuel doping. Target value of the additional oil dosage is the double volume of engine oil consumption. For each ashing run a new DPF is used. To avoid cross influences of differences in production all DPFs are from the same batch. The backup DPF is uncoated and no ash has been ever found on it.

The time-elapsing factors of increased sulphated ash content in the oil does not correlate completely with the increased sulphated ash content, because the ash capture ratio is lower compared to reference. The burner generated ash with blue burner in ashing run number 4 shows deposits in the burning chamber. That is the reason for the lower ash capture ratio compared to the yellow burner.

No.	Description	Duration [h]	Ash mass [g]	Oil consumption engine [kg]	Additional oil [kg]	Sulphated ash content in oil [%]	Time acceleration factor [-]
1	Reference	300	74.4	9.11	–	0.9	1
2	Doubling sulphated ash content	150	68.3	4.94	–	1.7	1.83
3	Triplication sulphated ash content	102	71.9	3.28	–	2.8	2.84
4	Blue burner	54	57.8	1.69	3.49	1.7	4.32
5	Yellow burner	55	69.7	1.62	3.72	1.7	5.11
6	Oil injection inlet manifold	88	68.4	1.7	3.98	1.7	3.13
7	Fuel doping	36	52.1	1.11	2.02	1.7	5.84

TABLE 1 Overview of ashing runs © TU Braunschweig

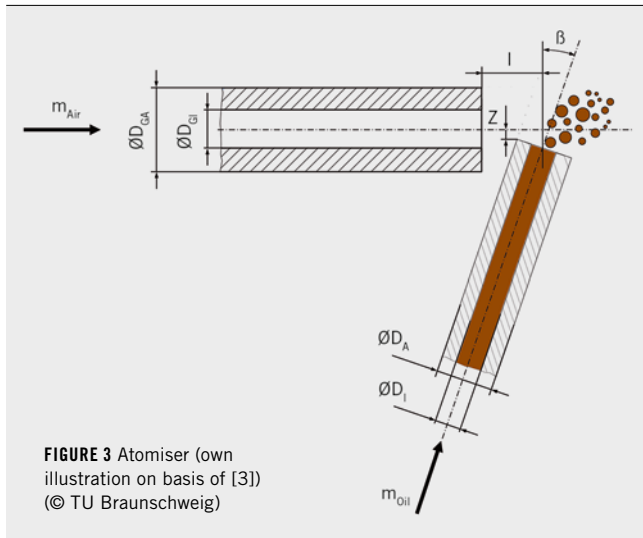


FIGURE 3 Atomiser (own illustration on basis of [3])
© TU Braunschweig

By using oil injection into inlet manifold the normal engine oil consumption is reduced respectively and additional oil is found in the sump. That is a reason for the low time-lapsing factor.

FIGURE 4 shows the difference pressure corrected for same ash mass after external thermal regeneration in an oven. The difference pressure is measured under standard temperature and pressure conditions at a mass flow of 400 kg/h. Due to the regeneration the soot is completely burnt and therefore only the differential pressure of the ash is measured. Since all filters come from the same production batch, the differential pressures of the empty filters differ very little. The differences of the ashed filters lead back to the properties of the embedded ashes. A higher differential pressure at the same ash loading of two filters shows a lower ash permeability.

The difference pressure will be interpolated at lower ash mass loads. Basis for the evaluation is the reference, because the ash mass of all other processes was corrected to this ash mass. The difference pressure of the increased sulphated ash content oil (1.7%) is with 75.4 mbar tightly higher than the reference with 72.1 mbar. Further increase of sulphated ash content (2.8%) leads to a decrease of 7.2% of difference pressure compared to reference. The ashing run number 5 (yellow burner) results in a 14 mbar decreased difference pressure, which means 18.1% lower pressure. This is due to a different ash permeability. A decreased difference pressure of 10.7% is the result of the injection of oil into the inlet manifold. This ashing process shows the lowest differences to the reference aside from the increased sulphated ash oil ashing runs.

Dosing the fuel in the ashing run number 7 results in a significant increase of difference pressure. Due to the low ash permeability there is only an ash mass of 52.1 g on the filter. This high difference pressure led to an abort (premature discontinuation) of the ashing run. So the gap of ash mass between reference run and fuel doping is quite high. This results in a wide extrapolation of the difference pressure in combination with a high calculation error. Under consideration of the maximum calculation error the extrapolated difference pressure is still higher than for the reference.

The ash layer characteristic along the filter channels is analysed with automated picture methology. For this, one unit-brick is divided in length direction into four parts. From the three sites of fracture pictures are taken with a microscope. The results are presented in **FIGURE 5**. The maximum of the Y-axis has been scaled to represent the half height of the inlet channel and to show the filter in full length. Ash layer thickness is linearly increasing with filter length at the reference in the investigated area. The ash generated from the oil with increased sulphated ash content (1.7%) showed a similar behaviour. At the first measurement position and in the middle of the filter the ash layer thickness is a little smaller the reference. The ashing run with high sulphated ash content in the oil (2.8%) shows a similar behaviour to reference and also the oil with 1.7%

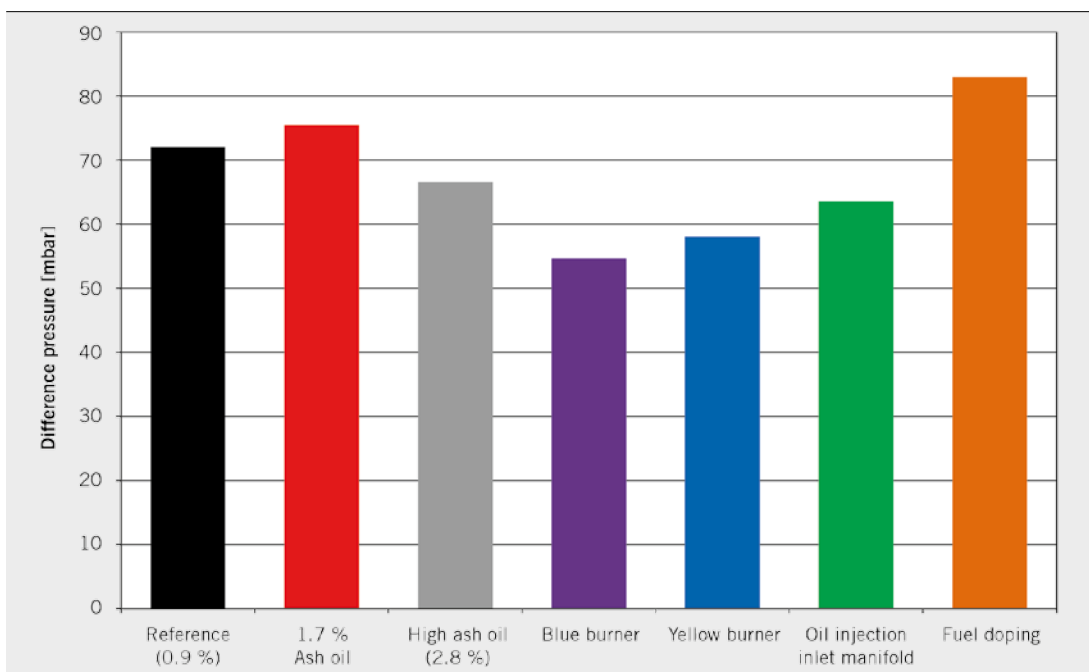


FIGURE 4 Difference pressure corrected for same ash mass
© TU Braunschweig

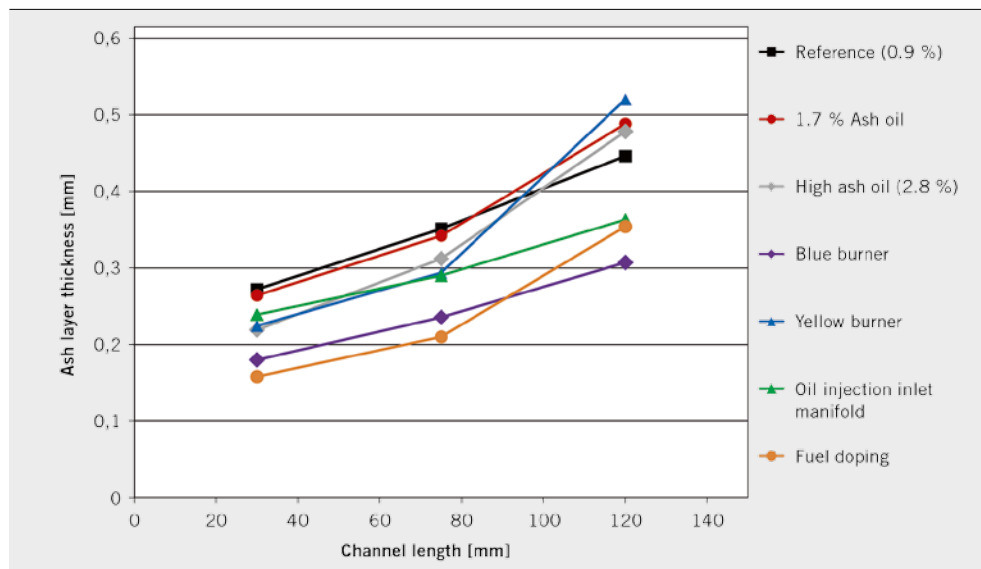


FIGURE 5 Ash layer thickness in the inlet channel of the filter (© TU Braunschweig)

of sulphate ash content. In the inlet area and in the middle the ash layer thickness is a little bit smaller than by the use of the oil with 1.7% sulphate ash content. The application of the blue burner shows a course parallel to the reference of the ash layer. The ash layer thickness is clearly lower and the whole ash mass is lower too. The run with the yellow burner led to a raised ash aggregation at the channel end. Among other things this leads back to the fact, that the exhaust of the yellow burner is thinned with air to ensure an exhaust temperature lower than 480 °C. Due to the increased exhaust mass flow the axial flow velocity in the filter increases. So more particles are transported to the end of the channel.

The ashing run with oil injection into inlet manifold leads to an ash deposition which rises not so strongly as the reference at the channel end. The explanation for the lower level is an 8% lower ash mass on the whole filter. If the oil is introduced with the fuel in the cylinder, the ash deposits in the input area differently compared to the other

ashing runs. The ash does not lie completely close on the wall. Instead of this, a gap appears between the ash layer and the filter wall.

FIGURE 6 shows SEM images from the middle of the filter at an 80-times magnification. The ash of the reference (a) and of the higher sulphated ash oil with 1.7% (b) show high comparable ash morphology. The ash of the further increased sulphated ash oil with 2.8% (c) shows increased diameter of the agglomerates as well as clear spaces. Burner generated ashes (d, e) are in this zoom-position optical similar to the reference and the increased ash content (1.7%). The ash generated with oil injection into inlet manifold (f) shows a similar morphology to high sulphated ash content oil (2.8%). Fuel doping (g) results in a completely different ash structure. There is an unstructured layer of about 100 µm on the channel wall which show layer-like structure.

The structure of the ashes is clearly better visible in FIGURE 7 with 700-times enlargement. The higher ash content oils (1.7% and

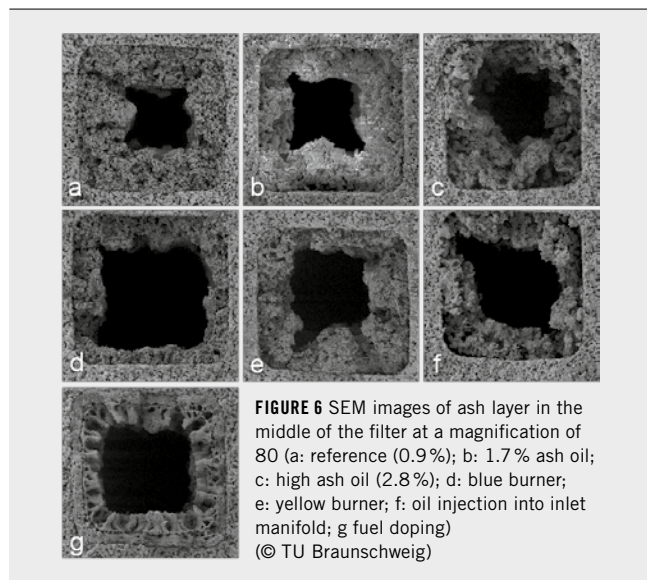


FIGURE 6 SEM images of ash layer in the middle of the filter at a magnification of 80 (a: reference (0.9%); b: 1.7% ash oil; c: high ash oil (2.8%); d: blue burner; e: yellow burner; f: oil injection into inlet manifold; g: fuel doping) (© TU Braunschweig)

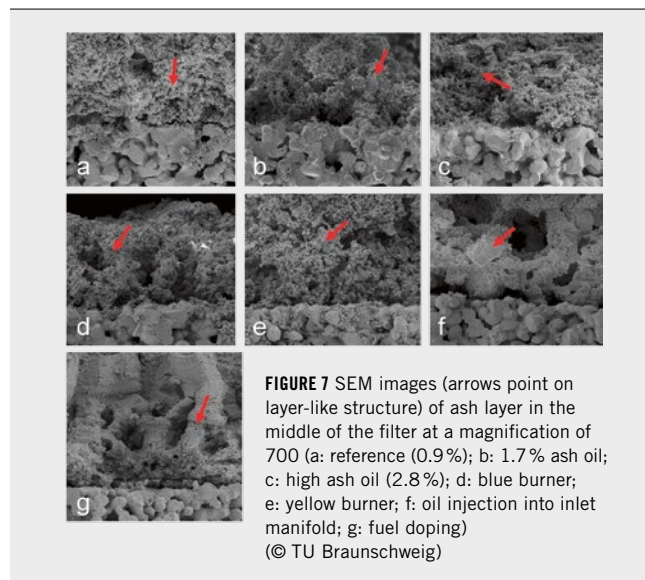


FIGURE 7 SEM images (arrows point on layer-like structure) of ash layer in the middle of the filter at a magnification of 700 (a: reference (0.9%); b: 1.7% ash oil; c: high ash oil (2.8%); d: blue burner; e: yellow burner; f: oil injection into inlet manifold; g: fuel doping) (© TU Braunschweig)

		Double sulphate ash content	Triplicate sulphate ash content	Yellow burner	Oil injection into inlet manifold	Fuel doping
Criteria	Weighting coefficient [%]	Grading				
Ash morphology and characteristics	40	171	149	109	156	86
Economic parameters	30	36	77	127	101	144
Process parameters	25	87	86	93	73	85
Further system properties	5	12.5	14	18	9	15
Final score		306.5	326	347	339	330

TABLE 2 Evaluation matrix (© TU Braunschweig)

2.8%) (b and c) show layer-like structures which grow up to a certain length and then break. In **FIGURE 7** these layer structures are marked with arrows. This structure also exists with the oil injection into inlet manifold (f). Fuel doping (g) make this layer structure to develop especially strongly. The cross section surface of the single accumulations is clearly stronger developed in comparison to the other ashes. The burner-generated ash and the reference show this layer build up only in a low amount. The ashes from both oils with increased sulphated ash content and the burner-generated ash show at this enlargement a good correspondence to the reference.

5 EVALUATION OF RESULTS

The evaluation is divided into the following four main categories:

- ash morphology and characteristics (40%)
- economic parameters (30%)
- process parameters (25%)
- further system properties (5%).

The main categories are subdivided into single evaluation criteria. Hence the first main category ash morphology and characteristics is subdivided into the single criteria difference pressure, ash packaging density, ash layer characteristic within the channel length, optical similarity, influence on conversion efficiency, ash particle size distribution und chemical composition.

Evaluation is done on a scale from 0 points (criterion not or very bad fulfilled) to 5 points (complete or best fulfilled). Each single criterion is evaluated for all ashing runs. The grading is multiplied with a weighting coefficient. The product is the individual score. All scores are condensed in an evaluation matrix. The ashing process with highest score is most suitable for ashing of particulate filters. From burner-generated ashing processes only the yellow burner is taken into account, because this showed throughout better results. Taking all parameters into consideration the ashing process with burner-generated ash shows the best properties. This is demonstrated with the high number of 347 evaluation points, **TABLE 2**. With exception of fuel doped ash also the other processes are appropriate to generate ash.

6 SUMMARY AND OUTLOOK

Within this project different promising methods for the quick ashing of particulate filters are investigated under carefully controlled laboratory conditions. The processes are further developed and applied on one test bench. Thereby, generated ash is analysed in detail and

compared to a reference run. The doubling of the sulphate ash content produces very similar results to the reference. A further increase on three times sulphated ash content does not produce these unequivocal results. Anyway this shows without any additional efforts a good possibility to generate the triple amount of ash per time unity. The parallel application of an oil burner produces good results if the ash particle reaches the filter together with the soot. Ash can be generated with relatively low operating costs with the help of the burner. The effort for the construction and the parameterisation of the system is high. The very high flexibility is a further advantage. If the oil is injected into the inlet manifold the normal oil consumption of the engine can simply be increased. The ash generated with this process shows differences to the reference in a row of evaluation criteria. Doping the fuel with oil is a very simple method to generate high amounts of ash in a short time. The ash morphology is not comparable to the reference and other ashing processes.

The results presented here are developed within the project quick ashing, which was supported by the Research Association for Combustion Engines e. V. This project is a precursor project for a interdisciplinary project with five research centres involved. In the main project investigations are planned which deal around ash behaviour in the filter. Aim of the precursor project is to have an appropriate process for the quick generation of ash.

REFERENCES

- [1] Dittler, A.: Abgasnachbehandlung mit Partikelfiltersystemen in Nutzfahrzeugen. Shaker-Verlag, 2014
- [2] Sappok, A. et al.: A Novel Accelerated Aging System to Study Lubricant Additive Effects on Diesel Aftertreatment System Degradation. In: SAE Technical Paper 2008-01-1549, 2008
- [3] Richter, T.: Zerstäuben von Flüssigkeiten: Düsen und Zerstäuber in Theorie und Praxis. Expert-Verlag, 2011
- [4] Eilts, P.; Sonntag, F.: Schnellveraschung. Abschlussbericht FVV-Vorhaben No. 1122, 2015

THANKS

This report is the scientific result of the research project Quick Ashing, which was made by Research Association for Combustion Engines (FVV, Frankfurt). The project was supported by a research committee of the FVV. The authors thank for the great support.